Accepted Manuscript

Neogene to Quaternary stratigraphic evolution of the Antarctic Peninsula, Pacific Margin offshore of Adelaide Island: Transitions from a non-glacial, through glacially-influenced to a fully glacial state

F. Javier Hernández-Molina, Robert D. Larter, Andrés Maldonado

PII: S0921-8181(16)30351-4
DOI: doi: 10.1016/j.gloplacha.2017.07.002
Reference: GLOBAL 2604

To appear in: *Global and Planetary Change*

Received date: 20 August 2016
Revised date: 6 February 2017
Accepted date: 10 July 2017

Please cite this article as: F. Javier Hernández-Molina, Robert D. Larter, Andrés Maldonado , Neogene to Quaternary stratigraphic evolution of the Antarctic Peninsula, Pacific Margin offshore of Adelaide Island: Transitions from a non-glacial, through glacially-influenced to a fully glacial state, *Global and Planetary Change* (2017), doi: 10.1016/j.gloplacha.2017.07.002

Neogene to Quaternary Stratigraphic Evolution of the Antarctic Peninsula, Pacific Margin offshore of Adelaide Island: transitions from a non-glacial, through glacially-influenced to a fully glacial state

F. Javier Hernández-Molina[1*], Robert D. Larter[2], Andrés Maldonado[3]

[1] Dept. Earth Sciences, Royal Holloway University of London, Egham, Surrey TW20 0EX, UK
[2] British Antarctic Survey (BAS), High Cross, Madingley Road, Cambridge CB3 0ET, UK
[3] Instituto Andaluz de Ciencias de la Tierra (IACT), CSIC/Univ. Granada, Campus de Fuentenueva, s/n, 18002 Granada, Spain

* Corresponding author. *Email address*: javier.hernandez-molina@rhul.ac.uk

Abstract

A detailed morphologic and seismic stratigraphic analysis of the continental margin offshore of Adelaide Island on the Pacific Margin of the Antarctic Peninsula (PMAP) is described based on the study of a regular network of reflection multichannel seismic profiles and swath bathymetry. We present an integrated study of the margin spanning the shelf to the continental rise and establish novel chronologic constraints and offer new interpretations on tectonic evolution and environmental changes affecting the PMAP. The stratigraphic stacking patterns record major shifts in the depositional style of the margin that outline three intervals in its evolution. The first non-glacial interval (Early Cretaceous to middle Miocene) encompasses a transition from an active to a passive margin (early Miocene). The second glacially-influenced interval (middle to late Miocene) is marked by pronounced aggradational sedimentary stacking and subsidence. Ice sheets advanced over the middle shelf of the margin at the end of this second interval, while the outer shelf experienced rare progradational events. The third, fully glaciated interval shows clear evidence of glacially dominated conditions on the margin. This interval divides into three minor stages. During the first stage (late Miocene to the beginning of the early Pliocene), frequent grounded ice advances to the shelf break began, depositing an initial progradational unit. A major truncation surface marked the end of this stage, which coincided with extensive mass transport deposits at the base of the slope. During the second progradational glacial margin stage (early Pliocene to middle Pleistocene), stacking patterns record clearly prograding glacial sequences. The beginning of the third aggradational glacial margin stage (middle Pleistocene to present) corresponded to an important shift in global climate during the Mid-Pleistocene Transition. Morphosedimentary characteristics observed along the margin today began to develop during the latest Miocene but did not become fully established until sometime during the interval between the end of the Pliocene and middle Pleistocene. Between these two time intervals, the northeast lateral migration of the Marguerite Trough also played a critical role in margin evolution, as it controlled ice sheet drainage pathways across the shelf, which in turn influenced development of slope and rise morphologies. Areas offshore from Adelaide Island differ from other areas of the PMAP due to changes in sedimentary processes that resulted from migration of the trough. This study confirms that the PMAP represents an exceptional locality for decoding, reconstructing and linking past tectonic and climatic changes. The study area specifically records not only the most relevant changes in depositional style, but also the relative importance of persistent along- and down-slope sedimentary processes. Our study approach can be extended to other areas and integrated with additional techniques to understand the evolution and the global linkages of the entire Antarctic continental margin and the ice sheets.

Key words: Antarctic Peninsula Pacific Margin, Neogene and Quaternary, seismic stratigraphy, sedimentary processes, morphology, bottom-current, ice sheets evolution

1. INTRODUCTION

The evolution and present morphology of polar margins derive from tectonic and environmental changes. In particular, environmental shifts during the Cenozoic have dictated the depositional style. The middle to latest Miocene saw major changes along the margin around West Antarctica, as the Antarctic Peninsula transitioned from a non-glaciated state, to a condition in which there had been intermittent alpine to marine-terminating glaciations, to a final fully glaciated state. This shift also strongly influenced sedimentation along the margin (Cooper *et al*., 1991; Powell and Domack, 1995; Larter *et al*., 1997; Nitsche *et al.*, 1997, 2000; Barker and Camerlenghi, 2002; Bart *et al.*, 2005; Rebesco *et al*., 2006; Lindeque et al., 2013; 2016). Major Pliocene and Quaternary climatic events include the late Pliocene to the early Quaternary (~2.6 Ma) and the Mid-Pleistocene transition (MPT, 1.2-0.65 Ma) (e.g., Shackleton and Opdyke, 1973; Ruddiman *et al*., 1989; Raymo *et al*., 1989; Clark *et al*., 1999; 2006; Zachos et al., 2008, Maslin and Ridgwell, 2005; McClymont et al., 2013), which coincided with eustatic sea level changes (Lowrie, 1986; Haq *et al*., 1987; Kitamura and Kawagoe, 2006; Miller *et al.*, 2011) and changes in global thermohaline circulation (THC) (Giosan *et al*., 2002; Knutz, 2008; Hernández-Molina *et al.*, 2014). These events also exerted a dramatic influence on Earth's climate state (Zachos *et al*., 2001, 2008), offering some of the most detailed long term evidence of a linkage between eustatic sea level, atmospheric dynamics, oceanic circulation and the volume and extent of ice cover (both continental and marine). Marine sediments record these processes, particularly in bottom circulation processes and associated contourite features (Boulton, 1990; Anderson, 1999; Harris *et al.*, 2001; Barker and Camerlenghi, 2002; Giosan *et al*., 2002; Maldonado *et al.*, 2006, 2014; Rebesco *et al*., 2006; Volpi *et al.*, 2011; Pérez *et al.*, 2014a, 2014b; 2015a,b).

1250 ka and was complete by 700 ka.

Continental margin sedimentation in polar regions is very sensitive to glacial changes. The Pacific Margin of the Antarctic Peninsula (PMAP) is an exceptional location for decoding and reconstructing past climatic changes due to its high subsidence rate and detailed sedimentary record. The West Antarctic Ice Sheet (WAIS) and Antarctic Peninsula Ice Sheet (APIS) have been very sensitive to the aforementioned climate changes with consequences for sea-level (Larter *et al*., 1997; Nitsche *et al.*, 2000; Bart, 2001; Naish *et al.*, 2009). The depositional style changed dramatically when the APIS first reached the shelf break along the PMAP. Although the margin has been studied extensively over the past 30 years, consensus has yet to emerge on the exact timing of major changes (Larter and Barker, 1989, 1991b; Bart and Anderson, 1995; Larter *et al*., 1997; Rebesco *et al*., 1997, 2002, 2006; Barker and Camerlenghi, 2002; Bart *et al*., 2005; Hernández-Molina *et al.*, 2006a).

Grounded ice advance across a continental shelf can generate indicative depositional and erosional features, seismic facies, unconformities, and stratal geometries (Cooper et al., 1991; Dowdeswell and Ó´cofaigh, 2002; Dowdeswell, et al., 2016) and if dated provide the timing of ice advance to the shelf edge, as well as its potential link with global climate dynamics (Larter and Barker, 1989; Bartek *et al*., 1991; Belknapp and Ship, 1991; Cooper *et al*., 1991, 2008; Larter and Cunningham, 1993; Bart *et al.,* 2005, 2007; Larter *et al*., 1997; Barker and Camerlenghi, 2002; Scheuer *et al.*, 2006; Rebesco *et al*., 2006; among others). Ice advances to the shelf are also recorded by changes in the continental slope, rise and abyssal plain, as sediment supply to deep-water environments increases and mass transport deposits (MTDs) deposited along the slope (Rebesco et al., 2006; Volpi *et al.*, 2011), specially in front of the trough, on the trough mouth fans (TMFs, O´Cofaigh et al., 2003; Laberg et al., 2010; Swartz et al., 2015). Polar margins are an ideal setting for the MTDs studies and they can potentially provide a record of when ice sheets reached the shelf edge (e.g. Rebesco and Camerlenghi, 2008; Rebesco et al., 2012; 2014). MTDs have been identified within the stratigraphic record of the East and West Antarctica (e.g., Lindeque et al., 2013, 2016) and Scotia Sea basins (Pérez et al., 2014a, 2014b, 2016), but eluded proper characterization on the Antarctic Peninsula, often being overlooked or misinterpreted as seamounts (Anderson, 1999). This is partly because much work has been done on both the continental shelf and the rise, but few researchers have correlated the two domains (Larter and Barker, 1989; Larter *et al*., 1997; Scheuer *et al.*, 2006; Rebesco *et al.*, 2006; Volpi *et al.*, 2011). Thus, the PMAP has been extensively studied but significant uncertainties persist regarding stratigraphic correlations along and across the margin.

This paper offers a detailed description of PMAP evolution in areas offshore of Adelaide Island (Fig. 1) from bathymetric and seismic stratigraphic analysis. The objectives of this research were to 1) perform an integrated study of the margin by tracing discontinuities, seismic facies and other seismic features across the shelf, slope and rise, 2) identify changes in deposition and evolutionary stages as they may relate to shifts in climate by a novel chronologic constraint, 3) determine when ice sheets first reached the shelf edge and how this affected margin geometry, and finally 4) determine the influence of grounded-ice development on past and present sedimentary processes.

2. GEOLOGICAL SETTING

a. Tectonic framework

The PMAP evolved throughout a complex Mesozoic to Cenozoic tectonic and sedimentary history (Fig. 2). The Antarctic Peninsula has been part of a stable East Antarctic Plate since at least the middle Eocene (Eagles *et al*., 2009). The margin was active from as early as the Early Cretaceous period (Pankhurst, 1990), but later became passive, once subduction ceased along most of the margin, and the Antarctic-Phoenix spreading ridge migrated into the trench (Figs. 2A and B). Subduction of ocean floor generated at this spreading ridge beneath the Antarctic Peninsula southwestward of the Hero Fracture Zone (HFZ) began before 50 Ma, and eventually led to ridge-crest trench (RC-T) collision (Figs. 1 and 2). As an individual ridge-crest segment arrived at the trench, subduction locally ceased and trench basement topography was eliminated (Fig. 2C). Cessation of subduction thus occurred in a diachronous manner, as ridge segments arrived at the trench sequentially from southwest to northeast, and the entire margin southwest of the HFZ became passive (Barker, 1982; Larter and Barker, 1991a). Arrival of Antarctic-Phoenix ridge-crest segments at the trench was followed by rapid uplift of the opposing margin segment. This tectonic activity occurred centered on the mid-shelf high (MSH) and lasted for a 1 to 4 Myr period. Following an interval of a few million years (Fig. 2D), a combination of thermal decay, sediment loading and compaction effects initiated a protracted period of subsidence that continues to the present day (Larter and Barker, 1989; 1991a). MSH uplift appears to have cut off the supply of terrigenous sediment to the slope and deeper domains, and subsequent subsidence of the margin favored the preservation of younger sedimentary units in more distal areas of the shelf (Larter *et al*., 1997). Southeastward projections of oceanic fracture zones (FZs) segregated segments according to their different subduction, uplift and subsidence histories. During the Pliocene, spreading ceased along the last remaining segments of the Antarctic-Phoenix ridge. These segments lay northwest of the HFZ, more than 250 km from the trench. Slow convergence continues today to the northeast of the HFZ, however, along the South Shetland Trench, accommodating extension within the Bransfield Strait marginal basin (Herron and Tucholke, 1976; Larter and Barker, 1991a; Livermore *et al*., 2000; Maldonado *et al.*, 2000; Jabaloy *et al.*, 2003; Galindo-Zaldivar *et al*., 2004).

The study area on this work lies between the Tula and Biscoe Fracture Zones, and is bisected by the Adelaide Fracture Zone (Fig. 1). These fracture zones formed along offsets of the Antarctic-Phoenix ridge, as it migrated towards a former trench along the Antarctic Peninsula margin. The ridge segment between the Tula and Adelaide Fracture Zones reached the trench at 19 ± 0.8 Ma, while the segment between the Adelaide and Biscoe Fracture Zones reached the trench at 16.7 ± 0.7 Ma (Larter *et al*., 1997). As the ridge migrated towards the trench, new ocean floor formed along its northwest flank constituted part of the Antarctic Plate. Following subduction of the ridge crest, features along this flank of the ridge remained stable relative to the Antarctic Peninsula (Barker, 1982; Larter and Barker, 1991a).

b. Stratigraphic and sedimentary framework

The continental shelf and upper slope of the PMAP include a thick Miocene to Quaternary sedimentary section exhibiting progradational and aggradational stacking patterns (Fig. SM-I in the supplementary material). In regional studies of this section, Larter and Barker (1989) and Larter *et al*. (1997) identified four major seismic units (S4 to S1) along the northeastern part of the margin . The oldest of these units (S4) formed prior to a series of ridge-trench collision. Reflections associated with the S4 unit dip steeply seaward while S4’s upper surface represents the first major regional unconformity for the margin. This remarkable truncation surface is referred to as the “uplift unconformity*”* (UU; used here) (Larter *et al*., 1997) or “collision unconformity*”* (CU) (Bart and Anderson, 1995). The UU formed due to uplift associated with the arrival of the ridge-crest segment at the margin (Fig. 2C), and therefore varies in terms of its chronostratigraphic position along the margin. The S3 to S1 units were deposited as a passive margin sedimentary wedge (Larter *et al.*, 1997). A second major regional unconformity marks the S3/S2 boundary. This surface was originally defined as the "base of glacial-margin sequences" (BGMS), and interpreted as marking the onset of extensive and synchronized advance of grounded ice to the shelf edge during the late Miocene (Larter *et al.*, 1997; Scheuer *et al.*, 2006),The S3 unit developed between the UU and BGMS unconformities.

Medium to high-resolution seismic studies by Bart and Anderson (1995, 1996) and Bart *et al. (*2005, 2007) on the post-collision wedges of the outer shelves revealed in more detail, three seismic stratal packages (1 to 3 from youngest to oldest). These were differentiated according to internal geometry and together contain 31 glacial erosion surfaces (Fig. SM-I). Bart and Anderson (1995, 1996) used robust evidence of glacial erosion and deposition appearing in the upper part of Package 3 to propose a model in which the ice sheet advanced onto the outer shelf during the middle Miocene. Bart *et al*. (2005) proposed at least 12 different episodes of grounded ice advance to the shelf edge occurring from 5.12 and 7.94 Ma. At the time, however, these age estimates were unconstrained by drilling. Ocean Drilling Program (ODP) Leg 178 (Fig. 1) results subsequently showed that they were actually late Miocene, as Larter and Barker (1989, 1991b) had determined from careful correlation to sequences overlying Miocene oceanic basement on the continental rise. The lower bound of the above age range given by Bart *et al.* (2005), which the authors based on biostratigraphic constraints from ODP Leg 178, Site 1097 (Fig. 1 and SM-I), slightly predates the age inferred for the BGMS by Larter *et al*. (1997) and Scheuer *et al.* (2006).

The continental rise also hosts a thick succession of clastic sediments that have been extensively studied using Deep Sea Drilling Project (DSDP) Leg 35, Site 325 data, multichannel seismic reflection profiles and data from ODP Leg 178, Sites 1095-1103 (Fig. 1). The upper continental rise contains several large sedimentary mounds (Fig. 1), separated from the base of the slope and from each other by turbidite channels (Tucholke and Houtz, 1976; Rebesco *et al*., 1996; 1997; Pudsey and Camerlenghi, 1998; Pudsey, 2000; Lucchi *et al*., 2002; Lucchi and Rebesco, 2007; Uenzelmann-Neben, 2006). The sedimentary mounds have been interpreted as mixed contourite drifts, constructed primarily of fine-grained input from turbidity currents entrained within the nepheloid layer of ambient, along-slope bottom water flows (Rebesco *et al*., 1996, 1997, 2002). McGinnis and Hayes (1995) and McGinnis *et al. (*1997) alternatively stressed the importance of downslope turbidity currents in the formation of these mounds, interpreting them as channel levees modified by bottom currents. Rebesco *et al*. (1996, 1997, 2002) used regional seismic stratigraphic analysis to identify six depositional sequences within the continental rise and three major stages of sedimentation. These include (1) a pre-drift stage (sequences M6 and M5; 36-15 Ma), (2) a drift-growth stage (sequences M4 and M3; 15-5.3 Ma) and (3) a drift-maintenance stage (sequences M2 and M1; 5.3 Ma to the present) (Fig. SM-I). These authors observed that the upper three units (M3 – M1) consisted primarily of glacially-derived sediments, and thus assigned them late Miocene to Pleistocene ages based on correlation with DSDP Leg 35, Site 325 results (Rebesco *et al*., 1997). These age interpretations were subsequently confirmed by results from ODP Leg 178, Sites 1095 and 1096 (Barker and Camerlenghi, 2002). The main regional drift-growth stage (sequences M4 and M3) included a high proportion of terrigenous material from the glaciated continent, with large volumes of sediment transported down-slope by turbidity currents. These turbiditic currents arose from numerous minor debris flows along the slope (Larter and Cunningham, 1993; Vanneste and Larter, 1995; Volpi *et al.*, 2011), being the fine-grained component of these currents redistributed along the rise by southwest-flowing bottom currents (Rebesco *et al*., 1996, 1997, 2002; Amblas *et al*., 2006).

3. OCEANOGRAPHIC SETTING

The PMAP and the adjacent Drake Passage and Scotia Sea (Fig. 3) are areas of active surface to deep water-mass circulation (Whitworth *et al.*, 1994; Orsi *et al.*, 1999, Naveira Garabato *et al.*, 2002a, b, 2003; Hernández-Molina *et al.*, 2006; Hillenbrand *et al.* 2008; Carter *et al.*, 2009; Tarakanov, 2009, 2012; Morozov *et al.*, 2010; Palmer *et al.*, 2012; Meredith *et al.*, 2001, 2013). The Antarctic Circumpolar Current (ACC) flows eastward around the Antarctic continent, driven by eastward wind stress that generates velocities of 20-60 cm/s at the surface and 7-12 cm/s near the sea floor (Orsi *et al.*, 1995; Carter *et al.*, 2009). The ACC comprises bottom-reaching fronts —namely, from north to south: the Subantarctic Front (SAF), the Polar Front (PF), the Southern Antarctic Circumpolar Current Front (SACCF), and the Southern Boundary (SB) of the ACC. Ocean depth profiles have revealed that these fronts are not vertical, but rather dip to the north (Naveira Garabato *et al*., 2002a,b; 2003). South of the SB and extending eastward from the northern tip of the Antarctic Peninsula lies the Weddell Scotia Confluence (WSC), where dense shelf waters enter a band of eastward flow.

The deep-water masses of the Southern Ocean consist of two distinct components, the voluminous Circumpolar Deep Water (CDW) and the Antarctic Bottom Water (AABW), which flows locally beneath it (Fig. 3). The CDW flows primarily towards the east with the ACC, and is internally sub-divided into Upper Circumpolar Deep Water (UCDW) and Lower Circumpolar Deep Water (LCDW). Along the PMAP, the CDW is located below surface water masses, the Antarctic surface water (AASW) and the Winter Water (WW) (Nowlin and Zenk, 1988; Patterson and Whithworth, 1990). Near the study area, the CDW flows northeastward between approximate water depths of 0.5 to 3 km (Sievers and Nowlin, 1984, Whitworth and Nowlin, 1987, Whitworth *et al.*, 1998). The AABW is the deepest water mass generated by brine rejection on the continental shelf and by cooling of different water masses beneath floating ice shelves, primarily in the Weddell Sea (~50% of the total AABW production) (Foldvik *et al.*, 2004; Tarakanov, 2009, 2012; Morozov *et al.*, 2010; Steig and Orsi, 2013). A A branch of the AABW (the Weddell Sea Deep Water, WSDW) spills over the South Scotia Ridge and spreads westward through the Drake Passage (Orsi *et al.*, 1999; Naveira-Garabato *et al.*, 2002; Tarakanov, 2009, 2012; Morozov *et al.*, 2010; Palmer *et al.*, 2012). This branch reaches the

Drake Passage between the SACCF and the SB (Fig. 3). After passing the HFZ, it mixes with the overlying LCDW. A branch of the LCDW derived from water that has circulated within the Weddell Gyre (WDW) also flows along the slope of the South Shetland Trench's southern flank, above the WSDW. This water mass continues southwestward along the Antarctic Peninsula Pacific Margin (Fig. 3). Evidence for westward flow over the Pacific margin of Antarctica has been found as far as 120° W, in the Amundsen Sea (Giorgetti *et al*., 2003). Along the margin offshore of the Antarctic Peninsula, the LCDW branch from the Weddell Sea flows at an approximate water depth of 3.5 km (Giogetti *et al*., 2003; Hernández-Molina *et al*., 2006b; Hillenbrand *et al*., 2008) and follows contours around large drifts (Fig. 3) located along central and upper areas of the rise. This LCDW branch has been verified by direct current meter measurements, which have recorded mean current speeds of ~6 cm/s, maximum speeds of < 20 cm/s and potential temperatures of 0.11-0.13 °C at water depths of 3475-3338 m (Camerlenghi *et al*., 1997; Giorgetti *et al*., 2003). Physical properties of the water mass, short-term current measurements and sedimentary wave migration patterns indicated the presence of this southwestward-flowing bottom current before detailed current meter data were collected (Tucholke and Houtz, 1976). A water mass with a potential density of 28.27 kg/m^3 at water depths below 4 km has also been identified in the region, and likely represents the AABW flowing along a primarily north-eastwards path (Orsi *et al.*, 1995).

Three tectonic events were pre-requisites to the development of this modern oceanographic circulation pattern. These include the establishment of a deep-water pathway through the Drake Passage once the Scotia Sea began to develop (Livermore *et al*., 1994; Barker, 2001; Lawver and Gahagan, 2003; Maldonado *et al.*, 2003, 2005, 2014), the opening of gaps between the eastern continental arc fragments in the Scotia Sea (Barker, 2001; Maldonado *et al.*, 2014), which enabled the ACC to develop to the full extent of its current depth, and the opening of gaps along the South Scotia Ridge (Maldonado *et al.* 2006, 2014; Pérez *et al*., 2014a, b, 2015a,b), which enabled WSDW to flow first from the Weddell Gyre into the Scotia Sea, and then westwards. Along the PMAP rise, active northeasterly flowing bottom currents influenced the margin during the early Miocene (Hernández-Molina *et al*., 2006b). Middle Miocene deposits record the initial incursions of the WSDW into the Scotia Sea (Maldonado *et al.,* 2003, 2006) and evidence for southwesterly flow of the LCDW branch from the Weddell Sea along the PMAP (Hernández-Molina *et al*., 2006b). Since the Mid-Miocene to Quaternary period the ACC and AABW circulation developed fully (Maldonado *et al.*, 2006, 2014; Uenzelmann-Neben and Gohl, 2012; Pérez *et al.*, 2014a, b, 2015a,b; Lindeque et al., 2016; Uenzelmann-Neben et al., 2016).

4. METHODS AND DATASETS

We analyzed multibeam echosounder and seismic data, especially multichannel seismic (MCS) refection profiles, collected by several international research projects. This study specifically interprets MCS profiles from the Spanish

ANTPAC 1997/1998 Project along with data provided by the British Antarctic Survey (BAS). The Italian Instituto Nazionale di Oceanografía e di Geofisica Sperimentale (OGS), the Brazilian Antarctic Program, and Rice University (Texas, USA) also provided data used to assess morphology and stratigraphic correlation of seismic units and discontinuities within the study area (Scientific Committee on Antarctic Research Seismic Data Library System, Cooper *et al.*, 1991, SCAR, 2001; Wardell et al., 2007). Figure 4 shows the network of seismic profiles compiled for the study area, which has the densest bathymetric and seismic coverage of any region along the PMAP. We also used stratigraphic and chronological records from ODP Leg 178, Sites 1095-1103 (Barker *et al*., 1999) and DSDP Leg 35, Site 325 (Hollister *et al.*, 1976) (Fig. 1). Correlation of seismic units and discontinuities among sites helped to constrain the timing of specific depositional processes and to establish a chronology for the development of the continental margin. We evaluated chronologic constraints for the seismic units and discontinuities by correlating them with features found in regional seismic datasets, and by using previously established chronostratigraphic interpretations for the shelf (Larter and Barker, 1991b; Larter and Cunnigham, 1993; Bart and Anderson, 1995; Bart *et al.*, 2005) and rise (Rebesco *et al.*, 1996, 1997, 2002; McGinnis and Hayes, 1995; McGinnis *et al*., 1997; Barker *et al.*, 1999; Barker and Camerlenghi, 2002). The age of the oceanic crust, as inferred from marine magnetic anomalies (Larter and Barker, 1991a), was used to constrain the age of basal sediments along the rise. Magnetic anomaly ages were interpreted according to the magnetic reversal timescale of Cande and Kent (1995) and thus differ slightly from those given in Larter and Barker (1991a) which were based on the earlier magnetic reversal time scale of LaBrecque et al. (1977).

ANTPAC 1997/1998 (Spanish) seismic data were obtained during a 1997/98 austral summer research cruise aboard the B/O *Hespérides* (Fig. 4). The BAS collected MCS data aboard RRS *Discovery's* cruise 172 during the 1987/1988 austral summer. The OGS collected MCS data on several cruises aboard the RV *OGS-Explora* during the 1989/90, 1991/92, 1994/95 and 1996/97 austral summers. The Brazilian Antarctic Program collected MCS data on research cruises of the RV *Almirante Câmara*, during the 1986/87 and 1987/88 austral summers. MCS data were processed independently by research groups working in the respective national Antarctic programme with a standard sequence.

In addition to MCS profiles, we also obtained and analyzed higher resolution single-channel seismic profiles. High frequency data collected with the nearest hydrophone group to the vessel deployed on the ANTPAC 1997/1998 cruise were digitized and processed using the Geoacoustic SES-4 system. This contribution provided higher resolution imaging of seismic units, thus clarifying shelf stratigraphy. We also analyzed single-channel seismic data collected by Rice University aboard the RV *Polar Duke* during the 1987/1988 austral summer (Anderson *et al*., 1990; Bart and Anderson, 1995; 1996; Bart *et al.*, 2005). These data were acquired with a seismic source consisting of either one or two waterguns discharged at volumes of 1.6 l. Shots were fired at intervals of 8 s and ship speeds 13-15 km/h, resulting in an approximate 30 m shot spacing.

Seismic data interpretation included five steps. First, seismic units and sedimentary environments were identified by studying seismic facies. Secondly, seismic stratigraphic analysis was conducted according to standard practices established over the past three decades, tracing seismic units and discontinuities from shelf localities across the slope to the rise (thickness of units is measured in s or ms two-way travel time, twt). Third, the 3D shape, orientation and seismic facies of units were used to distinguish between down- and along-slope sedimentary processes. Fourth, major stratigraphic boundaries were identified by correlating features in seismic profiles with those recorded in ODP Leg 178 and DSDP Leg 35 data. Lastly, we correlated seismic units and discontinuities with features observed in data previously described by other groups, and then interpreted these units and horizons in terms of regional and global climatic and palaeoceanographic changes. Figures 5 and SM-I (supplementary material) show a composite regional stratigraphic interpretation of the continental margin, summarizing the results of a shelf-to-rise correlation, along with the main morphological domains, stratigraphic discontinuities, seismic facies, seismic units and evolutionary intervals. Figure SM-II shows a 3-D stratigraphic diagram indicating the major spatial differences between the northern, central and southern sectors of the margin.

The morphological study used the aforementioned seismic records as well as bathymetric data collected (using a SIMRAD EM12 multibeam echo-sounder system) aboard the B/O *Hespérides* during the ANTPAC 1997/1998 cruise. Data were post-processed with Simrad Neptune software and visualized with FLEDERMAUS software. We also considered bathymetric data compiled by the GLOBEC project (*Digital Bathymetry for the Southern Ocean*, http://msg.whoi.edu/GLOBEC/AGU_2002.html; Bolmer, 2008) as well as multibeam echo sounder data published by Dowdeswell *et al*. (2004). Lastly, we analyzed multibeam echo sounding data imaging the central continental rise collected aboard the RRS *James Clark Ross* during a Jan-Feb 2004 cruise (JR104) using a Kongsberg Simrad EM120 system.

The term 'contourite' refers to sediments deposited or substantially reworked by the persistent action of bottom currents (e.g., Stow *et al.*, 2002; Rebesco, 2005; Rebesco and Camerlenghi, 2008). Contourites include a wide array of sediments affected to varying degrees by different types of currents (Rebesco *et al.*, 2014). Contourite drifts or simply, drifts, refer to thick, extensive contourite accumulations. For the present work, we adopted the classification of Faugères *et al.*, (1999) and its updated version (Faugères and Stow, 2008).

5. MARGIN MORPHOLOGICAL CHARACTERISTICS

Based on gross morphology, we differentiated the following major physiographic domains: shelf, slope and rise. Each of these consists of southern, central and northern sectors (Figs. 1, 6 and SM-III). The southern sector of the rise refers to the northeast portion of the oceanic crust segment between the Tula and Adelaide FZs. The central and northern sectors refer to the oceanic crust segment between the Adelaide and Biscoe FZs, according the interpretation of fracture zones by Larter *et al*. (1997). The Adelaide FZ trends in a northwest direction along the southwest flanks of Drift 5 (Figs. 1 and 6).

The continental shelf is ~140 km wide and can be divided into inner, middle and outer areas (Fig. 6). The Marguerite Glacial Trough runs obliquely across the shelf in an approximately north-south direction. The Marguerite Trough is ~50 km across on the inner shelf and reaches 70 km width on the outer shelf. The trough extends to depths of up to ~150 m (from its axis to neighboring banks) in the southeastern corner of the study area. The trough incises more than 1 km into the inner shelf, where it reaches maximum water depths of about 1600 m (Rebesco *et al*., 1998; Graham *et al.*, 2011), and then grades into a more subtle depression with only ~70-50 m relief on the outer shelf. Its widespread and U-shaped morphology reflects ice stream influence and is characterized on the outer shelf by an asymmetric northeast boundary that it is steeper than its southwest boundary. Seafloor morphology within the trough includes drumlins and minor lineations along the inner and middle shelves, as well as Megascale Glacial Lineations (MSGL) on the outer shelf (Fig. 6), as previously identified by Ó Cofaigh *et al*. (2002, 2005) and Livingstone *et al.* (2013, 2016).

The inner shelf consists of basement outcrop and glacially-scoured seafloor incised by small troughs and other features that suggest erosion. A few recent sedimentary bodies appear in the central and northern sectors of the inner shelf (Fig. 6). The middle shelf consists of two sub-domains strongly influenced by erosive processes, the Mid-Shelf Basin (MSB) and Mid-Shelf High (MSH) (Fig. 6). The MSB is an eroded sedimentary remnant of an asymmetric, synclinal structure, which represents a relict, 24 km wide, NE-SW trending forearc basin. The MSB ranges from 300 to 500 m water depth. Fractures trending in a northwest direction bisect the MSB, bound a morphologic high in the central sector (Fig. 6) and also form the northeastern boundary of the Marguerite Trough. The MSH is a NE-SW trending elongated structural high exhibiting distinctive characteristics in the southern and northern sectors of the study area (Fig. 6). In the northern sector, the MSH forms the present seafloor as a bathymetric shelf high with locally thin sediment cover. In the southern sector however, young sedimentary cover has buried the MSH. The boundary between the two MSH sectors coincides with the southern boundary of the aforementioned morphologic high in the MSB's central sector. The boundary therefore represents a northwest trending structural lineation referred to here as the Adelaide shelf structural lineation (ASL) (Fig. 6).

The major features on the outer shelf include troughs and highs (or banks), the latter of which developed primarily due to depositional processes. The outer shelf reaches about ~52 km width and exhibits an average landward gradient of 0.08°, becoming gradually shallower towards a sharp shelf break (Fig. 6). Banks along the northern (Bank-3, the Matha Bank) and southern (Bank-4, the Adriasola Bank) sectors of the outer shelf overlie or fall just landward of progradational Lobes 3 and 4 (defined by Larter *et al*., 1997). The Marguerite Trough, located in the central sector, separates these banks. Study area images also show a minor secondary glacial trough in northerly areas of the Matha Bank, referred to here as the Matha Trough. Amblas *et al*. (2006) referred to this feature as the T8 trough and identified a similar feature, referred to as the T7 trough in an area northeast of the Matha Bank.

The shelf edge resides at an average depth of ~488 m (Fig. 6) and exhibits a pronounced, sinuous morphology (in plan view) that includes concave and convex zones (relative to deeper areas of the ocean). Convex areas occur in front of major banks and concave areas occur in front of troughs. These patterns are consistent except along northern part of the Adriasola Bank where the shelf edge does not show any evidence of convex (seaward) trends.

The continental slope exhibits a steeper gradient (10.1° on average) relative to the global average slope (3°, Kennett, 1982). It lacks submarine canyons and can be divided into upper, middle and lower slope domains (Fig. 6). The upper slope is an erosive surface, with an average gradient of 7.6°, and occurs between water depths of 488 and 1135 m. This area exhibits numerous gullies incising into underlying deposits, frequent internal erosive surfaces and chaotic seismic facies (Figs. 6 and 7). As previously reported by Noormets *et al.* (2009), the upper slope seaward of the Marguerite Trough consists of a more gradual surface with fewer gullies (Figs. 6 and 7). Here, a trough mouth fan is not fully developed. The middle slope, between water depths of 1135 and 2170 m, forms a convex surface and exhibits the steepest observed gradients (16.8° on average). Extending to 3.7 km width, this area is incised by gullies and overlies deposits that display high acoustic response and poor internal organization in seismic profiles (Fig. 7). The narrowest sections of the middle slope occur in the central sector seaward of the Marguerite Trough, with a minimum gradient of 13° and has fewer gullies, coinciding with the area where the upper slope is more gradual. The lower slope exhibits an average gradient of 5.3°, a 9.3 km width and water depths between 2170 and 3045 m. Its smooth and concave form overlies deposits with well-organized seismic facies. Locally, high amplitude reflections appear in basal areas of the slope indicating the occurrence of small channels (Fig. 7). In the central sector seaward of the Marguerite Trough, the lower slope exhibits a lower gradient (3°) and more small channels (Fig. 7). We identified large, buried debris flow deposits within lower slope areas of the southern sector, mapping these features between Drifts 5 and 5A, off the northern part of the Adriasola Bank (Fig. 6). Several relict mounded drifts occur along lower slope areas of the central sector, seaward of the Marguerite Trough. These drifts are unevenly distributed and highly eroded. The largest example is adjacent to the northern boundary of the trough.

The continental rise begins at water depths of ~3045 m and includes both depositional and erosional morphological features (Fig. 6). These consist of mounded asymmetric contourite drifts and large turbidite canyon-channel systems (CCSs). Seismic and bathymetric images show four major drifts, referred to as Drifts 4A, 4B, 5 and 5A, as well as four CCSs referred to as the Biscoe, Lavoisier, Adelaide and North Tula systems, following Rebesco *et al*. (2002). In the northern sector, areas seaward of shelf Bank-3 primarily include depositional features, where Drifts 4A and 4B developed between the Biscoe and Lavoisier, and the Lavoisier and Adelaide CCSs, respectively (Fig. 6). The central sector seaward of the Marguerite Trough includes extensive erosional features but the upper slope exhibits a gentler gradient and has fewer gullies around the Adelaide Channel. The southern sector of the rise between Drifts 5 and 5A also includes an extensive erosional zone seaward of the northern part of the Adriasola Bank and related to the North Tula CCS. The location of this second erosional zone is unusual given that large mounds typically develop off the region's shelf banks, as reported by Amblas *et al.* (2006).

Mounded drifts show elongation in a direction roughly orthogonal to the dominant trend of the margin (Fig. 6). The most elongate drift (Drift 5) extends 120 km in length, ~70 km in width and reaches an elevation of nearly 1 km above the bounding channel floor. The drift exhibits a generally asymmetric external shape characterized by a relatively steep and rough southwest side (2°) contrasted by a gently-dipping and smooth northeast side (0.8°). On the proximal part of the drift, the two sides meet to form a long narrow ridge that connects the drift to the continental slope. Drift summits exhibit a general NW trend and extend to average depths of 2900-3000 m, with the exception of Drift 5, on which the shallowest part of the drift crests rises to shallower than 2600 m water depth. The drift crest axes connect with the nearby areas of the lower slope, except for Drifts 4A and 5, whose crests intersect the middle slope (Fig. 6). V-shaped gullies occur along the steep sides of the drifts, exhibiting average widths of 1 km and depths of less than 100 m. These gullies trend in an E-W direction, oblique to the main crest of the drifts. The floor of the large CCSs trend in a NW to NNW direction (Fig. 6), reach widths of up to 4 km and arise from networks of tributary channels at the foot of the continental slope at average water depths between 2900 and 3200 m.

6. STRATIGRAPHIC ANALYSIS

Nine seismic units (SU) bounded by regional discontinuities (VIII to I) have been recognized over the acoustic basement (Fig. 5 and SM-I). On the shelf, the Mid-Shelf High (MSH) represents the acoustic basement. The underlying reflections above the MSH dip seaward beneath the outer shelf until they disappear into seafloor multiple reflections. The basement exhibits remarkably high amplitude and irregular reflections for its upper material and a distinctive transparent seismic facies below this. On the rise, the igneous basement of oceanic Layer 2 occurs below the sedimentary succession at an average depth of 6 s (twt). Layer 2 in this region forms a more consistently smooth surface than that of oceanic igneous basement elsewhere, but also appears fractured by small-scale faults, evident from reflections and closely-spaced diffraction hyperbolae in unmigrated MCS profiles.

The oldest seismic unit on the shelf and slope (SU9) does not correlate (seismically) to the oldest unit on the rise, but the remaining units (SU8-SU1) can be regionally traced along the entire margin (Figs. 8 to 12). The oldest units (SU9-SU5) appear most clearly in areas beneath the central sector of the shelf and slope. Prior to SU3 deposition, this sector experienced less subsidence than southern and northern sectors below the Adriasola and Matha Banks (Figs. 5, SM-II). Three major intervals of evolution (I-III) have been determined and described below based on the stratigraphic stacking pattern of seismic units (Fig. 5, SM-I and SM-II). Seismic facies are summarized in Table-I and sedimentary thickness of each unit is included in the Table-II.

6.1. *Interval-I*

This interval consisted of three minor stages.

a) Stage I.1

Seismic unit SU9 records initial deposition along the shelf and slope, and is particularly apparent along the outer shelf of the margin's central sector (Table-I and II). This unit overlies shelf basement, tilting seaward and pinching out against basement of the MSG in a landward direction (Figs. 10A and C). SU9 reflections tilt seaward and then are truncated by an overlying unconformity, which corresponds with a prominent, seaward-dipping erosional surface (Fig. 5). Towards the slope, this unit is deeply folded and fractured. Along the rise, SU9 directly overlies basement and occurs near a relict seamount (Figs. 5 and 9). It is located within the depression in the top of the basement below a Fossil Mounded Sedimentary Body (MB) defined by Hernández-Molina *et al.* (2006b).

b) Stage I.2

SU7 and SU8 record the second stage, whose expression varies at different shelf, slope and rise localities (Figs. 5, Table-I and II). These units developed as sheeted deposits covering the outer shelf and slope, where they appear clearly in the central sector (Fig. 10). Both units pinch out landward in this sector, but tilt in a seaward direction from the MSH. SU7 and SU8 appear on the slope but are truncated by a more recent significant erosional surface as they approach the Marguerite Trough (Fig. 10D). Emplacement of the MSH appears to have strongly affected SU9, SU8 and SU7 expression on the outer shelf. A channel cut and fill appears in the central sector, associated with SU8's upper surface. This base of the channel erodes into SU9 and consists of aggradational fill evident as concave-up reflections (Fig. 10B). The discontinuities and internal reflections for both units dip in a seaward direction. The palaeo-shelf edges associated with the upper boundaries of these two units exhibit a smooth, convex-up shelf break (Fig. 5 and 10). SU7 and SU8 generally outlines folded and faulted strata along the middle and lower slope (Figs. 5 and 10). At the base of the slope, both units consist of similar deposits exhibiting irregular to semi-chaotic seismic features represented by an amalgam of high amplitude reflections (Figs. 5, 10 to 12). On the rise, SU7 and SU8 represent a progradational mega-wedge deposited above the oceanic basement, which thickens towards the margins (Figs. 5, Table-II). SU8 pinches out seaward along the central rise. A wavy seismic facies appears locally within SU7.

The AISM13 seismic profile shows a certain degree of along-slope spatial variation between SU7 and SU8 at the transition between the lower slope and upper rise (Fig. 12). This part of the profile shows two buried structural highs. The first appears to relate to the Adelaide FZ in the southern sector. In this area, the high has deformed the SU8. SU7 partially buries the high by onlap onto SU8's upper surface (Fig. 12B). The second high appears within the Adelaide/Biscoe oceanic segment between the central and northern sectors in the studied area and thus does not relate to any previously defined fracture zone (Fig. 12). This high has affected SU8, SU7 and SU6, but SU5 onlaps onto it and the youngest part of SU5 continues over the high (Fig. 12E). Both SU7 and SU8 exhibit greater thicknesses within a large depression between these two highs (Fig. 12), relative to adjacent areas. In contrast, the central sector of the outer shelf appears to have occupied a relatively high position, persisting through deposition of SU9, SU8 and SU7, until SU5-SU4 deposition. Both SU7 and SU8 are tilted, deformed and truncated by the base of SU6, beneath the outer shelf (Fig. 5).

c) Stage I.3

The third stage of the non-glacial margin interval, recorded by SU6, represents a major change in margin deposition. Relative to the other units, deposits form more consistent sheets and are less obviously affected by MSH emplacement along the shelf. SU6 displays an aggradational stacking pattern with reflections onlapping in a landward direction onto SU7's upper surface (Figs. 5, Table-I). Along the outer shelf, the unit progrades seaward at a very low angle (Fig. 5). Although well defined in all sectors, SU6 pinches out towards the inner part of the outer shelf in the northern and the southern sectors. Its upper surface is a locally erosional discontinuity. Along the slope, SU6 thins and disappears just in front of the Marguerite Trough, due to erosional truncation (Fig. 10).. Some reflections show good lateral continuity and locally include seismic facies that we interpret as small contourite deposits and sediment waves (Figs. 5).

6.2. *Interval-II*

This interval was recorded by SU5, which exhibits a clearly tabular shape and aggradational stacking pattern along the shelf (Figs. 5, 8, SM-I and SM-II). SU5 shows a back-stepping configuration relative to SU6 and landward onlap onto its basal discontinuity. Along the outer shelf, it shows clear, narrowly focused seaward progradation. In the central sector, SU5 is well defined, but thins out toward the northern and the southern sectors (Table-I and II), where the unit is eroded by SU4's basal unconformity, especially towards the northeast, below the shelf Lobe-3. The unit pinches out along the inner parts of the outer shelf. (Figs. 10). We interpret a few glacially related features within SU5, where it occurs along the middle shelf and the proximal areas of the outer shelf. These include small troughs and erosional surfaces that dip in a landward direction (Figs. 10 and 13). The upper boundary represents a prominent erosional unconformity affecting the entire outer shelf.

SU5 thins along the slope and disappears just seaward of the Marguerite Trough due to erosional truncation (Fig. 10D, Table-II). In the transition between the lower slope and upper rise, SU5 only appears in the northern sector, where it contains minor subunits with mounded and lens shaped deposits and chaotic seismic facies (Table-I).. On a regional basis, SU5 occurs throughout the continental rise (Figs. 5 and 8), with variable thickness (Table-II). Although it clearly appears on the upper rise near the slope, it disappears in local areas of the central and upper rise, due to truncation by SU4's basal unconformity (Figs. 8, 10, and 11).

6.3. *Interval-III*

Four seismic units SU4, SU3, SU2 and SU1 comprise this last major interval. Based on stratigraphic stacking patterns, these units are divided into three stages of margin evolution (Figs. 5, SM-I and SM-II): a transitional stage, a progradational stage and an aggradational stage.

a) Stage III.1: Transitional stage

SU4 appears over middle and distal areas of the outer shelf, shelf edge and slope, but pinches out landward (Fig. 5) . It does not appear along the upper slope, just seaward of the Marguerite Trough, due to incision by a major erosional unconformity (Fig. 10). SU4 also does not appear within the transition between the lower slope and rise of the southern and central sectors, but it does appear in these areas of the northern sector (Table-II).

Within the shelf and slope, SU4 exhibits greater thicknesses in the southern sector than in the northern sector (Table-II). Its basal and upper surfaces are both erosional unconformities (Figs. 8, 10, 11 and 12). Its upper boundary represents a major erosional surface, which as described above, incises SU4, SU5, SU6 and SU7 in the central sector (Fig. 10C). In the southern and northern sectors however, the erosional surface only incises SU4. SU4 assumes a wedge shape with a general sigmoid-oblique configuration and varied seismic facies (Table-I). SU4 is the first high-angle progradational unit on the upper slope of the shelf break (Figs. 5 and 10C) and exhibits some internal reflections and a clear, landward dipping, upper discontinuity surface along the outer shelf. SU4 therefore records another important change in the stacking pattern of the margin..

We interpreted several large, irregular, lens-shaped deposits with chaotic, transparent seismic facies (Table-I), as debris flows. These occur at the toe of the lower slope, in association with the SU4's upper boundary (Figs. 5, 8, 10 and 11). Locally, these deposits outcrop at the sea floor (Fig. 10D), constituting some of the relict and partially buried mass-transport deposits mapped in the lower slope of the southern sector, that acoustically mask the seismic returns from units below them.

The contrasting thickness of SU4, as it occurs in the upper rise (well developed) and in areas between the upper rise and lower slope (thin or absent from a wide, smooth depression), indicates that this unit also represents an important depositional change along the rise (Figs. 5). Its basal boundary represents a regional erosional surface (Figs. 8E and 9). SU4 is relatively thick in the rise (Table-II) and some mound shaped deposits and sediment wave facies appear locally, especially near obstacles along the central rise (Figs. 5 to 9).

b) Stage III.2: Progradational margin stage

SU3 and SU2 record the progradational margin stage. These units exhibit a very small landward dip along the outer shelf and are bounded by discontinuities on both the outer shelf and slope (Figs. 5, SM-I and SM-II). Seismic profiles indicate massive (transparent, no features observable in reflections) units along the outer shelf (Fig. 8B), but some material beneath the shelf break and slope thickens in a progradational pattern. The lateral expression of SU2 and SU3 mimics that of the modern physiographic domains (Table-II), with shifts in facies across the upper and middle slope (Fig. 7, Table-I). Along the upper slope, chaotic facies appear with frequent internal erosion surfaces, and then transition at the middle slope into poorly organized facies, with high acoustic response and highly irregular reflections. Towards the lower slope, more uniform facies with a transparent-to-weak acoustic response include occasional higher amplitude reflections with concave patterns that indicate minor palaeochannels.

SU3 comprises three wedge-shaped progradational subunits (Subunits a, b and c) (Figs. 5). The youngest one, Subunit a, represents the most important progradational stage along the margin (Figs. 8, 10 and 11). Subunit c exhibits a sigmoid-oblique configuration, Subunit b, an oblique-tangential configuration, and Subunit a, an oblique-parallel configuration. SU2 includes both progradational and aggradational reflection patterns, indicating that it marks another shift in margin development (Fig. 5). It comprises Subunits a and b, the younger of which (Subunit a) extends further landward.

Along the rise, SU3 and SU2 comprise a thin sedimentary wedge that thickens in a landward direction (Figs. 5, 8, 10 11 and Table-II). A major stratigraphic change along the rise occurs above SU3's Subunit c, which consists of an elongate, mounded deposit that runs parallel to the slope. In contrast, Subunits a and b formed deposits with a transverse orientation relative to the margin. These subunits also prograde seaward at a low-angle and their depocenters formed closer to the slope than those of Subunit c (Fig. 5). The upper boundary of SU3 is a truncation surface that correlates with the erosion surface between SU3 and SU2 along the outer shelf and slope, and therefore marks the cessation of major progradation along the margin. Along the rise, SU2 constitutes a thin aggradational deposit (Table.-II), especially in the southern sector (Figs. 8, 11 and 12).

c) Stage III.3: Aggradational margin stage

SU1 records the aggradational margin stage. Its base represents a significant shift in the margin's depositional style and geometry. SU1 occurs as a thick sedimentary wedge that covered the shelf and slope (Figs. 5, SM-I and SM-II).

Along the shelf, the unit consists of thin deposits (Figs. 8, 10, 11 and Table-I, II). For the outer shelf and upper slope, we identified four subunits (a, b, c and d) within SU1's sedimentary lobes, which are separated by minor discontinuities with high amplitude reflections (Fig. 13). SU1 is thinner over drifts and mounds along the rise, especially in the southern sector (Table-II). The unit disappears laterally around turbidite channels where erosional processes efficiently remove material (Figs. 8, 10 and 11).

6.4. Marguerite Trough occurrence and lateral migration

SU4's upper surface as it occurs in the southern sector beneath present-day Lobe-4 (Figs. 13 and SM-II) marks the earliest development of the Marguerite Trough axis. Variations in the lateral and vertical position of the axe of the trough and its boundaries for each unit and sub-unit are identified based on the seismic lines. SU3 records the trough's migration from this original position, in alignment with the present North Tula CCS (southeastern part of the oceanic Tula-Adelaide segment) at the Adriasola Bank. Sediments spanning from SU3's upper surface to the upper surface of SU2's Subunit b specifically record the trough's northeast, stepwise, lateral migration towards its present position (*i.e.*, landward of the Adelaide CCS, which overlies the southeastern portion of the Biscoe-Adelaide segment). The Marguerite Trough axis did not reach its present-day position however until a time equivalent to the upper surface of SU2 Subunit a (Fig. 13). We have identified three respective events in the upper surfaces of Subunits 3a, 2b and 2a that represent temporal steps in the northeast migration of the Marguerite Trough.

7. DISCUSSION

Due to their implications for PMAP evolution, three major aspects of the morphological and stratigraphic analysis deserve further consideration. These include (1) growth patterns of the margin and their tectonic implications, (2) the influence of glacial evolution on morphosedimentary features and (3) mixed drift formation.

7.1. Stratigraphic model: chronology and tectonic implications

We identified several shifts in margin depositional patterns apparently influenced by Cenozoic tectonics and environmental changes. Figure SM-I shows chronological constraints for the identified seismic units described above and their discontinuities. Constraints were inferred from correlation with a) IODP Leg 178 (sites 1095-1103) and DSDP Leg 35 (site 325) results, b) previously defined continental shelf units (Larter and Barker, 1991b; Larter *et al.*, 1997; Bart and Anderson, 1995; Barker *et al.*, 1999; Jabaloy *et al.*, 2003 Bart *et al.*, 2005; García *et al.*, 2008), c) units previously defined along the rise (Rebesco *et al.*, 1996, 1997; 2002; Hernández-Molina *et al.*, 2006b; Uenzelmann-Neben, 2006) and d) age of the oceanic crust, based on interpretation of marine magnetic anomalies (Larter and Barker, 1991a). The margin's transition from an active to a passive state has influenced the distribution and other characteristics of the main seismic units that we have identified (Fig. 14). Correlation of shelf and rise units specifically indicated that the three major evolutionary intervals I, II and III correspond with; a non glacial margin; a glacially-influenced margin and a fully glaciated margin, which are described below.

7.1.1. Interval I: Non glacial margin interval (Early Cretaceous to late Miocene)

a) Stage I.1: Active margin phase (Early Cretaceous to early Miocene).

SU9 is very thin or absent along the rise but well developed along beneath the outer shelf and slope (Fig. 5). This unit records the active margin phase along the shelf and slope, thus taking the form of a pre-collision wedge. Subduction occurred in both oblique and orthogonal orientations relative to the trench (McCarron and Larter, 1998), and likely generated an accretionary wedge that contributed to a complex slope with numerous slope-basins, and a forearc basin along the shelf (Macdonald, 1993; Watts, 2001). SU9 therefore pre-dates the time when the ridge segment between the Tula and Adelaide FZs reached the trench (Larter *et al*., 1997). We interpret SU9 as early Miocene (e.g., at least 19 ± 0.8 Ma) or older in age (Figs. 14 and SM-I). SU9 is deeply folded and fractured beneath the slope, but thins along the rise. The oceanic basement at DSDP Leg 178, site 325 is late Oligocene in age (anomaly 6Cn.3n: Larter and Barker, 1991a, or 24 Ma on the magnetic reversal time scale of Cande and Kent, 1995). SU9 overlies the rise in an area that runs parallel to the regional magnetic anomalies, specifically between anomaly 6AAn (21.8 Ma) and the younger edge of anomaly 6Bn (22.6 Ma) (Hernández-Molina *et al.*, 2006b). We can therefore infer that SU9 sediments that overlie igneous basement along the rise are younger than 22.6 Ma. SU9 exhibits a thin and sheeted appearance and infills irregular basement features along the rise (Hernández-Molina *et al.*, 2006b).

These observations suggest two scenarios for SU9 development, which are not mutually exclusive. In the first scenario, this segment of the ocean crust did not receive a significant sediment supply from the margin until after the ridge crest had migrated into the trench. While the margin was active, mass transport and turbiditic processes served as the primary mechanisms for transporting material from the shelf to the trench axis (as in Fig. 2B). The intervening trench depression trapped most of the sediment, while the seaward flexural bulge and spreading ridge posed additional barriers hindering transport to deeper areas of the basin. In the second scenario, significant bottom current activity prevented deposition of fine-grained material in this area of the basin, as proposed by Hernández-Molina *et al*. (2006b) and supported by Uenzelmann-Neben (2006). This mechanism would indicate strong bottom currents coursing through the study area since the late Oligocene as has been suggested by other authors in other areas (Maldonado *et al.*, 2014; Eagles and Jokat, 2014). The Drake Passage seaway may have been deep enough by the early Oligocene as to allow deep circulation (Livermore *et al.*, 1994, 2004; Lawver and Gahagan, 2003; Lagabrielle *et al.*, 2009; Maldonado *et al.*, 2010, 2014, 2016) and initiation of a full, active ACC flow around the Antarctic continent (Fig. 14). Full onset of the

ACC coincided with expansion of ice cover in East Antarctica (Barrett, 1996) and with the initiation of a new thermohaline circulation (THC) pattern that strongly influenced the southern hemisphere (Van Andel *et al.*, 1977; Kennett, 1982; Niemi *et al.*, 2000; Hernández-Molina *et al.*, 2009; Carter *et al.*, 2004; Katz et al., 2011; Houben et al., 2013; Uenzelmann-Neben et al., 2016; Lindeque et al., 2016).

The active margin phase ceased about 16.7 ± 0.7 Ma when the Antarctic-Phoenix ridge crest (between the Adelaide and Biscoe FZs) migrated into the trench (Fig. 14). The arrival of the ridge-crest segment at the trench eliminated trench basement topography and initiated rapid uplift of an intervening margin segment centered near the Mid-Shelf High (Larter and Barker, 1989; 1991a,b; Macdonald, 1993). Along the middle to outer shelf, the upper surface of SU9 records this event as an angular unconformity (Fig. 10c), and has thus been referred to as the "uplift unconformity" (UU) (Larter *et al*., 1997), or the "collision unconformity" (CU) (Bart and Anderson, 1995). The adjacent segment of the margin to the northeast (the Biscoe - South Anvers segment) remained active as uplift occurred.

b) Stage I.2: Compressional deformation phase (early Miocene)

The second phase of the margin's evolution is depicted by SU8 and SU7 units. The configuration of these units indicates deformation following the margin's transition to a passive style (Fig. 14). SU7 and SU8 form a large sedimentary wedge along the rise on both sides of the Adelaide FZ. SU8 is thinner in the northern part of the area between the Adelaide and Biscoe FZs, but gradually thickens towards the margin, indicating that it was mostly formed after the Antarctic–Phoenix ridge segment had reached the margin in this spreading corridor (i.e., no earlier than 17.4 Ma). Consequently, deposition of SU8 primarily occurred during the later part of the early Miocene. SU9 must be younger than 19.8 Ma, but its upper boundary, along with SU7, probably formed after 16.7 Ma. The thinner, older sections of SU9 identified on the rise represent very slow accumulation of sediment (over a several million year interval) following emplacement of igneous basement. As such, they lend support to margin evolution models described above. SU7 and SU8 units correlate (Fig. SM-I) with the pre-drift stage of the upper rise drifts defined by Rebesco *et al*. (1996, 1997, 2002).

SU7 and SU8 comprise a sedimentary wedge thinning out from the slope towards the rise. Their overall structure indicates a slope and upper rise depositional setting dominated by downslope processes (e.g., mass wasting and turbidity currents). This interpretation is consistent with that of Rebesco *et al*. (1997) and McGinnis *et al.* (1997) concerning other areas of the slope and rise along the margin, but contrasts that given in Uenzelmann-Neben (2006). Regardless, a vigorous bottom current regime that flowed towards the northeast likely prevailed, however over the central continental rise, as previously described in Hernández-Molina *et al. (*2006b). We therefore propose a depositional setting influenced by along-slope processes for the central rise during this phase. Along-slope processes specifically refer to a vigorous bottom current during the early Miocene, which weakened slightly towards the end of the early Miocene. Uenzelmann-Neben (2006) observed similar phenomena in other parts of the PMAP, and Sykes *et al.* (1998) reached a similar conclusion from palaeobathymetric analyses. Seismic units that record a drift growth stage described by Rebesco *et al.* (1997, 2002) from the beginning of the middle Miocene previously served as earliest indication of strong bottom current activity along the continental rise west of the Antarctic Peninsula. However, our data indicate that along-slope processes associated with northeastward flow prevailed along the central rise from before 19.8 Ma to roughly 15 Ma. These processes did not affect the upper rise or lower slope, where downslope mass transport processes (MTDs) prevailed and high sediment supply masked along-slope processes. Uenzelmann-Neben (2006) suggested that bottom currents flowed southwest during this stage. Although during the early Miocene there was certainly a deep-water pathway through Drake Passage for Circumpolar Deep Water (CDW), there may not have been a seaway for significant proportions of WSDW and LCDW from the Weddell Sea to reach the continental rise west of the Antarctic Peninsula through the South Scotia Ridge. The first major incursion of water masses from the Weddell Sea into the central Scotia Sea apparently occurred during the middle Miocene, once tectonic movements had produced sufficient gaps in the South Scotia Ridge to allow deep-water inflow from the northern Weddell Sea (Maldonado *et al.*, 2003, 2005, 2006; Bohoyo, 2004; Pérez *et al.* 2014a, 2014b). Assuming Uenzelmann-Neben's (2006) conclusions are correct, the water mass that flowed along the upper rise in a southwest, along-slope direction for areas corresponding to present-day Drifts 6 and 7 could not have been the modern southwestward-flowing bottom current. The potential effects of a putative, alternative bottom current along the upper rise of areas corresponding to the present-day location of Drifts 4 and 5 are unfortunately masked by high sedimentary input from MTDs. On the other hand, the alternative water mass may not have influenced these areas.

The compressional deformation phase also included thermal uplift of the margin. SU9, SU8 and SU7 were each markedly affected by uplift associated with MSH emplacement. Local channel cut and fill along SU8's upper surface (Fig. 10B), which incises SU8 and SU9 as they occur along the outer shelf, may represent fluvial incision, coeval with the thermal uplift of the margin (Fig. 14), subsequent cooling and lowstand intervals during the early Miocene (Haq *et al*., 1997; Zachos *et al*., 2001, 2008; Miller *et al.*, 2011).

The base-of-the slope also includes two buried structural highs separated by a depression. The tectonic high southwest of the Adelaide FZ may be analogous to the "base-of-slope transition high" described by Jabaloy *et al*. (2003) at the lateral terminus of the South Shetland Trench (Fig. 12). Compressional deformation can occur between two oceanic crust segments if one becomes passive while the adjacent one remains active and there is a slight change in plate convergence direction, thus generating a compressive high at the base of the slope (as in Fig. 2C). The deformation of the younger sections of SU7 and SU8 may thus reflect post ridge-trench collisional tectonics. MTDs associated with large debris flows indicate that these processes were particularly influential along transitional areas between the lower slope and upper rise.

The second high, located farther northeast, in the middle of the Adelaide/Biscoe oceanic segment requires further consideration. It may have formed from deformation associated with a minor and previously unknown fault zone between the Adelaide and Biscoe FZs, or from seamount emplacement during the previous ridge-crest collision, with later deformation during SU7 and SU8 deposition. Whatever its origin, this second structural high also affected SU7. We therefore suggest gradual migration of subtle deformation from southwest to northeast based on current data. Progressive deformation could relate to the lateral effects of the active margin located to the northeast during this time (Biscoe- South Anvers Segment), until its ridge-crest collision (RC-T) at around 15 to 14.1 ± 0.6 Ma (Larter *et al*., 1997), which coincided with thermal uplift of the shelf between the Adelaide and Biscoe segments.

A possible explanation for subtle deformation continuing following RC-T collision in this area is a final phase of extension on the West Antarctic Rift System (WARS; Cande et al., 2000). Granot et al. (2010) argued that a small amount of extension on the WARS continued into the Miocene, and perhaps even the late Miocene. Eagles et al. (2009) and Bingham et al. (2012) suggested that the Oligocene to Miocene WARS continued into the southern part of the Antarctic Peninsula and connected to the trench at the Pacific margin. If these interpretations are correct, most of the Antarctic Peninsula was part of the East Antarctic plate during the mid-Cenozoic, but Alexander Island, the part of the margin offshore from it and the trailing flank of the Antarctic-Phoenix Ridge were part of the West Antarctic plate. In this case, RC-T collisions in this area involved a triple junction and would have been more complex than in the simple two-plate scenario described by Barker (1982) and Larter & Barker (1991a).

Tectonic deformation during SU8 and SU7 deposition is significant to margin evolution for three reasons. First, it explains why the shelf and slope were persistently elevated (high) in the central sector relative to the northern and southern sectors until the latter part of SU3 deposition. Second, it controlled the initial position of the Marguerite Trough and ice flow pattern during the initial expansion of the ice-sheets along this area of the PMAP. Lastly, it caused downslope mass transport processes that dominated the lower slope and upper rise.

c) Stage I.3: Passive margin phase (latter part of the early Miocene)

An important change in margin growth depositional patterns occurred during SU6 deposition. We interpret SU6 as corresponding to the Type IIA sequences identified by Cooper *et al*. (1991). The overall aggradational stacking pattern likely relates to the onset of subsidence after margin uplift and rising sea-levels associated with warmer conditions during the middle Miocene (Fig. 14), which preceded dramatic cooling during the Mid Miocene Climate Transition (MMCT) between ~14 Ma and ~12.4 Ma (Haq *et al*., 1997; Zachos *et al*., 2001, 2008; Shevenell et al., 2004; Lewis et al., 2007, 2008; Haywood et al., 2009). The initial subsidence in the central sector of the margin proceeded at a lower rate than that occurring in the southern and the northern sectors, as indicated by relatively thin expression of older seismic units in this central area. Along the rise, SU6 forms a regionally sheeted unit, although Hernández-Molina *et al*. (2006b) have also reported drift features influenced by bottom current circulation flowing toward the northeast during this time.

Biostratigraphic constraints on sedimentation rates at Site 325 indicate that SU6 contains a hiatus or condensed sequence that spans most of the middle Miocene (<6 m/Ma, 15–8 Ma; Hollister *et al*., 1976). Correlation between line BAS878-19 and Site 325 data indicates that most of SU6 must predate the middle Miocene condensed sequence at Site 325 (i.e., > 15 Ma). Therefore, SU6 along with previous SU7 and SU8 subunits developed rapidly over a < 2.4 M.y. interval during the latter part of the early Miocene and the beginning of the middle Miocene (Fig. 14). Dominant downslope mass transport processes on the lower slope and upper rise probably formed these units. Deposition of SU6 coincided with regional formation of canyon-channel systems and the initial development of the upper rise drifts (Fig. SM-I), as identified by Rebesco *et al*. (1997). The inception of a vigorous bottom current along the slope and rise generated these features. Uenzelmann-Neben (2006) proposed a sedimentary model for a different area in which downslope processes (mass movements) strengthened due to growth of Antarctic Peninsula ice cover at this time, while the along-slope processes weakened. Based on our data, we propose a mixed sedimentary model during SU6 deposition, in which downslope and along-slope processes interact along the upper and central rise.

The basal boundary of SU6 correlates with Reflector-II identified in Barker *et al*. (1998, 1999) for which we propose a 15-16 Ma, middle Miocene age (Figs. 14 and SM-I). A coeval discontinuity occurs within other Southern Hemisphere oceanic basins (Hinz *et al.*, 1999; Niemi *et al.*, 2000; Carter *et al.*, 2004; Hernandez-Molina *et al.*, 2009, 2010). Several important events also coincided with SU6 deposition, including widening of the Drake Passage (Livermore *et al.*, 2000; Eagle, 2003; Lagabrielle *et al.*, 2009), inception of the East Scotia Ridge (Eagles, 2003; Larter et al., 2003), the end of compressional tectonics in the Patagonian Cordillera (Barreda and Palamarczuk, 2000), a massive aggradational phase along the South American margin, which may have been associated with major regional subsidence (Van Andel *et al.*, 1977; Kennett, 1982; Aceñolaza, 2000; Malumian and Olivero, 2006; Potter and Szatmari, 2009), global third-order highstand intervals (Haq *et al.*, 1987) and the restriction of deep bottom current activity associated with the proto-AABW to depths below ~5.5 km (Sykes *et al.*, 1998; Hernández-Molina et al., 2010).

7.1.2. Interval II: Glacially-influenced margin interval (middle to late Miocene) *a) The subsidence phase*

SU5 records the progressive subsidence phase of the glacially-influenced margin, which brought clear but restricted seaward progradation along the outer shelf. During this phase, the palaeo-shelf break exhibits a convex morphology and resembles the Type IIA sequences of Cooper *et al*. (1991). Seismic facies overlying the shelf generally resemble those of SU6. A regional unconformity between the two units however indicates that MSH uplift exerted a stronger influence on SU6 than on SU5, and that SU5 developed coevally with the margin's main subsidence stage during a period of relative tectonic stability. These factors led to burial and preservation of the northern structural high in the transitional area between the lower slope and upper rise (Fig. 12E).

SU5's lower boundary formed around the end of the middle Miocene (ca. 10 Ma; Figs. 5 and SM-I), with the rest of SU5 developing through the middle to late Miocene (Fig. 14). Along the rise however, SU5 can be absent or appear as a very condensed sequence (i.e., SU4 directly overlies SU6) (Figs. 7 and SM-I). A discontinuity in the middle Miocene has been described in areas of nearby ocean basins, including the southern Atlantic Ocean (Viana *et al.*, 2003; Hernández-Molina *et al.*, 2009, 2010; Preu et al., 2012) and in the Weddell and Scotia Seas (Maldonado *et al.*, 2006; Pérez *et al.*, 2014a, b, 2015a,b).

SU5 records the main phase of regional drift development along the PMAP (Fig. SM-I), as recognized by Rebesco *et al*. (1997, 2002), who correlated it with initiation of substantial glacial sedimentary transport from the shelf. In contrast, Uenzelmann-Neben (2006) interpreted less voluminous sedimentary input during this time, which coincides with relocation of the bottom current towards the north. We interpret SU5's sedimentary history as resembling that of SU6, except that along-slope processes exerted a greater influence than down-slope processes, enabling more drift-mounded morphologies to develop within SU5. Deposition of this unit may have coincided with a middle to late Miocene increase in bottom water circulation in the Southern Hemisphere (Kennett, 1982; Carter *et al.*, 2004; Joseph *et al.*, 2004; Uenzelmann-Neben et al., 2016). NADW circulation intensified first in the Atlantic and subsequently in the Southern Hemisphere thus contributing to a more vigorous LCDW around Antarctica (Kennett, 1982; Nisancioglu *et al.*, 2003). Examples of this intensification occur around the Argentine margin (Hernández-Molina *et al.*, 2009, 2010) and in the northern Weddell Sea and Scotia Sea (Maldonado *et al.*, 2006). Hernández-Molina *et al.* (2006b) previously interpreted a regional palaeoceanographic change in SU5 data from along the central rise as indicating more vigorous intermediate and deep-water flow towards the southwest. This shift and the aforementioned increase in bottom water circulation following events related to the expansion of the eastern Antarctic ice sheet (EAIS) (Flower and Kennett, 1994; Vincent and Berger, 1985; Zachos *et al.*, 2001) and opening of gaps in the South Scotia Ridge (SSR, Fig. 14) enabled WSDW and LCDW incursion from the Weddell Sea into the central Scotia Sea (Maldonado *et al.*, 2003, 2004, 2005; Bohoyo, 2004: Pérez *et al.*, 2014a, b, 2015a,b).

b) The Base of Glacial Margin Sequences (BGMS)

Previous studies have attempted to establish the timing of glacial margin sequence initiation along the shelf (Type IA glacial sequences, as defined by Cooper *et al*., 1991). Larter and Barker (1989, 1991b) conducted the first seismic-based study using MCS profiles. Larter *et al*. (1997) defined the BGMS as the S3/S2 boundary (late Miocene) based on the occurrence of Type IA glacial sequences in the overlying S2 and S1 units. Following the results of Bart and Anderson (1995), Bart *et al.* (2005) analyzed deposition of the upper part of their Seismic Package 3 (SP3) to interpret 12 grounded ice advances across the outer shelf occurring between 7.94 and 5.12 Ma.

We interpret the onset of glacial margin sequences (BGMS) as occurring at the base of SU4 (Transitional Unit), which marks the time that regular ice advances began to reach the shelf break. The base of SU4 marks a major change in PMAP stratal geometry and correlates with the original S3/S2 boundary from Larter and Barker (1989). The S`3/S2´ boundary from Larter and Barker (1989, 1991b) and Larter et al. (1997), however does not correspond with the S3/S2 boundary considered by Barker and Camerlenghi (2002) in relation to ODP Leg 178 results. Using the AISM-06 profile, these latter authors placed the S3/S2 boundary in a higher stratigraphic position that that indicated in Larter *et al.* (1997). The Type IA glacial sequences along the outer shelf therefore began earlier than the age assigned by Barker and Camerlenghi (2002), as shown in Fig. SM-IV. At Site 1097, the base of SU4 corresponds to the upper part of SP3 (Fig. SM-I) as reported in Bart and Anderson (1995) and Bart *et al.* (2005).

This revised correlation is relatively consistent with lithologic observations from the Ocean Drilling Program (ODP) Leg 178 data (Eyles *et al*., 2001; Barker *et al.*, 2002), which indicate a transition from glaciomarine sediments in SU5 to subglacial sediments in SU4 and SU3 as interpreted from Site 1097 data along the outer shelf. Core recovery from Site 1097 however was poor and results from this site do not clearly resolve the question of whether or not ice was frequently grounded on the outer shelf before the latest Miocene (Eyles *et al*., 2001; Larter, 2007). Based on results from that site, SU4's basal discontinuity correlates with Reflector III and with the transition between Units III and II (Fig. 5), or the Tau and Upsilon diatom zone (Barker *et al*., 1998, 1999; Barker and Camerlenghi, 2002). More recent studies of Sites 1097 and 1103 data place the S2/S3 boundary from Larter and Barker (1989, 1991b) at ca. 5.12 to 7.94 Ma, although S2 is absent at Site 1103 (Lavelle *et al*., 2002; Iwai and Winter, 2002). As previously mentioned, SU4 correlates with the lowest section of the S2 seismic unit of Larter and Barker (1989, 1991b) and Larter *et al.* (1997). These researchers estimated a basal boundary of S2 at ca. 6.5 Ma based on correlation with sediments overlying oceanic basement of known age. This age matches reasonably well with interpretation by Bart *et al.* (2005, 2007) and chronostratigraphic constrains from ODP Leg 178, sites 1097 and 1101 (Barker et al., 1999). Consequently, SU4's basal boundary formed between the end of the late Miocene and the beginning of the early Pliocene, perhaps between 5.12 and 6.5 Ma according to our data and stratigraphic correlations. A coeval discontinuity has been detected in stratigraphic data from Southern Hemisphere ocean basins, including sections described from the South Atlantic Ocean (Ledbetter and Ciesielski, 1986; Viana *et al.*, 2003; Hernández-Molina *et al.*, 2009), Indian Ocean (Niemi *et al.*, 2000), South Pacific Ocean (Carter *et al.*, 2004) and Antarctica's Weddell and Scotia Seas (Maldonado *et al.*, 2006). Based on the attributed age for the SU4's basal boundary the regular ice advances began to reach the shelf break in the margin offshore from Adelaide Island later compare with other areas around Antarctica. In the East Antarctica it is considered about 15 Ma (Escutia et al., 2005, 2011), similar to the age recently proposed for the West Antarctica (Lindeque et al., 2016). But, a different time range is proposed for the advancing ice sheets grounding on the outer shelf in the Weddell Sea, being variable (17.7–10.8 Ma) from southeast to northwest (Lindeque et al., 2013).

The margin offshore from Adelaide Island experienced some glacial influence during later SU5 deposition. This unit includes a few moderately erosive, glacial features (minor troughs and irregular surfaces) that appear in seismic profiles from the middle shelf and very proximal areas of the outer shelf, as reported by Bart and Anderson (1995), by Bart *et al.* (2005) for the lower part of SP3 and by Hernández-Molina *et al.* (1999, 2000, 2006a,b). These subtle features apparently formed beneath grounded ice, but are not associated with the broad glacial troughs extending to the shelf break and evident in younger sequences. They cannot be linked to Type IA glacial sequences, as defined by Cooper *et al*. (1991) and suggest that the grounded ice rarely advanced beyond the MSH during SU5 deposition. This interpretation is consistent with the fact that the topography of SP3 seismic reflectors mapped by Bart *et al.* (2005) does not clearly indicate that they were formed below grounded ice. Our interpretation, that the ice sheets covered mainly the inner and middle shelves, glacial maxima grounding lines occurred around the middle shelf, but some progradational events reached proximal areas of the outer shelf. This idea is consistent with earlier interpretations of the margin described above.

The MSH still represented a major barrier to grounded ice advance during SU5 deposition. Consequently, ice advances to the shelf edge may have started earlier along the margin offshore of Alexander Island and then progressed north along the Peninsula. The earliest large ice sheets may have nucleated on the vast, subaerially exposed areas of Alexander Island and Palmer Land (Smellie *et al.*, 2009). Alternatively, the first grounding line advances across the outer shelf may have preceded the BGMS, which marked a widespread change in subglacial processes. If grounded ice had yet to reach the shelf break, subglacial transport across the shelf would be very efficient, given the depths established along the outer shelf by the middle Miocene. If ice did extend across the outer shelf, its flow may have been more sheet-like, and included broaded zones of rapid ice flow than the focussed ice streams that characterize most parts of more recent ice sheets. These interpretations are supported by the following lines of evidence: a) the BGMS being located at the top of the S3 (Larter *et al.*, 1997); b) interpretation of ODP Leg 178, sites 1095-1103 data (Barker *et al.*, 2002), c) evidence that full glacial conditions have affected the outer shelf of the Antarctic Peninsula since the late

Miocene (Eyles *et al*., 2001; Barker and Camerlenghi, 2002), d) high sedimentation rates from 9.5 to 4 Ma along the rise (Hollister *et al.,* 1976; Barker and Camerlenghi, 2002) and e) the younger age of Drift 5's main drift growth stage relative to those proposed by (Rebesco *et al.,* 2002) for Drifts 6 and 7. This last line of evidence arises from the higher sediment supply and more frequent sedimentary cycles occurring on the Antarctic Peninsula's continental rise. These evidences indicate grounding events (as noted by Bart *et al.* 2005) across the entire shelf during the latest Miocene.

7.1.3. Interval III: Fully glaciated margin interval (latest Miocene to present)

Seismic units 1-4 characterize this interval, which divides into three minor stages: transitional, progradational and aggradational margin stages (Fig. 14).

a) Stage III.1: Transitional stage (late Miocene to the beginning of the early Pliocene)

SU4 represents the first progradational unit containing truncated foreset reflections for distal areas of the outer shelf. These indicate one of the most significant shifts in margin deposition since the margin became tectonically passive. SU4 exhibits internal reflections that are generally less continuous and contains sequences with distinctive topset and foreset reflections as well as oblique truncation of foresets near the palaeo-shelf break. It thus conforms to Cooper *et al*.'s (1991) definition for Type IA glacial sequences. Hernández-Molina *et al.* (2006a, 2006a,b) defined SU4 as a 'Transitional Unit (TU)' because it recorded the transition to conditions of a fully glacially-dominated margin, when grounding cycles of APIS on the outer shelf were more frequent (Zachos et al., 2001). Although the unit probably includes several phases of advance and retreat, SU4 records the advance of the glacial maxima grounding line position up to the shelf edge.

SU4's upper boundary for slope areas of the central sector consists of a major truncation surface that cuts across underlying units SU4, SU5, SU6 and SU7. At the base of the slope, large debris flow deposits formed just above this boundary. These features provide indirect evidence of slope instability resulting from: 1) significant erosion along the shelf and rapid delivery of sediment to the upper slope; and 2) recording the maximum (or first) advances to the shelf edge of the grounded ice sheet or derive from smaller debris flows formed by a multiphase episode of continental margin collapse at the end of SU4. These debris flows deposits are very well developed but have not been previously described at this stratigraphic position.

SU4 also represents a major shift in deposition along the continental rise, evident from the regional erosive surface at the base of SU4's contourite drift. The drift is a separated body of mounded and elongated deposits along the rise. It exhibits moderate-to-high acoustic response in its expression along lower slope areas. These facies become more laminar in a basinward direction. The prominent erosive discontinuity at the base of SU4 along the rise correlates to a seismic reflection identified at 0.370 s (twt) bsf in DSDP Site 325 data (Fig. 9). We correlate SU4's upper surface with

'Horizon R', defined previously by Tucholke and Houtz (1976), which occurs at 0.225 s (twt) bsf in Site 325 data. This correlation implies that the base of SU4 formed between the latest Miocene and the early Pliocene (Fig. SM-I). SU4's basal surface also correlates with a possible hiatus at ODP Leg 178, Site 1095 interpreted from biostratigraphic evidence, spanning from 6.14 to 5.04 Ma (Hillenbrand and Fütterer, 2002, 2003). The estimated age ranges for SU4 also coincide with those derived from outer shelf deposits (IODP Leg 178 1097 data).

The erosional base of SU4, its external mounded shapes evident in profiles and the high-to-very-high acoustic response and high lateral continuity of SU4 reflections all indicate deposition under more energetic deep water conditions than those inferred for SU5–SU7. The base of SU4 may have therefore marked the final establishment of more intensive bottom water circulation (Fig. 14) and reorganization of deep water flows into a regional pattern similar to the one observed at present (Billups, 2002; Hernández-Molina *et al*., 2006b). As such, LCDW from the Weddell Sea may have extended over a greater area of the central rise along the Antarctic Peninsula, thereby displacing CDW and forcing it into a more distal position.

These palaeoceanographic changes established a mixed sedimentary regime along the margin that involved interaction of down- and along-slope sedimentary processes. Debris flow and turbiditic processes became the primary processes operating on the slope. Drift deposits indicate that bottom currents dominated in areas along the rise and water-mass circulation resembled that observed at present (Hernández-Molina *et al*., 2006b). Lateral relations between SU4's shelf and rise deposits and chronostratigraphic constraints from DSDP Leg 35, Site 325 (Hollister *et al.*, 1976) and ODP Leg 178, Site 1097 (Barker *et al*., 1999) indicate that the main phase in which the present drift morphologies developed along the rise coincided with the initiation of glacial margin sequences along the outer shelf. Thus, the main phase of drift growth along this part of the margin began later than the time interpreted by Rebesco *et al*. (1997, 2002), who estimated a 9.5 - 3 Ma growth phase synchronous with Drifts 6 and 7. Uenzelmann-Neben (2006) also interpreted seismic data from Drifts 6 and 7 areas to estimate an earlier depositional age of 15-9.5 Ma for drift growth.

Multiple lines of evidence indicate relatively strong intermediate and deep-water circulation from the late Miocene to the early Pliocene (Sykes *et al.*, 1998; Nisancioglu *et al.,* 2003; Uenzelmann-Neben et al., 2016). This change is likely associated with increased production of cold bottom water due to expansion of the WAIS and fringing ice shelves (Ledbetter and Ciesielski, 1986; Niemi *et al.*, 2000; Anderson and Shipp, 2001) and the initiation of ephemeral Northern Hemisphere ice sheets, coincident with a global cooling event (Jansen and Raymo, 1996).

b) Stage III.2: *Progradational glacial margin stage (early Pliocene to middle Pleistocene)*

SU3 and SU2 contain glacial sequences and widely distributed progradational facies for shelf break and slope areas. These sequences exhibit prograding palaeo-shelf edges above SU4's upper surface. The foreset and topset deposits accumulated as ice grounding lines advanced and retreated (Larter and Vanneste, 1995; Bart and Anderson, 1995; Larter *et al.*, 1997). SU2 and SU3 prograde across the outer shelf and include depositional lobes along the margin (Bank 3 and 4, Fig. 5). These correspond to grounding sequences (GS) as interpreted by Bart and Anderson (1995) or 'glacial margin sequences' described by Larter *et al*. (1997).

Of all the units analyzed, SU3 exhibits the greatest amount of sedimentary progradation (Fig. 14). Subunit a is the youngest and most progradational of the three subunits (a, b and c) identified within SU3 (Figs. 5 and SM-I). A mixed depositional regime continued to operate along the slope and rise as SU3 formed, with an active southwest-flowing bottom current contributing to down- and along-slope processes. Physiographic domains along the margins were positioned in a manner similar to those observed at present. The elongated lobe morphology that runs parallel to the slope in Subunit c demonstrates the prevalence of along-slope processes. Subunits a and b developed sedimentary wedges transverse to the margin, with relatively limited progradation and depocenters located closer to the slope than those of Subunit c. These characteristics indicate the prevalence of down-slope processes in slope areas as depocenters migrated landward.

Our sedimentary deposition model does not fit with the results of Uenzelmann-Neben (2006) for Drifts 7 and 6, in which she interpreted weaker bottom currents without drift growth, and a decline in sedimentary input after 5.3 Ma, resulting in a condensed sedimentary succession. Our model is fairly consistent with the maintenance stage described by Rebesco *et al.* (1997, 2002). Their interpretation holds that after 5 Ma, bottom current activity exerted less influence along the rise. This transition was due to an increase in down-slope sediment transport associated with the glacial sequences rather than to an actual decrease in current velocity.

SU3's upper surface represents a relevant significant change in margin accretion experienced by the PMAP, once ice sheet advance to the shelf edge begun. This boundary corresponds to Reflector IV of Barker *et al*. (1998, 1999), and was putatively dated at 2.4 Ma by Larter and Barker (1989, 1991b) and Barker *et al*. (1998, 1999). Rebesco *et al*. (2007) recently reassigned it an age 2.9 ± 0.2 Ma. Rebesco *et al.* (2006, 2007) also interpreted the boundary as a significant regional surface that records transition of West Antarctic ice sheets from temperate, wet and highly dynamic to cold, dry and relatively stable. Discontinuities marking this transition occur in other areas around Antarctica (Volpi *et al.*, 2007; Cooper *et al.*, 2004).

Major tectonic and global environmental changes occurred at end of the Pliocene and beginning of the Quaternary, between 3-2.6 Ma (Fig. 14). These included plate tectonic reorganization (Cloetingh *et al.*, 1990; Whyte and Lovell, 1997; Hernández-Molina *et al.*, 2014), global cooling (Shackleton *et al.*, 1984; Raymo *et al.*, 1989; Lear *et al.*, 2000), major fall in sea-level (Lowrie, 1986; Haq *et al.*, 1987; Morrison and Kukla, 1998), onset of major northern hemisphere glaciations (Raymo *et al.*, 1989; Maslin *et al.*, 1998; Zachos *et al.*, 2001, 2008) and growth of Northern Hemisphere ice sheets (Moran *et al*. 2006). This transition also marked a major shift in climatic cycles from predominance of the asymmetric 4th-order climatic (and sea-level) cycles having ~20 k.y. periods (precessional cycles), to the predominance of 42 k.y. obliquity orbital cycles (e.g., Shackleton and Opdyke, 1973; Ruddiman *et al*., 1989; Raymo *et al*., 1989; Clark *et al*., 1999).

Diviacco *et al*. (2005) identified buried mega-debris flow deposits at a stratigraphic position coinciding with SU3's upper surface, beneath the deep sea Alexander Channel, between Drifts 6 and 7 as described by Rebesco *et al*. (2002). Large debris flow deposits do not appear in lower slope or upper rise areas of SU3's upper surface described here. Rebesco *et al.* (2006) interpreted major changes in the continental slope (a regional downlap surface) and rise (a decrease in accumulation rate) from features observed at and around the S1-S2 boundary (SU3's upper surface). Immediately above SU3, SU2 forms a primarily aggradational unit that does not include the continuous regional downlap surface described by Rebesco *et al.* (2006), whose seismic stratigraphic criteria were invalid for our studied area. SU2 is thinner or eroded along the upper and central rises indicating lower accumulation rates following SU3 deposition, as suggested by Rebesco *et al.* (2006).

Aggradational and progradational structures in SU2 indicate a late Pliocene to Pleistocene change in margin geometry. SU2 facies along the shelf and slope resemble those of SU3, while SU2 facies along the rise appear as thin, aggradational deposits with weak acoustic response. During SU2 deposition, the sedimentary processes resembled those operating during SU3's early Pliocene (SU3) deposition. As described by Rebesco *et al.* (1997), drift shape was preserved under these conditions of lower sedimentation rate and greater along-slope influence. However, this scenario disagrees with the results of Uenzelmann-Neben (2006) for Drifts 7 and 6, who interpreted that these drifts were no longer built up.

c) Stage III.3: Aggradational glacial margin stage (middle Pleistocene to present)

By the middle Pleistocene, margin deposition created a more aggradational stacking pattern (SU1) where the greatest sediment accumulation occurs on the outer shelf banks, similar to depositional systems operating at present (Fig. 14). SU1 forms a thick sedimentary wedge composed of thin aggradational subunits along outer shelf areas. A similar unit occurs along northern reaches of the Antarctic Peninsula margin (Jabaloy *et al.*, 2003) and the Bransfield basin (García *et al.*, 2008). SU1 formed from the middle Pleistocene to recent times. Its basal boundary represents the most recent major shift in margin deposition and geometry, which may coincide with a major change in the duration of global climatic cycles during the Mid-Pleistocene Transition (MPT, ~1.2–0.65 Ma) (Clark *et al*., 1999,,2006; Maslin and Ridgwell, 2005; McClymont et al. 2013). The MPT includes a significant fall in global sea level, specifically around 0.9 Ma (Lowrie, 1986; Haq *et al.*, 1987; Llave *et al.*, 2001; Hernández-Molina *et al.*, 2002, 2016; Kitamura and Kawagoe, 2006; Clark et al.,2006; McClymont et al. 2013), and a major change in climate, wherein glacial/interglacial cycles shifted to longer periods and greater amplitudes (Thunell *et al*., 1991). SU1's basal discontinuity may therefore represent transition from a climate most strongly influenced by the asymmetric climate and sea-level cycles associated with Earth's 41 k.y. obliquity cycles to subsequent predominance of the 100 k.y. eccentricity orbital cycles. During the Quaternary, the higher amplitude climatic and eustatic changes increased the frequency and duration of ice sheet grounding events (Bartek *et al.*, 1991), shifted depositional processes from erosion to net accumulation, developed aggradational/progradational deposits (Solheim *et al.*, 1996) and may have increased margin subsidence (Dahlgren *et al.*, 2005).

Flow of grounded ice has served as the primary erosion, transportation, deposition mechanisms for development of margins at higher latitudes. Advance of the grounding line to the continental shelf edge transported large volumes of sediment to the slope where mass flow processes carried them downslope to build base-of-slope systems. Extensive erosional surfaces developed on the shelf and eliminated previous deposits. During this last evolutionary period, downslope processes reactivated turbidite canyon-channel systems and prevailed during glacial periods, while contourite processes along the upper part of the continental rise played an ancillary role. A fairly uniform, thin layer of fine-grained sediments accumulated above contourite drifts between the large CCSs, where erosional processes prevailed. This sedimentary model agrees with interpretations of both Rebesco *et al.* (2002) and Uenzelmann-Neben (2006), who proposed that intensive Quaternary glacial phases diminished sedimentation rates and led to increased erosion along the upper rise.

7.2. Origin of the morphosedimentary features: the imprint of fully glacial conditions

A seaward change in facies trends between the upper and middle slope, reveals advance of grounded ice during the Pliocene and Quaternary. The present glaciogenic morphosedimentary features along the shelf and slope began developing during SU4 deposition and became fully established during a time corresponding to SU3's upper surface. The present erosional and depositional features along the shelf, slope and rise have evolved through many climatic and eustatic cycles. Changing ice-sheet drainage patterns associated with lateral migration of the Marguerite Trough also played a critical role in drastically altering slope and rise morphology.

Trough migration causes this area to differ from other regions of the PMAP and disrupts the relationship between the two major troughs along shelf, rise CCSs and inter-trough areas. Probably that migration if the reason because there is not a mature trough mouth fans identified in front of other glacial troughs (O´Cofaigh et al., 2003, 2016; Laberg et al., 2010; Swartz et al., 2015). It also affects inter-trough areas with major drifts along the rise, as was observed by Rebesco *et al*. (2002) and Amblas *et al*. (2006) for north and south areas. Lateral migration of the Marguerite Trough explains the differences between Drift 5 and the larger Drifts 6 and 7 identified by Rebesco *et al*. (1997, 2002). These authors suggest that over time, stable glacial troughs controlled the spacing between the major turbiditic canyon systems and determined the shape and dimensions of sediment drifts along the rise. During the Pliocene (SU4 and SU3 deposition), the Marguerite Trough was located southwestward of its present position, at the Adriasola Bank, in alignment with the current position of the North Tula CCS. It migrated to its present position, in front of the Adelaide channel, which also marks where the Adelaide shelf lineation (ASL) was located, during the Quaternary (SU2, Subunit 2a). The Marguerite Trough represents the largest palaeo-ice stream trough draining Pacific side of the Antarctic Peninsula Ice Sheet. Its northeast migration was associated with a positional change of ice streams and inter-trough areas along the shelf, and induced lateral migration of drifts and CCSs along the rise. It may also have affected (or been affected by) the ASL tectonics, a potential relationship that should be further investigated by future research.

The continental margin off Adelaide Island exhibits a complex array of erosional and depositional features clearly zoned from shelf to continental rise localities. Features reflect processes arising from the complex interplay of glacial, glaciomarine and marine conditions as they occur in different oceanographic domains. Lateral changes in dominant processes appear in other areas of the margin (Amblas *et al*., 2006), such as the Bransfield basin (García *et al.*, 2009). The present morphology of this locality includes overdeepened and foredeepened troughs, banks formed by multiple advance-retreat cycles of ice streams and sea floor features formed during the last glacial to glaciomarine transition (Ó Cofaigh *et al.*, 2002, 2005; Livingstone *et al.*, 2013, 2016). Erosional and depositional features reflect alternating advance and retreat of ice streams flowing rapidly over the shelf between inter-trough areas (Fig. 15).

During glacial periods progressive ice sheet advance to the shelf edge (Bentley and Anderson, 1998; Anderson *et al*., 2002) transported large volumes of unsorted glaciogenic sediments (Fig. 15). These generated prograding sequences along the outer shelf and slope (Larter and Barker, 1989; Larter and Cunninghan, 1993; Vanneste and Larter, 1995). Subglacial processes beneath ice streams were efficient in eroding and transporting debris to the shelf edge. Ice streams eroded the seafloor and transported sediment from inner drainage areas to the shelf edge, producing deep troughs along the shelf (Fig. 15), and forming streamlined bedforms in their path (Vanney and Johnson, 1974; Rebesco *et al*., 1998; Canals *et al*., 2000, 2002; Ó Cofaigh *et al.*, 2005; Amblas *et al*., 2006; Larter *et al*., 2009). Northwest of the troughs, the CCSs channelized sediment transfer towards the abyssal plain (Amblas *et al*., 2006). Turbid meltwater plumes and mass-wasting processes occurred at the base of ice stream termini, thereby increasing pelagic and hemipelagic accumulation rates (McGinnis *et al*., 1997; Pudsey and Camerlenghi, 1998; Lucchi *et al.*, 2002; Noormets *et al.*, 2009, Gales et al., 2013). Slope and shelf edge areas associated with ice stream termini experienced higher rates of sediment delivery than those located between ice streams. This flux can be expected to have resulted in greater downslope transport in front of fast-flowing ice streams than in front of slower moving ice as it reached the shelf edge (Rebesco, *et* *al*., 1998). Slopes in front of glacial troughs may have failed more often due to intrinsic physical properties of sediment transported beyond the troughs (Fig. 15), which consisted of low shear-strength material (due to shear remolding) that was poorly consolidated and had a higher degree of sorting relative to sub-glacial tills (Rebesco *et al*., 1998). Sediment slumps evolved downslope into debris flows and turbidity currents, as suggested by Larter and Cunningham (1993). During glacial periods, greater sediment supply along the slope increased rates of gravitational failure. Turbidity current flows within well-developed dendritic CCSs along the upper rise carried coarse-grained particles out to the lower rise and abyssal plain (Fig. 15).

Inter-trough areas (banks) between the major ice streams (e.g., the Marguerite Trough) probably experienced lower rates of ice movement and drainage (Amblas *et al.*, 2006). These areas exhibit well-developed sedimentary lobes and prograding wedge sequences containing high proportions of unsorted sediments (Fig. 15). Episodes of growth along the slope therefore occurred due to mass transport processes (primarily debris flows) along the outer edges of banks during glacial maxima. Numerous slumps along the upper slope facilitated down-slope sediment transport, which evolved quickly downslope into debris flows and turbidity current flows.

7.3. Mixed contourite drifts

The interaction between along-slope contour currents and other depositional processes, mainly down-slope flows, developed large mixed drift bodies on the slope and rise (Rebesco, 2005). The most effective interplay in building mixed drifts occurs between contourites and turbidites, but processes may also involve debrite, hemipelagite and glacigenic systems. The aforementioned types of interaction built the mixed contourite drifts of the Antarctic Peninsula (Camerlenghi *et al.*, 1997; Giorgetti *et al.*, 2003; Hillenbrand *et al.*, 2008). Mixed drifts are also observed at mid-latitudes along other margins (e.g., Camerlenghi and Rebesco, 2008; Hernández-Molina *et al.*, 2009; Llave *et al.*, 2007; Rebesco *et al.*, 2014). The PMAP, however reveals an combination of glacial, turbidite and contour current deposition (Fig. 15). High sedimentation rates along the shelf edge in front of ice streams caused sediment failure and debris flows along the continental slope. These in turn generated turbidity currents along the continental rise, where bathymetric irregularity at the base of the slope could cause hydraulic jumps and changes in flow density (Pudsey and Camerlenghi, 1998). Along the upper rise, interaction between down-slope turbidity currents and ambient southwest-flowing bottom currents (Fig. 15) redistributed the suspended, fine-grained components (from meltwater plumes and turbidity currents), forming large mixed contourite drifts on the rise between the CCSs, especially during glacial periods (Rebesco *et al*., 1996; Rebesco *et al*., 1998, 2002; Amblas *et al*., 2006). Turbidites were subsequently winnowed by contour currents and the material removed was redeposited along ridges. During interglacial periods, ice sheets retreated from the shelf edge while diatomaceous muds accumulated on the shelf, especially within trough depocenters (Pope and Anderson, 1992). These sedimentary processes contributed to drift growth through pelagic and hemipelagic settling, including accumulation of biogenic and glacially-derived material in a weak bottom current setting (Pudsey and Camerlenghi, 1998; Lucchi *et al*., 2002; Amblas *et al*., 2006). The sedimentary model described above resembles that proposed for the Southeast Greenland glaciated margin (Clausen, 1998), except that this latter margin includes a large moat zone formed along the base of the continental slope, below the high-velocity contour current core. The Antarctica Peninsula does not include a moat zone along the slope, probably because bottom currents were weaker and gravitational processes were stronger at this locality.

Based on our results two important aspects should be considered for improving this sedimentary model in the future. First, we show that the main phase of drift development on this part of the PMAP occurred during the late Miocene and early Pliocene, thus coinciding with higher sediment supply and initiation of glacial margin sequences along the outer shelf during SU4 deposition. Drift development therefore began later than inceptions estimated by Rebesco *et al*. (1997; 2002) and Uenzelmann-Neben (2006) for areas where Drifts 6 and 7 formed. These results suggest that drift development may have occurred over multiple episodes along the PMAP. Second, the crest of Drift 5 at water depths of around 2600 m impinges the lower slope. Drifts 1 and 2, located to the northeast, exhibit very shallow crests, while Drifts 6 and 7, located to the southeast occur at greater depths. Drifts located along the PMAP thus occur at different water depths. A particular drift reflects water mass dynamics over a specific water depth range while horizontal upper surfaces reflect density interfaces (pycnocline) between different water masses (e.g., Preu *et al.*, 2013; Rebesco *et al.*, 2014). Some PMAP drifts exhibit more horizontal upper surfaces but additional supporting evidence for a steepened pycnocline at the corresponding depth is lacking.

The overall influence on deposition exerted by the flow of deep Antarctic water masses on the Southern Hemisphere increases during glacial periods (Duplessy *et al.*, 1988; Mulitza *et al.*, 2007; Knutz, 2088). This evolution may have included increased AABW production (Ninnemann and Charles, 2002; Piotrowski *et al.*, 2008) but its interpretation is still under debate (e.g., Krueger *et al.*, 2012). Greater production of water from southerly areas would enhance the AABW layer. By contrast, NADW production weakened during cold periods (McCave *et al.*, 1995; Knutz, 2008), thus reducing the NADW layer in the southwest Atlantic (Kennett, 1982; Viana *et al.*, 2002; Preu *et al.*, 2013) and potentially weakening the LCDW, since this water mass derives primarily from the NADW. During cold (glacial) periods under this scenario, the oceanographic setting would differ from the present one and may have enhanced drift formation along the PMAP during the late Pliocene and Quaternary. While the discussion given above is somewhat speculative, questions of whether the observed drifts relate to the same water masses observed today, and the conditions and timing of their formation, remain unresolved. Different oceanographic conditions would certainly explain asymmetry between the drifts and their location at different depths. Future research should address these unresolved questions. The International Ocean Discovery Program proposal 732 is a timely initiative in this respect since it directly focuses on contourite drifts development along the Antarctic Peninsula Pacific Margin.

8. CONCLUSION

The Pacific Margin of the Antarctica Peninsula (PMAP) offshore of Adelaide Island provides an exceptional sedimentary record of how an active margin transitions into a passive style. This area became passive during the early Miocene, when ridge-crest segments arrived at the trench, causing the end of the subduction and subsequently trench basement topography was eliminated. The study area is particularly unique because the newly initiated passive margin has continued to deform (especially along its lower continental slope and rise) over several million years, due to continued subduction and later collision of an adjacent oceanic segment. In addition to the tectonics, the PMAP offers an excellent scenario to analyze the glacial history of West Antarctica and the timing of changes through which the passive margin shifted from a non-glacial margin to a glacially-influenced margin and finally to a fully glaciated margin. Neogene and Quaternary sedimentary basins recorded these transitions as unconformities and major shifts in sedimentary stacking patterns at the middle to late Miocene, the end of the Pliocene or base of the Quaternary and the Mid Pleistocene. These changes were initially influenced mainly by the tectonics of the region, which progressively was overtaken by climate that influenced long-term global cooling and ice sheet expansion onto the shelf. Our analysis indicates that the initial incursion of ice sheets over the shelf occurred during the late Miocene. A fully glaciated margin, characterized by frequent advances of grounded ice to the shelf break, was established in the study area by latest Miocene to earliest Pliocene time. The primary erosional and depositional features presently observed on the margin began to develop during this time, after the major drift growth and margin progradation, but become fully established at different steeps sometime between the end of the Pliocene, base of the Quaternary and the Mid Pleistocene.

This time frame coincides with the northeast lateral migration of the Marguerite Trough, which strongly influenced development of the margin. The Marguerite Trough migration during the Pliocene until the Mid Pleistocene in fact represents a major controlling factor in the margin's evolution, due to its influence on ice sheet drainage along the shelf, which in turn caused dramatic changes in slope and rise morphology. Trough migration differentiates this sector of the PMAP from other areas, in which major troughs along the shelf show no relationship to turbidite canyon-channel systems along the rise. Other areas also differ from the PMAP in terms of their inter-trough areas and major contourite mixed drifts along the rise.

Tectonics, climate, sea-level evolution, glacial and palaeoceanographic changes exerted major influence on margin growth pattern at specific time intervals. Their spatiotemporal influence is evident in deep-water sedimentation processes that constructed the margin, particularly the persistent along- and down-slope sedimentary processes. Key events described here also appear in other basins found in both the southern and northern hemispheres, thus supporting the global influence of these plate tectonic, oceanographic and climatic variations (e.g., Potter and Szatmari, 2009; Zachos *et al.*, 2001; Miller *et al.*, 2011; Maldonado *et al.*, 2006; 2014; Preu et al., 2012, 2013; Hernández-Molina *et al.*, 2014; 2016). Our approach can be more widely applied and integrated with other studies to understand other areas of the Antarctic continental margin, to document palaeoenvironmental and palaeoceanographic changes and to identify these events in sedimentary sections. Given the complexity of this PMAP multiphase margin evolution, many questions may be a subject of debate, mostly the global applicability of this margin's evolution. The scarcity of drill core data from deep-water sites as well as the relatively poor quality and low-resolution of lithostratigraphic and chronostratigraphic data acquired from these sites represents a major impediment to resolve questions and uncertainties described above. Further and more detailed analysis of high-resolution stratigraphic data will help constrain and enhance our understanding of the margin and its relation to global climate and ocean dynamics.

Acknowledgement

We began this study in 2003. More than a decade of extensive research on the morphology and seismic stratigraphy of this highly remote area leaves us with too many people to thank. The list of contributions given below is a summary but our gratitude to those not listed remains unabridged. We first thank several individuals who have shared their ideas through meetings, research collaboration and publications. This work was conducted during research periods F.J. Hernández-Molina spent at the British Antarctic Survey (BAS) in 2003, 2004, 2005 and 2007, as part of a Spanish-British scientific collaboration on the study of the continental margin offshore of Adelaide Island. These periods were funded by the Spanish Ministry of Education and Science Mobility Award (PR2002-0271 [2003] and PR2003-0421 [2004-2005]) and by the Royal Society of the UK, through an International Short Visit fellowship (2007). The Spanish Comisión Interministerial de Ciencia y Tecnología (CYCIT) supported our research through projects ANT96-1001 ANT99-0817, REN2001-2143 and REN2003-01498, CTM2008-06386-C02/ANT, CTM 2008-06399-C04/MAR (CONTOURIBER), CTM2011-30241-C02-01(ConPacA) and CTM 2012-39599-C03 (MOWER). Research was conducted in the framework of the "*Drifters Research Group*" of the Royal Holloway University of London (UK). Data from the Istituto Nazionale di Oceanografia e di Geofisica Sperimentale (OGS, Italy) and Brazilian Antarctic Program were obtained from the Scientific Committee on Antarctic Research Seismic Data Library System (SCAR-SDLS; SCAR, 2001; Wardell et al., 2007). The authors thank the captains, officers, crew, support staff and scientists who participated in research cruises that provided data for this study. A. C. Naveira Garabato (NOCS, UK), A. Piola (SHN, Argentina) and A. H. Orsi (University of Washington, USA) are thanked for thorough and constructive reviews and comments concerning the oceanographic setting of the study area. Finally, we also thank the editor, Dr. T. Cronin, and the two anonymous reviewers for their very positive and helpful feedback and suggestions, which helped us to improve the paper.

9. REFERENCES

Aceñolaza, F.G., 2000, La Formación Paraná (Mioceno medio): estratigrafía, distribución regional y unidades equivalentes. In: Aceñolaza F. G. and Herbst R. (Eds.), El Neógeno de Argentina. Tucumán: INSUGEO, Serie Correlación Geológica, 14: 9–-27.

Amblas, D., Urgeles, R., Canals, M., Calafat, A. M., Rebesco, M., Camerlenghi, A., Estrada, F., De-Batist, M., Hughes-Clarke, J. E. 2006. Relationship between continental rise development and palaeo-ice sheet dynamics, northern Antarctic Peninsula Pacific margin. Quat. Sci. Rev. 25, 933-944.

Anderson, J.B., 1999. Antarctic Marine Geology. Cambridge University Press, 288 pp.

Anderson, J.B., Pope, P.G., Thomas, M.A., 1990. Evolution and hydrocarbon potential of the northern Antarctic Penninsula continental shelf. In: StJohn, B. (Ed.), Antarctica as an Exploration Frontier – Hydrocarbon Potential, Geology an Hazards, Am. Assoc. Pet. Geol. Stud. Geol., 31:1-12.

Anderson, J.B., Shipp, S.S., 2001. Evolution of the West Antarctic ice-sheet. In: Alley, R.B., Bindschadler, R.A., (Eds), The West Antarctic ice-sheet: behavior and environment. AGU, Antar Jansen, E., Raymo, M.E., 1996. Leg 162: New Frontiers on past climates. In Proceeding of the Ocean Drilling Program, Initial Reports, Jansen, E., Raymo, M.E., Blum, P *et al.* (Eds.), 162: pp. 5-20.

Anderson, R.F., Chase, Z., Fleisher, M.Q., Sachs, J., 2002. The Southern Ocean’s biological pump during the Last Glacial Maximum. Deep-Sea Research II 49, 1909-1938.

Barker, P. F., 1982. The Cenozoic subduction history of the Pacific margin of the Antarctic Peninsula: Ridge crest-trench interactions, J. Geol. Soc. London, 139, 787– 801.

Barker, P.F., 2001. Scotia Sea regional tectonic evolution: implications for mantle flow and palaeocirculation. Earth-Science Review, 55:1–39.

Barker, P.F., Burrell, J., 1977. The opening of Drake Passage. Mar. Geol. 25, 15-34.

Barker, P.F., Camerlenghi, A., 2002. Glacial History of the Antarctic Peninsula from Pacific margin sediments. In: Barker, P.F., Camerlenghi, A., Acton, G.D., Ramsay, A.T.S. (Eds.), Proc. ODP, Sci. Results, 178, 1-40.

Barker, P.F., Camerlenghi, A., Acton G.D., Ramsay, A.T.S. et al., 2002. Proceedings of the Ocean Drilling Program, Scientific Results 178 (CD-ROM). Available from: Ocean Drilling Program, Texas A&M University, College Station, TX 77845-9547, U.S.A.

Barker, P.F., Camerlenghi, A., Acton, G., and the Leg 178 Scientific Party, 1998 Antarctic Glacial History and sea level change-Leg 178 samples Antarctic Peninsula margin sediments. JOIDES Journal, 24 (2): 7-10.

Barker, P.F., Camerlenghi, A., and the Leg 178 Scientific Party, 1999. Proc. ODP, Init. Repts., 178: College Station, TX (Ocean Drilling Program), 90 pp.

Barreda, V., Palamarczuk, S., 2000. Estudio palinoestratigrafico del Oligoceno tardio-Mioceno en secciones de la costa patagonica y plataforma continental argentina. In: Aceñolaza, F.G., Herbst, R. (Eds.), El Neogeno de Argentina. INSUGEO, Serie Correlacion Geologica, vol. 14, pp. 103–138. Tucuman.

Barrett, P.J. 1996. Antarctic paleoenvirornment through Cenozoic times &endash; A review. Terra Antartica, 3(2), 103-119.

Bart P.J., Anderson J.B., 1997. Grounding Zone Wedges on the Antartic Continental Shelf, Antartic Peninsula. In: Glaciated Continental Margins: An Atlas of Acoustic Images (T. A. Davies; T. Bell; A.K. Cooper; H. Josenhans; L. Polyak; A. Solheim; M. S. Stoker and J.A. Stravers. Eds). Chapman & Hall.London.96-97.

Bart, P.J. Anderson, J.B., 2000. Relative temporal stability of the Antarctic ice sheets during the Late Neogene based on the minimum frequency of outer grounding events. Earth and Planetary Science Letters 182 (3), 259-272.

Bart, P.J., 2001. Did the Antarctic ice sheets expand during the early Pliocene? Geology 29, 67-70.

Bart, P.J., Anderson, J.B., 1995. Seismic record of glacial events affecting the Pacific Margin of the Northwestern Antarctic Peninsula. In: Cooper, A.K., Barker, P.F., Brancolini, G. (Eds.), Geology and Seismic Stratigraphy of the Antarctic Margin, AGU, Antarct. Res. Ser. 68, 74-95.

Bart, P.J., Anderson, J.B., 1996. Seismic expression of depositional sequences associated with expansion and contraction of ice sheets on the northwestern Antarctic Peninsula continental shelf. In: de Batist, M. and Jacobs, P. (eds.), Geology of Siliciclastic Shelf Seas. Geological Society Special Publication, 117: 171-186.

Bart, P.J., C.D. Hillenbrand, W. Ehrmann, M. Iwai, D. Winter and S.A. Warny, 2007. Are Antarctic Peninsula Ice Sheet grounding events manifest in sedimentary cycles on the adjacent continental rise? Marine Geology, 236, 1-13.

Bart, P.J., Egan, D.E., Warny, S.A., 2005. Direct constraints on Antarctic Peninsula Ice Sheet grounding events between 5.12 and 7.94 Ma. J. Geophys. Res. 110, F04008.

Bartek, L.R., Vail., P.R., Anderson, J.B., Emmet, P.A., Wu, S., 1991. Effect of Cenozoic ice sheet fluctuations in Antarctica on the stratigraphic signature of the Neogene. J. Geophys. Res., 96: 6753-6778.

Belknap, D.F., Shipp, R.C., 1991. Seismic Stratigraphy of glacial marine units, Maine Inner shelf. In: Anderson, J.B., Ashley, G.M. (eds.), Glacial Marine Sedimentation: Paleoclimatic Significance. Geological Society of America, Special Paper, 261: 137-157.

Bentley, M.J., Anderson, J.B., 1998. Glacial and marine geological evidence for the ice sheet configuration in the Weddell Sea- Antarctic Peninsula region during the Last Glacial Maximum. Antarctic Science 10, 309–325.

Berger, W.F., Yasuda, M.K., Bickert, T., Wefer, G., Takayamat, T., 1994. Quaternary time scale for Ontong Java plateau: Milankovitch template for ocean drilling program site 806. Geology 22, 463–467.

Billups, K., 2002. Late Miocene through early Pliocene deep water circulation and climate change viewed from the sub-Antartic South Atlantic. Palaeogeogr. Palaeoclimatol. Palaeoecol. 185, 287-307.

Bingham, R.G., Ferraccioli, F., King, E.C., Larter, R.D., Pritchard, H.D., Smith, A.M. & Vaughan, D.G. 2012. Inland thinning of West Antarctic Ice Sheet steered along subglacial rifts. *Nature*, 487, 468–471.

Bohoyo, F., 2004. Fragmentación continental y desarrollo de cuencas oceánicas en el sector meridional del Arco de Scotia, Antártida, Thesis. Universidad de Granada, Spain, 252 pp.

Bolmer, S.T. 2008. A note on the development of the bathymetry of the continental margin west of the Antarctic Peninsula from 65° to 71°S and 65° to 78°W. Deep-Sea Research II 55(3-4): 271-276.

Boulton, G.S., 1990. Sedimentary and sea level changes during glacial cycles and their control on glaciomarine facies architecture. In: Dowdeswell, J.A., Scourse, J.D., (eds.). Glaciomarine Environments: Processes and Sediments. Geological Society Special Publication, 53: 15-52.

Camerlenghi, A., Crise, A., Pudsey, C.J., Accerboni, E., Laterza, R., Rebesco, M., 1997. Ten month observation of the bottom current regime across a sediment drift of the Pacific margin of the Antarctic Peninsula. Antarctic Science 9, 426-433.

Canals, M., Casamor, J.L., Urgeles, R., Calafat, A.M., Domack, E.W., Baraza, J., Farran, M., De Batist, M., 2002. Seafloor evidence of a subglacial sedimentary system off the northern Antarctic Peninsula. Geology 30, 603–606.

Canals, M., Urgeles, R., Calafat, A.M., 2000. Deep sea-floor evidence of past ice streams off the Antarctic Peninsula. Geology 28, 31–34.

Cande, S. C., Stock, J.M., Müller, R.D., Ishihara, T., 2000. Cenozoic motion between East and West Antarctica, Nature, 404(6774), 145–150.

Cande, S.C., Kent, D.L., 1995, Revised calibration of the geomagnetic polarity timescale for the Late Cretaceous and Cenozoic. *J. Geophys. Res.* **100**, 6093-6095.

Carter L., Carter, R.M., McCave, I.N., 2004, Evolution of the sedimentary system beneath the deep Pacific inflow off eastern New Zealand: Marine Geology, 205: 9–27.

Carter, L., McCave, I.N., Williams, M.J.M., 2009. Circulation and Water Masses of the Southern Ocean: A Review. In: Fabio Florindo and Martin Siegert (Eds.), Developments in Earth and Environmental Sciences. Antarctic Climate Evolution, The Netherlands: Elsevier, vol 8: 85–114.

Clark P.U., Alley, R.B., Pollard, D., 1999. Northern Hemisphere Ice-Sheet Influences on Global Climate Change. Science 286:1104-1111.

Clark, P.U., Archerb, D., Pollard, D., Blumd, J.D., Riale, J.A., 2006. The middle Pleistocene transition: characteristics, mechanisms, and implications for long-term changes in atmospheric pCO2. Quaternary Science Reviews 25: 3150–3184.

Clausen, L. 1998. The Southeast Greenland glaciated margin: 3D stratal architecture of shelf and deep sea. In: Stoker, M., Evans, D., Cramp, A. (eds.) Geological Processes on Continental Margins: Sedimentation, Mass-Wasting and Stability. Geological Society, London, Special Publications, 129, 173-203.

Cloetingh, S., Gradstein, F.M., Kooi, H., Grant, A.C. and Kaminski, M., 1990, Plate reorganization: a cause of rapid late Neogene subsidence and sedimentation around the North Atlantic?. Journal of the Geological Society, London, 147: 495-506.

Cooper, A.K., Barrett, P., Stagg, H., Storey, B., Stump, E., Wise, W., 2008. Antarctica: A Keystone in a Changing World. Proceedings of the 10th International Symposium on Antarctic Earth Sciences, Polar Research Board, Division on Earth and Life Studies, National Research Council, U.S. Geological Survey. National Academies Press, 164 pp.

Cooper, A.K., Barrett, P.J., Hinz, K., Traube, V., Leitchenkov, G., and Stagg, H.M.J., 1991. Cenozoic prograding sequences of the Antarctic continental margin: a record of glacio-eustatic and tectonic events. *Mar. Geol.,* 102:175–213.

Cooper, A.K., O'Brien, P.E., Richter, C. (eds.), 2004. Proceedings of the Ocean Drilling Program, Scientific Results, College Station, Texas, Ocean Drilling Program, doi:10.2973/odp.proc.sr.188.2004.

Cramer, B.S., Toggweiler, J.R.,Wright, J.D., Katz, M.E., Miller, K.G., 2009. Ocean overturning since the late Cretaceous: inferences from a new benthic foraminiferal isotope compilation. Paleoceanography 24 (PA4216), 1–14.

Dahlgren, K.I.T., Vorren, T.O., Stoker, M.S., Nielsen, T., Nygard, A., Sejrup, H.S., Sejrup, H.P., 2005. Late Cenozoic prograded wedges on the NW European continental margin: their formation and relationship to tectonics and climate. Mar. Pet. Geol. 22, 1089–1110.

Dowdeswell, J. A., Canals, M., Jakobsson, M., Todd, B. J., Dowdeswell, E. K., Hogan, K. A., (eds) 2016. Atlas of Submarine Glacial landforms: Modern, Quaternary and Ancient. Geological Society, London, Memoirs, 46, http://doi.org/10.1144/M46.

Dowdeswell, J.A., Ó Cofaigh, C., (ed.s), 2002. *Glacier-Influenced Sedimentation on High Latitude Continental Margins*, Geological Society, London, Special Publication, No. 203, 378 pp.

Dowdeswell, J.A., Ó Cofaigh, C., Pudsey, C.J., 2004. Continental slope morphology and sedimentary processes at the mouth of an Antarctic palaeo-ice stream. *Mar. Geol.* 204, 203-214.

Duplessy, J.C., Shackleton, N.J., Fairbanks, R.G., Labeyrie, L., Oppo, D., Kallel, N., 1988. Deep water source variations during the last climatic cycle and their impact on the global deep water circulation. Paleoceanography, 3(3): 343–360.

Eagles, G., 2003. Plate tectonics of the Antarctic–Phoenix plate system since 15 Ma. Earth Planet. Sci. Lett. 88, 289–307.

Eagles, G., Gohl, K., Larter, R.D., 2009. Animated tectonic reconstruction of the Southern Pacific and alkaline volcanism at its convergent margins since Eocene times. Tectonophysics 464: 21―29.

Eagles, G., Jokat, W., 2014. Tectonic reconstructions for paleobathymetry in Drake Passage. Tectonophysics, 611, 28-50, http://dx.doi.org/10.1016/j.tecto.2013.11.021.

Eagles, G., Larter, R.D., Gohl, K., Vaughan, A.P.M. 2009. The West Antarctic Rift System in the Antarctic Peninsula. *Geophysical Research Letters*, 36, L21305, doi:10.1029/2009GL040721.

Escutia, C., Brinkhuis, H., Klaus, A. and the Expedition 318 Scientists, 2011. Proceedings IODP, 318. Integrated Ocean Drilling Program Management International, Inc., Tokyo http://dx. doi.org/10.2204/iodp.proc.318.2011 (101 pp.).

Escutia, C., De Santis, L., Donda, F., Dunbar, R.B., Cooper, A.K., Brancoli, G., Eittreim, S.L., 2005. Cenozoic ice sheet history from East AntarcticWilkes Land continental margin sediments. Glob. Planet. Chang. 45, 51–81. http://dx.doi.org/10.1016/j.gloplacha.2004.09.010.

Eyles, N, Daniels, J., Osterman, L.E., Januszczak, N., 2001. Ocean Drilling Program Leg 178 (Antarctic Peninsula): sedimentology of glacially influenced continental margin topsets and foresets. *Mar. Geol.* 178, 135-156.

Faugères, J.-C., Stow, D.A.V., 2008. Contourite drifts: Nature, evolution and controls, in: Rebesco, M., Camerlenghi, A. (Eds.), Contourites. Elsevier, Amsterdam, Developments in Sedimentology 60, pp. 257–288.

Faugères, J.-C., Stow, D.A.V., Imbert, P., Viana, A.R., 1999. Seismic features diagnostic of contourite drifts. Marine Geology 162, 1-38.

Flower, B.P., and Kennett, J.P., 1994, The middle Miocene climatic transition: East Antarctic ice sheet development, deep ocean circulation and global carbon cycling: Palaeogeography, Palaeoclimatology, Palaeoecology, v. 108, p. 537-555.

Foldvik, A., Gammelsrød, T., Østerhus, S., Fahrbach, E., Rohardt, G., Schröder, M., Nicholls, K.W., Padman, L., Woodgate, R.A., 2004. Ice shelf water overflow and bottom water formation in the southern Weddell Sea. Journal of Geophysical Research C 109 (2), C02015 1-15.

Gales, J.A., Larter, R.D., Mitchell, N.C. & Dowdeswell, J.A. 2013. Geomorphic signature of Antarctic submarine gullies: Implications for continental slope processes. *Marine Geology*, 337, 112-124.

Galindo-Zaldívar, J., Gambôa, L.A.P, Maldonado, A., Bochu, Y., Nakao S., 2004. Tectonic deformations along the South Shetland block boundaries and the development of Bransfield Strait. Marine Geology 206: 267-282.

García, M., Ercilla, G., Alonso, B., 2009. Morphology and sedimentary systems in the Central Bransfield Basin, Antarctic Peninsula: sedimentary dynamics from shelf to basin. Basin Research 21, 295–314.

García,M., Ercilla, G., Anderson, J.B., Alonso, B., 2008. Newinsights on the post-rift seismic stratigraphic architecture and sedimentary evolution of the Antarctic Peninsula margin (Central Bransfield Basin). Marine Geology 251, 167–182.

Giorgetti, G., Crise, A., Laterza, R., Perini, L., Rebesco, M., Camerlenghi, A., 2003. Water masses and bottom boundary layer dynamics above a sediment drift of the Antarctic Peninsula Pacific Margin. Antarct. Sci. 15, 537-546.

Giosan, L., Flood, R.D., Grützner, J., Mudie, P., 2002. Paleoceanographic significance of sediment color on western North Atlantic Drifts: II. Late Pliocene-Pleistocene sedimentation. Mar. Geol. 189, 43-61.

Graham, G. C., Nitsche, F.O., Larter, R.D., 2011. An improved bathymetry compilation for the Bellingshausen Sea, Antarctica, to inform ice-sheet and ocean models. The Cryosphere, 5, 95-106, 2011.

Granot, R., S., Cande, C., Stock, J.M., Davey, F.J., Clayton, R.W., 2010. Postspreading rifting in the Adare Basin, Antarctica: Regional tectonic consequences, Geochem. Geophys. Geosyst., 11, Q08005, doi:10.1029/2010GC003105.

Haq, B.U., Hardenbol, J., Vail, P.R., 1987. Chronology of fluctuating sea levels since the Triassic: Science, 235: 1156–1167.

Harris, P.T., Brancolini, G., Armand, L., Busetti, M., Beaman, R.J., Giorgetti, G., Presti, M., Trincardi, F., 2001. Continental shelf drift deposits indicates non-steady state Antarctic bottom water production in the Holocene. Marine Geology, 179: 1-8.

Haywood, A.M., Smellie, J.L., Ashworth, A.C., Cantrill, D.J., Florindo, F., Hambrey, M.J., Hill, D., Hillenbrand, C.D., Hunter, S.J., 2Larter, R.D., Lear, C.H., Passchier, S., van de Wal, R., 2009. Middle Miocene to Pliocene History of Antarctica and the Southern Ocean. In: Antarctic Climate Change (F. Florindo and M. Siegert, eds). Developments in Earth and Environmental Sciences, 8 . Elsevier, Amsterdam, pp- 401-463.

Hernández-Molina, F.J., Llave, E., Sierro, F.J., Roque, C., Van der Schee, M., Williams, T., Ledesma, S., Arnais, A., Rosales, C., Brackenridge, R.E., Stow, D.A.V., 2016. Evolution of the Gulf of Cadiz Margin and west Portugal contourite depositional system: tectonic, sedimentary and paleoceanographic implications from IODP Expedition 339. *Marine Geology*,, 377:7-39. doi:10.1016/j.margeo.2015.09.013

Hernández-Molina, F.J., Maldonado, A., Somoza, L., Vázquez, J.T., Barnolas, A., 2000. Arquitectura estratigráfica de la plataforma continental de Adelaida (Península Antártica). Geo-Temas, 1(4): 159-162.

Hernández-Molina, F.J., Paterlini, M., Somoza, L., Violante, R., Arecco, M.A., de Isasi, M., Rebesco, M., Uenzelmann-Neben, G., Neben, S., Marshall, P., 2010. Giant mounded drifts in the Argentine Continental Margin: Origins, and global implications for the history of thermohaline circulation. Marine and Petroleum Geology, 27: 1508-1530.

Hernández-Molina, F.J., Paterlini, M., Violante, R., Marshall, P., de Isasi, M., Somoza, L., Rebesco, M., 2009. A contourite depositional system on the Argentine Slope: an exceptional record of the influence of Antarctic water masses. Geology, I37 (6): 507-510.

Hernandez-Molina, F.J., Somoza, L., Vázquez, J.T., Lobo, F., Fernández-Puga, M.C., Llave, E., Diaz-del Rio, V., 2002. Quaternary stratigraphic stacking patterns on the continental shelves of the southern Iberian Peninsula: their relationship with global climate and palaeoceanographic changes. Quat Inter 92:5-23

Hernández-Molina, F.J., Stow, D.A.V., Alvarez-Zarikian, C.A., Acton, G., Bahr, A., Balestra, B., Ducassou, E., Flood, R., Flores, J.A., Furota, S., Grunert, P., Hodell, D., Jimenez-Espejo, F., Kim, J.K., Krissek, L., Kuroda, J., Li, B., Llave, E., Lofi, J., Lourens, L., Miller, M., Nanayama, F., Nishida, N., Richter, C., Roque, C., Pereira, H., Sanchez

Goñi, M.F., Sierro, F.J., Singh, A.D., Sloss, C., Takashimizu, Y., Tzanova, A., Voelker, A., Williams, T., Xuan, C., 2014b. Onset of Mediterranean Outflow into the North Atlantic, *Science*, 344: 1244-1250.

Hernández-Molina, F.J.; Larter, R. D.; Maldonado, A. and Rodríguez-Fernández, J., 2006a. Evolution of the Antarctic Peninsula Pacific margin offshore from Adelaide Island since the Late Miocene: An example of a glacial passive margin. *Terra Antarctica Reports, 12: 81-90.*

Hernández-Molina, F.J.; Larter, R. D.; Rebesco, M. and Maldonado, A., 2006b. Miocene reversal of bottom water flow along the Pacific margin of the Antarctic Peninsula: Stratigraphic evidences from a "Contourite Sedimentary Tail". *Marine Geology*, 1-4: 93-116.

Herron, E.M., Tucholke, B.E., 1976. Sea-floor magnetic patterns and basements structure in the southeastern Pacific. Initial Rep. Deep Sea Drill. Proj., 35: 263-278.

Hillenbrand, C-D, D.K. Futterer, 2003. Distribution of clay minerals and proxies for productivity in surface sediments of the Bellingshausen and Amundsen seas (West Antarctica) - Relation to modern environmental conditions. Mar. Geol. 193, 253-271.

Hillenbrand, C.D., Camerlenghi, A., Cowan, E.A., Hernández-Molina, F.J., Lucchi, R.G., Rebesco, M., Uenzelmann-Neben, G., 2008. The present and past bottom-current flow regime around the sediment on the continental rise of the Antarctic Peninsula. *Marine Geology*, 255: 55-63.

Hillenbrand, C.D., Futterer, D.K., 2002. Neogene to Quaternary deposition of opal on the continental rise west of the Antarctic Peninsula, ODP Leg 178, Sites 1095,1096, and 1101. In: Barker, P.F., Camerlenghi, A., Acton, G.D., Ramsay, A.T.S. (Eds.), Proc. ODP Sci. Results 178. Ocean Drilling Program, College Station, TX, pp. 1-33 [CD ROM]. Available from: Ocean Drilling Program, Texas A&M University, College Station, TX 77845-9547, U.S.A.

Hinz, K., Neben, S., Schreckenberger, B., Roeser, H.A., Block, M., Goncalves de Souza, K., Meyer, H., 1999. The Argentine continental margin north of 48º S: sedimentary successions, volcanic activity during break-up: Marine and Petroleum Geology, v.16, pp. 1–25.

Hollister, C.D., Craddock, C. *et al*., 1976. *Initial Reports of the Deep Sea Drilling Project*, 35. U.S. Government Printing Office, Washington, D.C., 930 pp.

Houben, A.J.P., Bijl, P.K., Pross, J., Bohaty, S.M., Passchier, S., Stickley, C.E., Röhl, U., Sugisaki, S., Tauxe, L., van de Flierdt, T., Olney, M., Sangiorgi, F., Sluijs, A., Escutia, C., Brinkhuis, H., and the Expedition 318 Scientists, 2013. Reorganization of Southern Ocean Plankton Ecosystem at the Onset of Antarctic Glaciation. Science, 340, 6130: 341-344.

Iwai, M., and Winter, D., 2002. Data report: Taxonomic notes on Neogene diatoms from the western Antarctic Peninsula: Ocean Drilling Program Leg 178, in Barker, P.F., et al., eds., Proceedings of the Ocean Drilling Program, Scientifi c Results, Volume 178: College Station, Texas, Ocean Drilling Program: http://www-odp.tamu.edu/publications/178_SR/ chap_35/chap_35.htm (September 2006).

Jabaloy, A., Balanyá, J.C., Barnolas, A., Galindo-Zaldívar, J., Hernández, F.J., Maldonado, A., Martínez, J.M., Rodríguez-Fernández, J., Sanz de Galdeano, C., Somoza, L., Suriñach, E., Vazquez, T., 2003. The transition from an active margin to a passive one (SW end of the South Shetland Trench, Antarctic Peninsula). Tectonophysics 336, 55– 81.

Jansen, E., Raymo, M.E., 1996. Leg 162: New Frontiers on past climates. In Proceeding of the Ocean Drilling Program, Initial Reports, Jansen, E., Raymo, M.E., Blum, P *et al.* (Eds.), 162: pp. 5-20.

Joseph, L.H., Rea, D.K., van der Pluijm, B.A., 2004. Neogene history of the Deep Western Boundary Current at Rekohu sediment drift, Southwest Pacific (ODP Site 1124): Marine Geology, 205: 185–206.

Katz, M.E., Cramer, B.S., Toggweiler, J.R., Esmay, G., Liu, C., Miller, K.G., Rosenthal. Y., Wade, B.S., Wright, J.D., 2011. Impact of Antarctic Circumpolar Current Development on Late Paleogene Ocean Structure. Science, 332, 6033: 1076-1079.

Kennett, J.P., 1982. Marine Geology. Prentice Hall, 813 pp.

Kitamura, A., Kawagoe, T. 2006. Eustatic sea-level change at the Mid-Pleistocene climate transition: new evidence from the shallow-marine sediment record of Japan. Quat Sci Rev 25:323-335.

Knutz, P.C., 2008, Palaeoceanographic significance of contourite drifts. In *Contourites. Developments in Sedimentology* (eds Rebesco, M. & Camerlenghi, A.) 60, 511-535 (Elsevier, Amsterdam).

Kominz,M.A., Browning, J.V.,Miller, K.G., Sugarman, P.J., Mizintseva, S., Scotese, C.R., 2008. Late Cretaceous to Miocene sea-level estimates from the New Jersey and Delaware coastal plain coreholes: an error analysis. Basin Res. 20 (2), 211–226.

Krueger, S., Leuschner, D.C., Ehrmann, W., Schmiedl, G., Mackensen,A., 2012. North Atlantic Deep Water and Antarctic Bottom Water variability during the last 200 ka recorded in an abyssal sediment core off South Africa. Global Planet. Change 80–81,180–189.http://dx.doi.org/10.1016/j.gloplacha.2011.10.001.

Laberg, J.S., Andreassen, K., Knies, J., Vorren, T.O., Winsborrow, M., 2010. Late PlioceneePleistocene development of the Barents Sea ice sheet. Geology 38, 107e 110.

LaBrecque, J.L., Kent, D.V., Cande, S.C., 1977. Revised magnetic polarity time scale for Late Cretaceous and Cenozoic time. Geology, 5: 330-335.

Lagabrielle, Y., Goddéris, Y., Donnadieu, Y., Malavieille, J., Suarez, M., 2009. The tectonic history of Drake Passage and its possible impacts on global climate. Earth and Planetary Science Letters, 279: 197-211.

Larter, R. D., Graham, A. G.C., Gohl, K., Kuhn, G., Hillenbrand, C.-D., Smith, J. A., Deen, T. J., Livermore, R. A., Schenke, H.-W., 2009. Subglacial bedforms reveal complex basal regime in a zone of paleo-ice stream convergence, Amundsen Sea embayment, West Antarctica. Geology, 37. 411-414. doi:10.1130/G25505A.1

Larter, R.D., 2007, Margin architecture reveals the transition to the modern Antarctic ice sheet ca. 3 Ma: Geology: Comment, doi: 10.1130/ G23422C.1.

Larter, R.D., and Barker, P.F., 1989, Seismic stratigraphy of the Antarctic Peninsula Pacific margin: A record of Pliocene–Pleistocene ice volume and paleoclimate: Geology, v. 17, p. 731–734, doi: 10.1130/0091-7613 (1989)017<0731:SSOTAP>2.3.CO;2.

Larter, R.D., Barker, P.F., 1991a. Effects of ridge crest-trench interaction on Antarctic-Phoenix spreading: forces on a young subducting plate, *J. Geophys. Res.* 96, 19, 583-607.

Larter, R.D., Barker, P.F., 1991b, Neogene interaction of tectonic and glacial processes at the Pacific margin of the Antarctic Peninsula, in Macdonald, D.I.M., ed., Sedimentation, Tectonics and Eustasy: International Association of Sedimentologists Special Publication, v. 12, p. 165–186.

Larter, R.D., Cunningham, A.P., 1993. The depositional pattern and distribution of glacial-interglacial sequences on the Antarctic Peninsula Pacific margin. Mar. Geol. 109, 203-219.

Larter, R.D., Rebesco, M., Vanneste, L.E., Gambôa, L.A.P., and Barker, P.F., 1997, Cenozoic tectonic, sedimentary and glacial history of the continental shelf west of Graham Land, Antarctic Peninsula. In Barker, P.F., and Cooper, A.K., eds., Geology and Seismic Stratigraphy of the Antarctic Margin, 2: American Geophysical Union Antarctic Research Series, v. 71, p. 1–27.

Larter, R.D., Vanneste, L.E., 1995. Relict subglacial deltas on the Antarctic Peninsula outer shelf. Geology, 23: 33-36.

Larter, R.D., Vanneste, L.E., Morris, P., Smythe, D.K. 2003. Structure and tectonic evolution of the South Sandwich arc. *Geological Society, London, Special Publications*, 219, 255–284.

Lavelle, M., Barker, P.F., and Osterman, L.E., 2002, Data report: Strontium isotope dating of barnacle fragments, Antarctic Peninsula Site 1103, in Barker, P.F. et al., eds., Proceedings of the Ocean Drilling Program, Scientifi c Results, Volume 178: College Station, Texas, Ocean Drilling Program: http://www-odp.tamu.edu/publications/178_SR/ chap_27/chap_27.htm (September 2006).

Lawver, L.A., Gahagan, L.M., 2003. Evolution of Cenozoic seaways in the circum-Antarctic region: Palaeogeography, Palaeoclimatology, Palaeoecology, 198: 11–37.

Lear, C.H., Elderfield, H., Wilson, P.A., 2000. Cenozoic deep-sea temperatures and global ice volumes from Mg/Ca in benthic foraminiferal calcite. Science, 287, 269-272.

Ledbetter, M.T., Ciesielski, P.F., 1986. Post-miocene disconformities and paleoceanography in the Atlantic sector of the Southern Ocean: Palaeogeography, Palaeoclimatology, Palaeoecology, 52 (3-4): 185–214.

Lewis, A. R., Marchant, D. R., Ashworth, A. C., Hemming, S. R., Machlus,M. L., 2007. Major middle Miocene global climate change: Evidence from East Antarctica and the Transantarctic Mountains. Geol. Soc. Am. Bull., 119, 1449–1461. DOI: 10.1130B26134.1

Lewis, A.R., Marchant, D.R., Ashworth, A.C., Hedenäs, L., Hemming, S.R., Johnson, J.V., Leng, M.J., Machlus, M.L., Newton, A.E., Raine, J.I., Willenbring, J.K., Williams, M., Wolfe, A.P., 2008. Mid-Miocene cooling and the extinction of tundra in continental Antarctica. Proc. National Acad. Sci., 105 (31): 10676-10680. DOI:10.1073/pnas.0802501105

Lindeque, A., Gohl, K., Henrys, S., Wobbe, F., Davy, B., 2016. Seismic stratigraphy along the Amundsen Sea to Ross Sea continental rise: A cross-regional record of pre-glacial to glacial processes of theWest Antarctic margin. Palaeogeography, Palaeoclimatology, Palaeoecology 443: 183–202

Lindeque, A., Martin, Y.M., Gohl, K., Maldonado, M., 2013. Deep-sea pre-glacial to glacial sedimentation in theWeddell Sea and southern Scotia Sea froma cross-basin seismic transect. Mar. Geol. 336, 61–83. http://dx.doi.org/10.1016/j.margeo.2012.11.004.

Livermore, R., Eagles, G., Morris, P, Maldonado, A., 2004. Shackleton Fracture Zone: no barrier to early circumpolar ocean circulation. Geology, 32:797–800.

Livermore, R., McAdoo D., Marks, K., 1994. Scotia Sea tectonics from high-resolution satellite gravity. Earth Planet Science Letter, 123:255–268.

Livermore, R.A., Balanyá, J.C., Maldonado, A., Martínez, J.M., Rodríguez-Fernández, J., Sanz de Galdeano, C., Galindo-Zaldívar, J., Jabaloy, A., Barnolas, A., Somoza, L., Hernández, J., Suriñach, E., Viseras, C., 2000, Autopsy on a dead spreading centre: the Phoenix Ridge, Drake Passage, Antarctica. *Geology* **18**, 607-610.

Livingstone, S.J., Ó Cofaigh, C., Stokes, C.R., Hillenbrand, C.-D.,Vieli, A., Jamieson, S.S.R., 2013. Glacial geomorphology of Marguerite Bay Palaeo-Ice stream, western Antarctic Peninsula, Journal of Maps, 9:4, 558-572, DOI: 10.1080/17445647.2013.829411

Livingstone, S.J., Stokes, C.R., Ó cofaigh, C., Hillebrand, C-D., Vieli, A., Jamieson, S.S.R., Spagnolo, M., Dowdeswell, J.A., 2016. Subglacial processes on an Antarctic ice stream bed. 1: Sediment transport and bedform genesis inferred from marine geophysical data. Journal of Glaciology, doi:10.1017/jog.2016.18

Llave, E., Hernández-Molina, F.J., Somoza, L., Díaz-del-Río, V., Stow, D.A.V., Maestro, A., Alveirinho Dias, J.M., 2001. Seismic stacking pattern of the Faro-Albufeira contourite system (Gulf of Cadiz): a Quaternary record of paleoceanographic and tectonic influences. Marine Geophysical Researches 22, 487-508.

Llave, E., Hernández-Molina, F.J., Somoza, L., Stow, D.A.V., Díaz del Río, V., 2007. Quaternary evolution of the contourite depositional system in the Gulf of Cadiz, in: Viana, A.R., Rebesco, M. (Eds.), Economic and Palaeoceanographic Significance of Contourite Deposits. Geological Society, London, Special Publication 276, 49-79.

Lowrie, A., 1986. Model for fine-scale mocements associated with climate and sea level changes along Lousiana shelfbreak growth faults. *Gulf Coast Association Geological Societies transactions,* 36: 497-508.

Lucchi, R.G., Rebesco, M., 2007. Glacial contourites on the Antarctic Peninsula margin: insight for palaeoenvironmental and palaeoclimatic conditions. In: Viana, A.R., Rebesco, M. (Eds.), Economic and Palaeoceanographic Significance of Contourite Deposits. Geol. Soc. London Special Publ. 276, 111-127.

Lucchi, R.G., Rebesco, M., Camerlenghi, A., Busetti, M., Tomadin, L., Villa, G., Persico, D., Morigi, C., Bonci, M.C., Giorgetti, G., 2002. Mid-late Pleistocene glacimarine sedimentary processes of a high-latitude, deep-sea sediment drift (Antarctic Peninsula Pacific margin). Mar. Geol. 189, 343-370.

Macdonald, D.I.M., 1993. Controls on sedimentation at convergent plate margins. Spc. Publ. Int. Ass. Sediment, 20: 225-257.

Maldonado, A., Balanyá, J.C., Barnolas, A., Galindo-Zaldívar, J., Hernández, J., Jabaloy, A., Livermore, R.A., Martínez, J. M., Rodríguez-Fernández, J., Sanz de Galdeano, C., Somoza, L., Suriñach, E., Viseras, C., 2000. Tectonics of an extinct ridge-transform intersection, Drake Passage (Antarctica). Marine Geophysical Researches 21, 43-68.

Maldonado, A., Barnolas, A., Bohoyo, F., Escutia, C., Galindo-Zaldívar, J., Hernández-Molina, F.J., Jabaloy, A., Lobo, F., Nelson, C.H., Rodríguez-Fernández, J., Somoza, L., Vázquez, J.T., 2005. Miocene to recent contourite drifts development in the northern Weddell Sea (Antarctica), in: Florindo, F., Harwood, D.M., Wilson, G.S. (Eds.), Long-term changes in Southern high-latitude ice sheets and climate: the Cenozoic history. Global and Planetary Change, 45: 99-129.

Maldonado, A., Barnolas, A., Bohoyo, F., Galindo-Zaldívar, J., Hernández-Molina, J., Lobo. F., Rodríguez-Fernández, J., Somoza, L., Vázquez, J.T., 2003. Contourite deposits in the central Scotia Sea: the importance of the Antarctic Circumpolar Current and the Weddell Gyre flows. Palaeogeography, Palaeoclimatology, Palaeoecology 198, 187-221.

Maldonado, A., Bohoyo, F., Galindo-Zaldívar, J., Hernández-Molina, F.J., Lobo, F.J., Martos-Martín, Y., Schreider, A., 2010. Cenozoic growth patterns and paleoceanography of the ocean basins near the Scotia-Antarctic plate boundary. Bollettino di Geofisica, 51: 227-231 (7-09).

Maldonado, A., Bohoyo, F., Galindo-Zaldívar, J., Hernández-Molina, F.J., Lobo, F.J., Lodolo, E., Martos, Y.M., Pérez, L.F., Schreider, A.A., Somoza, L., 2014. A model of oceanic development by ridge jumping: opening of the Scotia Sea. *Global and Planetary Change* 123:152-173. DOI: 10.1016/j.gloplacha.2014.06.010.

Maldonado, A., Larter, R., Aldaya, F., 1994. Forearc tectonic evolution of the South Shetland margin, Antarctic Peninsula. *Tectonics* 13, 1345-1370.

Maldonado, A.; Bohoyo, F.; Galindo-Zaldívar, J.; Hernández-Molina, F.J.; Jabaloy, A.; Lobo, F.; Rodríguez-Fernández, J.; Suriñach, E., Vázquez, J.T., 2006. Ocean basins near the Scotia–Antarctic plate boundary: Influence of tectonics and paleoceanography on the Cenozoic deposits. *Marine Geophysical Research, 27(2): 83-107.*

Malumian, N., Olivero, E.B., 2005. El Oligoceno–Plioceno marino del Rio Irigoyen, costa atlántica de Tierra del Fuego, Argentina: una conexión atlántico–pacifica. Rev. Geol. Chile 32 (1), 117–129.

Mascarelli, A.L., 2009. Quaternary geologists win timescale vote. *Nature*, 459: 264

Maslin, M.A., Li, X.S., Loutre, M.-F. and Berger, A., 1998, The contribution of orbital forcing to the progressive intensification of Northern Hemisphere glaciation. Quat. Sci. Rev. 17, 411–426.

Maslin, M.A., Ridgwell, A.J., 2005. Mid-Pleistocene revolution and the‘eccentrycity myth’. In: Head, M.J., Gibbard, P.L. (Eds.), Early–Middle Pleistocene Transitions: The Land–Ocean Evidence. Geological Society of London, Special Publication 247, pp. 19–34.

McCarron, J. J.; Larter, R. D. 1998. Late Cretaceous to early Tertiary subduction history of the Antarctic Peninsula. *Journal of the Geological Society, London*, 155, 255–268.

McCave, I.N., Manighetti, B.,Beveridge, N.A.S., 1995. Circulation in the glacial North Atlantic inferred from grain-size measurements. Nature, 374 (6518), 149–152.

McClymont, E., L., Sosdian, S.M., Rosell-Melé, A., Rosenathal, Y., 2013, Pleistocene sea-surface temperature evolution: Early cooling, delayed glacial intensification, and implications for the mid-Pleistocene climate transition. Earth-Science Reviews 123: 173–193

McGinnis J.P., Hayes, D.E., Driscoll, N.W., 1997. Sedimentary processes across the continental rise of the southern Antarctic Peninsula. Mar. Geol. 141, 91-109.

McGinnis, J.P., Hayes, D.E., 1995. The roles of down-slope and alongslope depositional processes: southern Antarctic Peninsula continental rise. In: Cooper, A.K., Barker, P.F., Brancolini, G. (Eds.), Geology and Seismic Stratigraphy of the Antarctic Margin. Antarct. Res. Ser. 68. American Geophysical Union, Washington DC, pp. 141-156.

Meredith, M.P., Naveira Garabato, A.C., Stevens, D.P., Heywood, K.J., Sanders, R.J., 2001. Deep and bottom waters in the eastern Scotia Sea: Rapid changes in properties and circulation. Journal of Physical Oceanography 31, 2157-2168.

Meredith, M.P., Schofield, O., Newman, L., Urban, E. and Sparrow, M., 2013. The vision for a Southern Ocean Observing System. Current Opinion in Environmental Sustainability.

Miller, K.G., Mountain, G.S. , Wright, J.D. Browning, J.V.,2011. A 180-million-year record of sea level and ice volume variations from continental margin and deep-sea isotopic records. Oceanography, 24(2):40–53, doi:10.5670/oceanog.2011.26. doi: 10.5670/oceanog.2011.26

Miller, K.G.,Wright, J.D., Browning, J.V., 2005. Visions of ice sheets in a greenhouse world. Mar. Geol. 217 (3–4), 215–231.

Moran, K., Backman, J., Brinkhuis, H., Clemens, S.C., Cronin, T., Dickens, G.R., Eynaud, F., Gattacceca, J., Jakobsson, M., Jordan, R.W. and others. 2006, The Cenozoic palaeoenvironment of the Arctic Ocean: Nature, v. 441, p. 601–605, doi: 10.1038/nature04800.

Morozov EG, Deminov AN, Tarakanov RY, Zenk W., 2010. Abyssal Channels in the Atlantic Ocean. Springer-Velag, Berlin, Heidelberg, New York

Morrison, R., Kukla, G., 1998. The Pliocene-Pleistocene (Tertiary-Quaternary) Boundary should be placed at about 2.6 Ma, not at 1.8 Ma!. *GSA Today*, 9.

Mulitza, S., Paul, A., Wefer, G., Scott, A.E., 2007. Late Pleistocene South Atlantic. Encyclopedia of Quaternary Science. Elsevier, Oxford, pp.1816–1831.

Naish, T., Powell, R., Levy, R., Wilson, G., Scherer, R., Talarico, F., Krissek, L., Niessen, F., Pompilio, M., Wilson, T., Carter, L., DeConto, R., Huybers, P., McKay, R., Pollard, D., Ross, J., Winter, D., Barrett, P., Browne, G., Cody, R., Cowan, E., Crampton, J., Dunbar, G., Dunbar, N., Florindo, F., Gebhardt, C., Graham, I., Hannah, M., Hansaraj, D., Harwood, D., Helling, D., Henrys, S., Hinnov, L., Kuhn, G., Kyle, P., Laufer, A., Maffioli, P., Magens, D., Mandernack, K., McIntosh, W., Millan, C., Morin, R., Ohneiser, C., Paulsen, T., Persico, D., Raine, I., Reed, J., Riesselman, C., Sagnotti, L., Schmitt, D., Sjunneskog, C., Strong, P., Taviani, M., Vogel, S., Wilch, T., Williams, T., 2009. Obliquity-paced Pliocene West Antarctic ice sheet oscillations. Nature, 458: 322-328.

Naveira Garabato, A.C., Heywood, K.J., Stevens, D.P., 2002a. Modification and pathways of Southern Ocean Deep Waters in the Scotia Sea. Deep-Sea Research Part I: Oceanographic Research Papers, 49(4), 681-705.

Naveira Garabato, A.C., McDonagh, E.L., Stevens, D.P., Heywood, K.J., Sanders, R.J., 2002b. On the export of Antarctic Bottom Water from the Weddell Sea. Deep-Sea Research Part II: Topical Studies in Oceanography, 49(21), 4715-4742.

Naveira Garabato, A.C., Stevens, D.P., Heywood, K.J., 2003: Water mass convertion, fluxes and mixing in the Scotia Sea diagnosed by an inverse model. J. Phys. Oceanogr. 33, 2565-2587.

Niemi, T.M., Ben-Avraham, Z., Hartnady, C.J.H., Reznikov, M., 2000, Post-Eocene seismic stratigraphy of the deep ocean basin adjacent to the southeast African continental margin: a record of geostrophic bottom current systems: Marine Geology, 162: 237–258.

Ninnemann, U.S., Charles, C.D., 2002. Changes in the mode of Southern Ocean circulation over the last glacial cycle revealed by foraminiferal stable isotopic variability. Earth Planet. Sci. Lett. 201(2),383–396.

Nisancioglu KH, Raymo ME, Stone PH., 2003. Reorganization of Miocene deep water circulation in response to the shoaling of the Central American Seaway. Paleoceanography 18:1006-1018. doi:10.1029/2002pa000767.

Nitsche, F.O., Cunningham, A.P., Larter, R.D., Gohl, K., 2000. Geometry and development of glacial continental margin depositional systems in the Bellingshausen Sea. *Mar. Geol*., 162:277-302.

Nitsche, F.O., Gohl, K., Vanneste, K., Miller, H., 1997. Seismic expression of glacially deposited sequences in the Bellingshausen and Amundsen seas, West Antarctica. *In* Barker, P.F., and Cooper, A.K. (Eds.), *Geology and Seismic Stratigraphy of the Antarctic Margin* (Pt 2). Am. Geophys. Union, Antarct. Res. Ser., 71:95-108.

Noormets, R., Dowdeswell, J.A., Larter, R.D., Ó Cofaigh, C., Evans, J., 2009 Morphology of the upper continental slope in the Bellingshausen and Amundsen Seas - implications for sedimentary processes at the shelf edge of West Antarctica. Marine Geology 258, 100-114.

Ó Cofaigh, C., Dowdeswell, J.A., Allen, C.S., Hiemstra, J.F., Pudsey, C.J., Evans, J., Evans, D.J.A., 2005. Flow dynamics and till genesis associated with a marine-based Antarctic palaeo-ice stream. Quaternary Science Reviews 24, 709–740.

Ó Cofaigh, C., Pudsey, C.J., Dowdeswell, J.A., Morris, P., 2002: Evolution of subglacial bedforms along a paleo-ice stream, Antarctic Peninsula continental shelf . *Geophys. Res. Lett.*, 29(8), doi: 10.1029/2001GL014488.

Ó Cofaigh, C., Taylor, J., Dowdeswell, J. A. & Pudsey, C. J. 2003. Palaeo-ice streams, trough mouth fans and high-latitude continental slope sedimentation. Boreas, Vol. 32, pp. 37–55.

Orsi, A.H., Johnson, G.C. and Bullister, J.L., 1999. Circulation, mixing, and production of Antarctic Bottom Water. Progress in Oceanography, 43(1), 55-109.

Orsi, A.H., Whitworth, T., III, Nowlin, W.D., Jr., 1995. On the meridional extent and fronts of the Antarctic Circumpolar Current. Deep-Sea Res. I 42, 641-673.

Palmer, M., Gomis, D., Flexas, M. D. M., Jordà , G., Jullion, L., Tsubouchi, T., Naveira-Garabato, A. C., 2012. Water mass pathways and transports over the South Scotia Ridge west of 50°W. Deep-Sea Research Part I: Oceanographic Research Papers, 59, 8-24.

Pankhurst, 1990. The Paleozoic and Andean magmatic arcs of West Antarctica and southern South America. Geol. Soc. Am. Spec. Publ. 241, 1-7.

Pérez, L. F., Bohoyo, F., Hernández-Molina, F.J., Casas, D., Galindo-Zaldívar, J., Ruano, P., Maldonado, A., 2016. Tectonic activity evolution of the Scotia-Antarctic Plate boundary from mass transport deposit analysis, J. Geophys. Res. Solid Earth, 121, doi:10.1002/2015JB012622.

Pérez, L. F., Maldonado, A., Hernández-Molina, F. J., Lodolo, E., Bohoyo, F., Galindo-Zaldívar, J., 2015b. Tectonic and oceanographic control of sedimentary patterns in a small oceanic basin: Dove Basin (Scotia Sea, Antarctica), *Basin Research*, 1:1-22. doi:10.1111/bre.12148.

Pérez, L.F., Hernández-Molina, F.J., Esteban, F.D., Tassone, A., Piola, A.R., Preu, B., Violante, R.A., Lodolo, E., 2015a. Erosional and depositional contourite features at the western Scotia Sea - Southern Atlantic Ocean Transition: correlations with regional water masses circulation. *Geo-Marine Letters*, 35(4): 271-288. DOI 10.1007/s00367-015-0406-6.

Pérez, L.F., Lodolo, E., Maldonado, A., Hernández-Molina, F.J., Bohoyo, F., Galindo-Zaldívar, J., Lobo, F.J., 2014a. Tectonic Development, Sedimentation and Paleoceanography of the Scan Basin (Southern Scotia Sea, Antarctica). *Global and Planetary Change,* 123:344-358*.* doi: 10.1016/j.gloplacha.2014.06.007.

Pérez, L.F., Maldonado,, A., Bohoyo, F., Hernández-Molina, F.J., Váquez, J.T., Lobo, F.J., Martos, Y.M., 2014b. Depositional Processes and Growth Patterns of Isolated Oceanic Basins: The Protector and Pirie Basins of the Southern Scotia Sea (Antarctica). *Marine Geology*, 357, 163-181.

Piotrowski, A.M., Goldstein, S.L., Hemming, S.R., Fairbanks, R.G., Zylberberg, D.R., 2008. Oscillating glacial northern and southern deep water formation from combined neodymium and carbon isotopes. Earth Planet. Sci. Lett. 272(1–2), 394–405, http://dx.doi.org/10.1016/j.epsl.2008.05.011.

Pope, P.G., Anderson, J.B., 1992. Late Quaternary glacial history of the northern Antarctic Peninsula's western continental shelf: evidence from the marine record. In: Elliot, D.H. (Ed.), Contributions to Antarctic Research III. Antarctic Research Series,vol. 57. AGU, Washington, D.C., pp. 63–91.

Potter, P.E. & Szatmari, P., 2009. Global Miocene tectonics and the modern world. *Earth Sci. Rev.* 96, 279-295.

Powell, R.D., Domack, E.W., 1995. Glaciomarine Environments, Chapter 13. In Menzies, J. (ed.), Glacial Environments - Processes, Sediments and Landforms (621 p.). Butterworth-Heinmann, Boston: 445-486.

Preu, B., Hernández-Molina, F.J., Violante, R., Piola, A.R., Paterlini, C.M., Schwenk, T., Voigt, I., Krastel, S., Spiess, V., 2013, Morphosedimentary and hydrographic features of the northern Argentine margin: The interplay between erosive, depositional and gravitational processes and its conceptual implications. Deep-Sea Research Part I: Oceanographic Research Papers, v. 75, p. 157-174. http://dx.doi.org/10.1016/j.dsr.2012.12.013

Preu, B., Schwenk, T., Hernández-Molina, F.J., Violante, R., Paterlini, M., Krastel, S., Tomasini, J., Spieß, V., 2012, Sedimentary growth pattern on the northern Argentine slope: The impact of North Atlantic Deep Water on southern hemisphere slope architecture. Marine Geology, v. 329–331, p. 113-125. http://dx.doi.org/10.1016/j.margeo.2012.09.009.

Pudsey, C.J., 2000. Sedimentation on the continental rise west of the Antarctic Peninsula over the last three glacial cycles. Mar. Geol. 167, 313-338.

Pudsey, C.J., Camerlenghi, A., 1998. Glacial-interglacial deposition on a sediment drift on the Pacific margin of the Antarctic Peninsula. Antarct. Sci. 10, 286-308.

Raymo, M., Ruddiman, W. Backman, J., Clement, B., Martinson, D., 1989. Late Pliocene variation in northern hemisphere ice sheets and North Atlantic deep water circulation. *Paleoceanography,* 4: 413-446.

Rebesco M., Camerlenghi A., Zanolla C., 1998. Bathymetry and morphogenesis of the continental margin west of the Antarctic Peninsula. Terra Antartica 5, 715-725.

Rebesco, M. Camerlenghi, A. (eds), 2008, Contourites. Developments in Sedimentology, vol 60. Elsevier, Amsterdam.

Rebesco, M., 2005. Contourites, in: Selley, R.C., Cocks, L.R.M., Plimer, I.R. (Eds.), Encyclopedia of Geology. Elsevier, Oxford, pp. 513–527.

Rebesco, M., Camerlenghi, A., Geletti, R., Canals, M., 2006, Margin architecture reveals the transition to the modern Antarctic ice sheet ca. 3 Ma: Geology, v. 34, p. 301–304, doi: 10.1130/G22000.1.

Rebesco, M., Camerlenghi, A., Volpi, V., Neagu, C., Accettella, D., Lindberg, B., Cova, A., Zgur, F., and the MAGICO party, 2007. Interaction of processes and importance of contourites: insights from the detailed morphology of sediment drift 7, Antarctica, in: Viana, A.R., Rebesco, M. (Eds.), Economic and Palaeoceanographic Significance of Contourite Deposits. Geological Society, London, Special Publication 276, pp. 95–110.

Rebesco, M., Laberg, J.S., Pedrosa, M.T., Camerlenghi, A., Lucchi, R.G., Zgur, F., Wardell, N., 2014. Onset and growth of Trough-Mouth Fans on the North-Western Barents Sea margin e implications for the evolution of the Barents Sea/Svalbard Ice Sheet. Quaternary Science Reviews 92:227-234

Rebesco, M., Larter, R.D., Barker, P.F., Camerlenghi, A., Vanneste, L.E., 1997. The history of sedimentation on the continental rise west of the Antarctic Peninsula. In: Barker, P.F., Cooper, A. (Eds.), Geology and Seismic Stratigraphy of the Antarctic Margin: Part 2. Antarct. Res. Ser. 71. American Geophysical Union, Washington DC, pp. 29-49.

Rebesco, M., Larter, R.D., Camerlenghi, A., Barker, P.F., 1996. Giant sediment drifts on the continental rise west of the Antarctic Peninsula. Geo-Mar. Lett. 16, 65-75.

Rebesco, M., Pedrosa, M.T., Camerlenghi, A., Lucchi, R.G., Sauli, C., De Mol, B.,Madrussani, G., Urgeles, R., Rossi, G., Böhm, G., 2012. One million years of climatic generated landslide events on the southern Storfjorden Trough Mouth Fan (western Barents Sea). In: Yamada, Y., et al. (Eds.), Submarine Mass Movements and Their Consequences, Advances in Natural and Technological Hazards Research, vol. 31, pp. 747-756.

Rebesco, M., Pudsey, C., Canals, M., Camerlenghi, A., Barker, P., Estrada, F., Giorgetti, A., 2002. Sediment drift and deep-sea channel systems, Antarctic Peninsula Pacific Margin. In: Stow, D.A.V., Pudsey, C.J., Howe, J.A., Faugeres, J.C., Viana, A.R. (Eds.), Deep-Water Contourite Systems: Modern Drifts and Ancient Series, Seismic and Sedimentary Characteristics. Geol. Soc. London Memoirs 22, pp. 353-371.

Rebesco, M.; Hernández-Molina, F.J.; Van Rooij, D., Wåhlin, A., 2014. Contourites and associated sediments controlled by deep-water circulation processes: state of the art and future considerations, Marine Geology, 352: 111-154.

Ruddiman, W.F., Raymo, M.E., Martinson, D.G., Clement, B.M., Backman, J., 1989. Pleistocene evolution: Northern Hemisphere ice sheets and North Atlantic Ocean. Paleoceanography, 4: 353-412.

SCAR, 2001, Report No. 9, ANTOSTRATA SCAR Seismic Data Library System for Cooperative Research (SDLS): Summary report of the International Workshop on Antarctic Seismic Data Oslo, Norway, April 11-15, 1991.http://www.scar.org/publications/reports/9/

Scheuer, C., Gohl, K., Larter, R.D., Rebesco, M., Udintsev, G, 2006, Variability in Cenozoic sedimentation along the continental rise of the Bellinghausen Sea, West Antarctica. Marine Geology, 227, 279-298.

Shackleton, N.J., Backman, J., Zimmerman, H., Kent, D.V., Hall, M.A., Robert. D.G., Schnitker, D., Baldauuf, J.G., Desprairies, A., Homrighausner, R., Huddlestone, P., Keen., J.B., Kaltenbach, A.J., Krumsiek, K.A.O., Morton, A.C., Murray, J.W., Westberg-Smith, J., 1984. Oxigen isotope calibration of the set of ice-rafting and history of glaciation in the North Atlantic region. *Nature*, 307: 620-623.

Shackleton, N.J., Berger, A., Peltier, W.R.,1990. An alternative astronomical calibration on the Lower Pleistocene time scales based on ODP site 677. Trans. R. Soc. Edinb. Earth Sci. 81, 251–261.

Shackleton, N.J., Opdyke, N.D., 1973. Oxygen isotope and paleomagnetic stratigraphy of equatorial Pacific core V28-238: oxygen isotope temperature and ice volume on a 10^6 year time scale. *Quaternary Research*, 3: 39-55.

Shevenell, A.E., Kennett, J.P., Lea, D.W., 2004. Middle Miocene Southern Ocean Cooling and Antarctic Cryosphere Expansion. Science, 305. 1766-1770. DOI: 10.1126/science.1100061.

Sievers HA, Nowlin WD., 1984. The stratification and water masses at Drake Passage. J Geophys Res: Oceans 89:10489-10514. doi:10.1029/JC089iC06p10489

Smellie, J.L., Haywood, A.M., Hillenbrand, C.D., Lunt, D.J., Valdes, P.J., 2009. Nature of the Antarctic Peninsula Ice Sheet during the Pliocene: Geological evidence and modeling results compared. Earth-Science Reviews, 94: 79-94.

Solheim, A., Andersen, E.S., Elverhøi, A., Fiedler, A., 1996. Late Cenozoic depositional history of the western Svalbard continental shelf, controlled by subsidence and climate. Glob. Planet. Change 12, 135–148.

Steig, E.S., Orsi, A.J., 2013. Climate science: The heat is on in Antarctica. Nature Geosci. 6, 87.88. doi:10.1038/ngeo1717.

Stow, D.A.V., Pudsey, C.J., Howe, J.A., Faugères, J.-C., Viana, A.R., 2002a. Deep-Water Contourite Systems: Modern Drifts and Ancient Series, Seismic and Sedimentary characteristics. Geological Society, London, Memoirs 22.

Swartz, J., Gulick, S., Goff, J.A., 2015, Gulf of Alaska continental slope morphology: Evidence for recent trough mouth fan formation: Geochemistry, Geophysics, Geosystems, v. 16, p. 165–177, doi:10.1002/2014GC005594.

Sykes, T.J.S., Ramsay, T.S. and Kidd, R.B., 1998. Southern hemisphere Miocene bottom-water circulation: a palaeobathymetric analysis. In: Cramp, A., C. J., MacLeod, S. V. Lee, and E. J. W. Jones (Eds). Geological evolution of Ocean Basin: results from the Ocean Drilling Program. Geological Society of London, 131: 43–54.

Tarakanov, R.Y. 2012. The Scotia Sea and the Drake Passage as an orographic barrier for the Antarctic Circumpolar Current. Oceanology 52:157-170.

Tarakanov, R.Y., 2009. Antarctic bottom water in the Scotia Sea and the Drake passage. Oceanology 49:607-621

Thunell, R., Rio, D., Sprovieri,R., Vergnaud-Grazzini, C., 1991. An overview of the post-Messinian paleoenvironmental history of the Mediterranean. Plaeoceanography, 6(1), 143-164.

Tucholke, B.E., Houtz, R.E., 1976. Sedimentary Framework of the Bellingshausen Basin from Seismic Profiler Data. In: Hollister, C.D., Craddock, C. *et al*. (Eds.), Initial Reports of the Deep Sea Drilling Project, 35, 197-228. U.S. Government Printing Office, Washington, D.C.

Uenzelmann-Neben, G., 2006. Depositional patterns at Drift 7, Antarctic Peninsula: along-slope versus down-slope sediment transport as indicators for oceanic currents and climatic conditions. Mar. Geol. 233, 49-62.

Uenzelmann-Neben, G., Gohl, K., 2012. Amundsen Sea sediment drifts: archives of modifications in oceanographic and climatic conditions.Mar. Geol. 299–302, 51–62. http:// dx.doi.org/10.1016/j.margeo.2011. 12.007/.

Uenzelmann-Neben, G., Weber, T., Grützner, J., Maik, T., 2016. Transition from the Cretaceous ocean to Cenozoic circulation in the western South Atlantic — A twofold reconstruction. *Tectonophysics*. http://doi.org/10.1016/j.tecto.2016.05.036

Van Andel, Tj. H., Thiede, J., Sclater, J.G., Hay, W.W., 1977. Depositional History of the South Atlantic during the last 125 Million Years. Journal of Geology, 85: 651-698.

Vanneste, L.E., Larter, R.D., 1995. Deep-tow boomer survey on the Antarctic Peninsula Pacific margin: an investigation of the morphology and acoustic characteristics of late Quaternary sedimentary deposits on the outer continental shelf and upper slope. In: Cooper, A.K., Barker, P.F., Brancolini, G. (Eds.), Geology and Seismic Stratigraphy of the Antarctic Margin. Antarct. Res. Ser., vol. 68, pp. 97–121.

Vanney, J.R., Johnson, G.L., 1976. Geomorphology of the Pacific continental Margin of the Antarctic Peninsula. In: Hollister, C.D. Craddock, C. *et al*. (Eds.), Initial Reports of the Deep Sea Drilling Project 35, 279-289, U.S. Government Printing Office, Washington, D.C.

Viana, A.R. Figueiredo, A.G., Feaugères, J.C., Lima, A.F., Gonthier, E., Brehme, I., Zaragosi, S., 2003. The São Paula Tomé deep-sea turbidite system (South Brazilian nasin): Cenozoic seismic stratigraphy and sedimentary processes. *American Association of Petroleum Geologists* Bulletin, 87, 873-894.

Viana, A.R.,Hercos,C.M., AlmeidaJr.,W., Magalhães, J.L.C.,Andrade,S.B.,2002. Evidence of bottom current influence on the neogene to quaternary sedimentation along the Northern Campos slope, SW Atlantic Margin. In: Stow, D.A.V., Pudsey, C.J., Howe, J.A., Faugeres, J.C, Viana, A.R. (Eds.), Deep-Water Contourite Systems: Modern Drifts and Ancient Series, Seismic and Sedimentary Characteristics, 22. Geological Society Memoir,pp.249–259.

Vincent, E., and Berger, W.H., 1985, Carbon dioxide and polar cooling in the Miocene: The Monterey hypothesis, in Sundquist, E.T., and Broecker, W.S., eds., The Carbon Cycle and Atmospheric CO2: natural Variations Archean to Present, Volume 32, Am. Geophys. Union Monogr. Ser.

Volpi, V. Rebesco, M. and Diviacco, P., 2007, New insights in the evolution of Antarctic glaciation from depth conversion of well-log calibrated seismic section of Prydz Bay: International Journal of Earth Sciences, 98 (8): 1991-2007.

Volpi, V., Amblas, D., Camerlenghi, A., Canals, M., Rebesco, M., Urgeles, R., 2011. Late Neogene to recent seafloor instability on the deep Pacific margin of the Antarctic Peninsula. In: Mass transport deposits in deep-water settings. R.C. Shipp, P. Weimer, H.W. Posamentier (Eds). Special Society for Sedimentary Geology (SEPM), Special Publication, 96: 161-177.

Wardell, N, Childs, J.R., Cooper, A.K., 2007. Advances through collaboration: Sharing seismic reflection data via the Antarctic Seismic Data Library System for Cooperative Research (SDLS), in Antarctica: A Keystone in a Changing World – Online Proceedings of the 10th ISAES, edited by A. K. Cooper and C. R. Raymond et al., USGS Open-File Report 2007-1047, Short Research Paper 001,4 p.; doi:10.3133/of2007-1047.srp001.

Watts, A.B., 2001. Isostasy and Flexure of the Lithosphere. Cambridge University Press, 458 pp.

Weber, M.E., Bonani, G., Fütterer, K.D., 1994. Sedimentation processes within channel-ridge systems, Southeastern Weddell Sea, Antarctica. Paleoceanography, 9(6): 1027–1048, http://dx.doi.org/10.1029/94pa01443.

Whitworth III, T., Nowlin Jr., W.D., 1987. Water masses and currents of the Southern Ocean at the Greenwhich Meridian. J. Geophys. Res. 92, 6462–6476.

Whitworth III, T., Nowlin, Jr., W.D.; Orsi, A.H.; Locarnini, R.A., Smith, S.G., 1994. Weddell Sea Shelf Water in the Bransfield Strait and Weddell-Scotia Confluence. Deep-Sea Res. I 41, 629-641.

Whitworth III, T., Orsi, A.H., Kim, S.-J., Nowlin, W.D., 1998. Water masses and mixing near the Antarctic Slope Front. Antarctic Research Series, 75, 1–27.

Whyte, N., Lovell, B., 1997. Measuring the pulse of a plume with the sedimentary record. Letter to Nature, 387: 888-891.

Zachos, J.C., Dickens, G.R., Zeebe, R.E., 2008. An early Cenozoic perspective on greenhouse warming and carbon-cycle dynamics. Nature, 451: 279-283.

Zachos, J.C., Pagani, M., Sloan, L., Thomas, E., and Billups, K., 2001, Trends, rhythms and aberrations in global climate 65 Ma to present: Science, v. 292, p. 686–693, doi: 10.1126/science.1059412.

FIGURES

Figure 1. Regional setting of the Pacific Margin of the Antarctic Peninsula (PMAP) offshore of Adelaide Island. Red filled circles represent ODP Leg 178, Sites 1095-1103 (Barker *et al*., 1999) and DSDP Leg 35, Site 325 (Hollister *et al.*, 1976) drill sites. Inset shows location of main figure. Black box represents the location of the study area. The maps show large mounded asymmetric contourite drifts and turbidite canyon-channel systems (CCSs). Four major drifts (Drifts 4A, 4B, 5 and 5A) and four CCSs have been identified in the study area: the Biscoe (BCCS), Lavoisier (LCCS), Adelaide (ACCS) and North Tula (NTCCS) systems. SM = seamount, HFZ = Hero Fracture Zone. Isobaths from Rebesco *et al.* (1998).

Figure 2. Sketches summarizing the evolution from an active (A and B) to passive margin (C and D). The margin became passive when the ridge-crest (RC) segment arrived at the trench, subduction ceased along the corresponding segment of the margin and trench basement topography was eliminated. Arrival of each Antarctic-Phoenix ridge-crest segment at the trench was followed by rapid uplift of the opposing segment of the margin. These events occurred at the MSH, for a period of 1 to 4 Ma (C) and were followed by long-term subsidence caused by a combination of thermal effects, sediment loading and sediment compaction (D). Active compressional deformation between the two oceanic crust segments occurred during a time when one segment became passive while the other remained active. This generated a compressive high (Transitional High) at the base of the slope (C).

Figure 3. A) General sketch of the area spanning the Pacific Margin of the Antarctic Peninsula (PMAP), Drake Passage and the Scotia Sea, showing circulation of the main regional water-masses (compilation based on Orsi *et al.*, 1999, Naveira-Garabato *et al.*, 2002a,b, 2003; Hernández-Molina *et al.*, 2006b; Hillenbrand *et al.*, 2008; Tarakanov, 2009, 2012; Morozov *et al.*, 2010; Palmer *et al.*, 2012; Meredith *et al.*, 2013). Legend for regional water masses: ACC= Antarctic Circumpolar Current, AABW= Antarctic Bottom Water, AAIW= Antarctic Intermediate Water, CBW= Circumpolar Bottom Water, SPDSW= Southeast Pacific Deep Slope Water, CDW= Circumpolar Deep Water, LCDW= Lower Circumpolar Deep Water, Lower LCDW/WDW= Lower Circumpolar Deep Water branch from the Weddell Sea, SPDW= South Pacific Deep Water, UCDW= Upper Circumpolar Deep Water, WSBW= Weddell Sea Bottom Water, WSDW= Weddell Sea Deep Water. Legend for oceanographic features: 54P= 54º-54º Passage, BaBk= Barker Bank, AI= Adelaide Island, BBk= Bruce Bank, BrP= Bransfield Strait, BuBk= Burdwood Bank, DaBk= Davis Bank, DBk= Discovery Bank, DP= Discovery Passage, EI= Elephant Island, FE= Falkland Escarpment, GP= South Georgia Passage, GR= South Georgia Rise, HBk= Herdman Bank, MEB= Malvinas Eastern Basin / Maurice Ewing Bank, M/F I= Malvinas/Falkland Islands, M/F V= Malvinas/Falkland Valley, NGP= North Georgia Passage, NGR= Northwast Georgia Rise, NSR= Nort Scotia Ridge; OI= South Orkney Islands, OP= Orkney Passage, OR= Orkney Ridge, PP= Phillip Passage, RP= Black Rocks Passage, SGI= South Georgia Island, SP= Shag Rocks Passage, SShI= Shetland Islands, SSR= South Scotia Ridge; SOM= South Orkney Microcontinent, SR= Shag (and Black) Rocks, SSI= South Sandwich Islands, TBk= Terror Bank. B) Vertical distribution of water masses across the Drake Passage (based on Naveira-Garabato *et al.*, 2002a, 2002b; Morozov *et al.*, 2010; Tarakanov, 2012). C) Detail of the main circulation paths along the PMAP offshore of Adelaide Island (based on Camerlenghi *et al*., 1997; Giorgetti *et al*., 2003; Hernández-Molina *et al.*, 2006b). Map also shows the surface position of the ACC fronts and present circulation pattern of bottom water masses with (a) CDW and (b) LCDW branch from the Weddell Sea. The Southern Boundary of the ACC (SB) dips in a northwest direction, while LCDW from the Weddell Sea flows

southwest beneath it. Red filled circles represent ODP Leg 178 (Barker *et al.*, 1999) and DSDP Leg 35 (Hollister *et al.*, 1976) drill sites. Black box represents location of the study area.

Figure 4. Sketch showing location of multibeam sonar and seismic profiles (study mostly used multichannel seismic (MCS) refection profiles) along the Pacific Margin of the Antarctic Peninsula (PMAP) offshore of Adelaide Island.

Figure 5. Regional stratigraphic sketch including the main morphological domains, stratigraphic discontinuities , seismic units and evolutionary intervals identified in this work by correlation with ODP Leg 178 (Barker *et al.*, 1999) and DSDP Leg 35 (Hollister *et al.*, 1976) data. Vertical scale is exaggerated to show major changes in the stratigraphic stacking pattern. See Figure SM-I in the supplementary material for a more complete sketch and Figure SM-II for stratigraphic correlations between northern, central and southern sectors of the study area.

Figure 6. Morphosedimentary map of the Pacific Margin of the Antarctic Peninsula offshore of Adelaide Island, showing the main features along the continental shelf, slope and rise.

Figure 7. Seismic and first-order morphological differences between the continental slopes in front of: A) the sedimentary lobes and banks (Lobe 4, Adriasola Bank in the southern sector) and B) the glacial trough in the central sector (Marguerite Trough). Major oceanographic domains are shown, along with the seismic facies for each domain. See Figure 4 for profile locations.

Figure 8. A) Interpretation of the AISM-12 seismic profile for the southern sector of the Antarctic Peninsula Pacific Margin offshore of Adelaide Island, showing the main morphologic domains, stratigraphic discontinuities and seismic units. See Figure 4 for profile location. Panels B-E show key stratigraphic seismic examples. B) Detail of seismic unit 4 (SU4), as the first shelf progradational body reaching the shelf break, C) stratigraphic stacking pattern for the slope in this sector, D) detail of the large debris flow deposits at the base of the slope, and E) example of Drift 5's sedimentary stacking pattern showing the main seismic facies and boundaries. The erosional surface at the base of SU4 is marked by a red line. BGMS= Base of the Glacial Margin Sequences.

Figure 9. A) F–k migrated multichannel seismic profile (BAS19) along the continental rise with a detailed stratigraphic interpretation and its correlation with DSDP Leg 35, Site 325 (Hollister *et al.*, 1976) data. Note relict mounded body and the related marginal troughs on both sides. SU5 is shaded dark grey to emphasize its truncation by SU4's basal discontinuity. See Figure 4 for profile location. B) Detail of DSDP Leg 35, Site 325 along the rise indicating the age, lithology, depth (km) and the two-way time (s) below sea floor (bsf) of the major reflectors.

Figure 10. A) Interpretation of the AISM-06 seismic profile for the central sector of the Antarctic Peninsula Pacific Margin offshore of Adelaide Island. Main morphologic domains, stratigraphic discontinuities and seismic units are included. See Figure 4 for profile location. Panels B-E show key stratigraphic seismic examples. B) Detail of channelized facies (fluvial incision) between SU8 and SU7, C) main seismic facies for the outer shelf near ODP Site 1097. Note truncation surface at the top of SU9. D) Stratigraphic staking pattern for the slope in this sector, E) detail of large debris flow deposits at the base of the slope. Abbreviations: BGMS= Base of the Glacial Margin Sequences, UU-CU= Uplift / Collision Unconformity.

Figure 11. A) Interpretation of AISM-14 seismic profile for the northern sector of the Antarctic Peninsula Pacific Margin offshore of Adelaide Island. Main morphologic domains, stratigraphic discontinuities and seismic units are included. See Figure 4 for profile location. Panels B and C show key stratigraphic seismic examples. B) Stratigraphic staking pattern for the slope in this sector, C) example of Drift 4B sedimentary stacking pattern showing the main seismic facies and boundaries. Abbreviations: BGMS= Base of the Glacial Margin Sequences; UU-CU= Uplift / Collision Unconformity.

Figure 12. A) Interpretation of AISM-13 seismic profile parallel to the lower slope and upper rise of the Antarctic Peninsula Pacific Margin offshore of Adelaide Island. Main morphologic domains, stratigraphic discontinuities and seismic units are included. See Figure 4 for profile location. Panels B-F show key stratigraphic seismic examples. B) Detail of seismic units above a buried slope structural high in the southern sector related to the position of the Adelaide Fracture Zone, C) detail of seismic facies in SU4, D) example of Drift 5 sedimentary stacking pattern showing the main seismic facies and boundaries, E) seismic units above the structural high in the central sector, F) Drift 4A sedimentary stacking pattern showing the main seismic facies and boundaries in the northern sector. Abbreviations: BGMS= Base of the Glacial Margin Sequences, UU-CU= Uplift / Collision Unconformity.

Figure 13. A) USAP-88b seismic profile parallel to the outer shelf of the Antarctic Peninsula Pacific Margin offshore of Adelaide Island. Main morphologic domains, stratigraphic discontinuities and seismic units are included. See Figure 4 for profile location. This profile shows the development of the Marguerite Trough axis starting from SU4's upper surface in the southern sector below the present Adriasola Bank. Lateral northeastward migration of the Marguerite Trough appears in SU2 Subunit a's upper surface. The trough moved to its present day position during deposition of this unit. B) USAP-5 seismic profile across the Matha Bank in the northern sector of study area showing the main stratigraphic discontinuities, seismic units and SU1's Subunits a, b, c and d. Abbreviations: BGMS= Base of the Glacial Margin Sequences, UU-CU= Uplift / Collision Unconformity.

Figure 14. Sketch of major Neogene to Quaternary global changes, including climatic, sea level, paleoceanographic and tectonic events. These events are correlated with the regional stratigraphy in the Pacific Margin of the Antarctic Peninsula (PMAP) offshore of Adelaide Island. Global sea level records: 1) global sea level (in dark blue) from 0 to 7 Ma (Miller *et al.*, 2005); 2) global sea level (in light blue) from 7 to 65 Ma (Miller *et al.*, 2005); 3) global sea level (in dark pink) from 7 to 65 Ma (Kominz *et al.*, 2008), base on deep sea oxygen isotope records: 4) oxygen isotopic (in red) synthesis (Cramer *et al.*, 2009) and 5) stacked deep sea benthic foraminiferal oxygen isotope curve (Zachos *et al.*, 2008). Major climatic changes and events synthetized from Zachos *et al.* (2001, 2008). Major Palaeoceanographic events summarized from different authors (Sykes *et al.*, 1998; Billups, 2002; Nisancioglu *et al.*, 2003; Maldonado *et al.*, 2006, 2014; Hernández-Molina *et al.*, 2006b, 2009, 2010, 2014). Abbreviations in alphabetic order: ACC= Antarctic Circumpolar Current, AABW= Antarctic Bottom Water, BGMS= Base of the Glacial Margin Sequences, BQ= Base of the Quaternary (2.6 Ma), CDW= Circumpolar Deep Water, CU= Collision Unconformity, EAIS= Eastern Antarctic Ice Sheets, LCDW= Lower Circumpolar Deep Water, MPT= Mid Pleistocene Transition, MT= Marguerite Trough, MTDs= mass transport deposits, NADW= North Atlantic Deep Water, NH= Northern Hemisphere, PMAP= Pacific Margin of the Antarctic Peninsula , UCDW= Upper Circumpolar Deep Water, UU= Uplift Unconformity, WAIS= Western Antarctic Ice Sheets.

Figure 15. Sketch indicating the main sedimentary processes affecting the Antarctic Peninsula Pacific Margin offshore of Adelaide Island operating during the latest Miocene, Pliocene and Quaternary.

Table-I. Main seismic facies for main seismic units (SU9 to SU1) along the continental outer shelf, continental slope and continental rise of the Pacific Margin of the Antarctic Peninsula offshore of Adelaide Island.

Table-II. Sedimentary thickness for the main seismic units (SU9 to SU1) along the outer shelf, slope and rise of the Pacific Margin of the Antarctic Peninsula offshore of Adelaide Island. Notice that changes between the different stages represent changes in the sedimentary thickness along the margin. Thicker deposits since the mid Miocene to the present time are associated to SU4 a (mainly on the rise), and to S3 (specially on the outer shelf and slope). SU4 is the first high-angle progradational unit on the upper slope of the shelf break and SU3 represents the most important progradational stage along the margin.

…….

Supplementary material

Figure SM-I. Regional stratigraphic correlation and age constraints on seismic units and discontinuities defined in this work by correlation with ODP Leg 178 (Barker *et al*., 1999) and DSDP Leg 35 (Hollister *et al.,* 1976) data, as well relation to regional units defined by previous research.

Figure SM-II. 3D fence diagram stratigraphic correlation between northern, central and southern sectors of the study area. N.B. The alignment of the main part of Marguerite Trough is approximately north-south, oblique to the margin, so although the trough reaches the shelf edge in the central sector, the basement high shown at the SE end of the central sector section lies on the eastern margin of the trough.

Figure SM-III. Regional Multibeam 3D sonar image of the Pacific Margin of the Antarctic Peninsula offshore of Adelaide Island, showing major oceanographic domains and morphologic features.

Figure SM-IV. Seismic line USAP-4 across the central sector of the Pacific Margin of the Antarctic Peninsula offshore of Adelaide Island showing main seismic units and discontinuities. The S3/S2 boundaries defined by Larter and Barker (1989) and Barker and Camerlenghi (2002) from ODP Leg 178 data are shown in a different stratigraphic position. The final onset of glacial margin sequences occurs at the base of SU4 (Transitional Unit), which marks the times when ice sheets became established on the shelf break. Nevertheless, a few moderately incisive, glacially-related features (little troughs and irregular surfaces) appear in upper sections of SU5 as it occurs on the outer shelf. Abbreviations: BGMS= Base of the Glacial Margin Sequences, UU-CU= Uplift / Collision Unconformity.

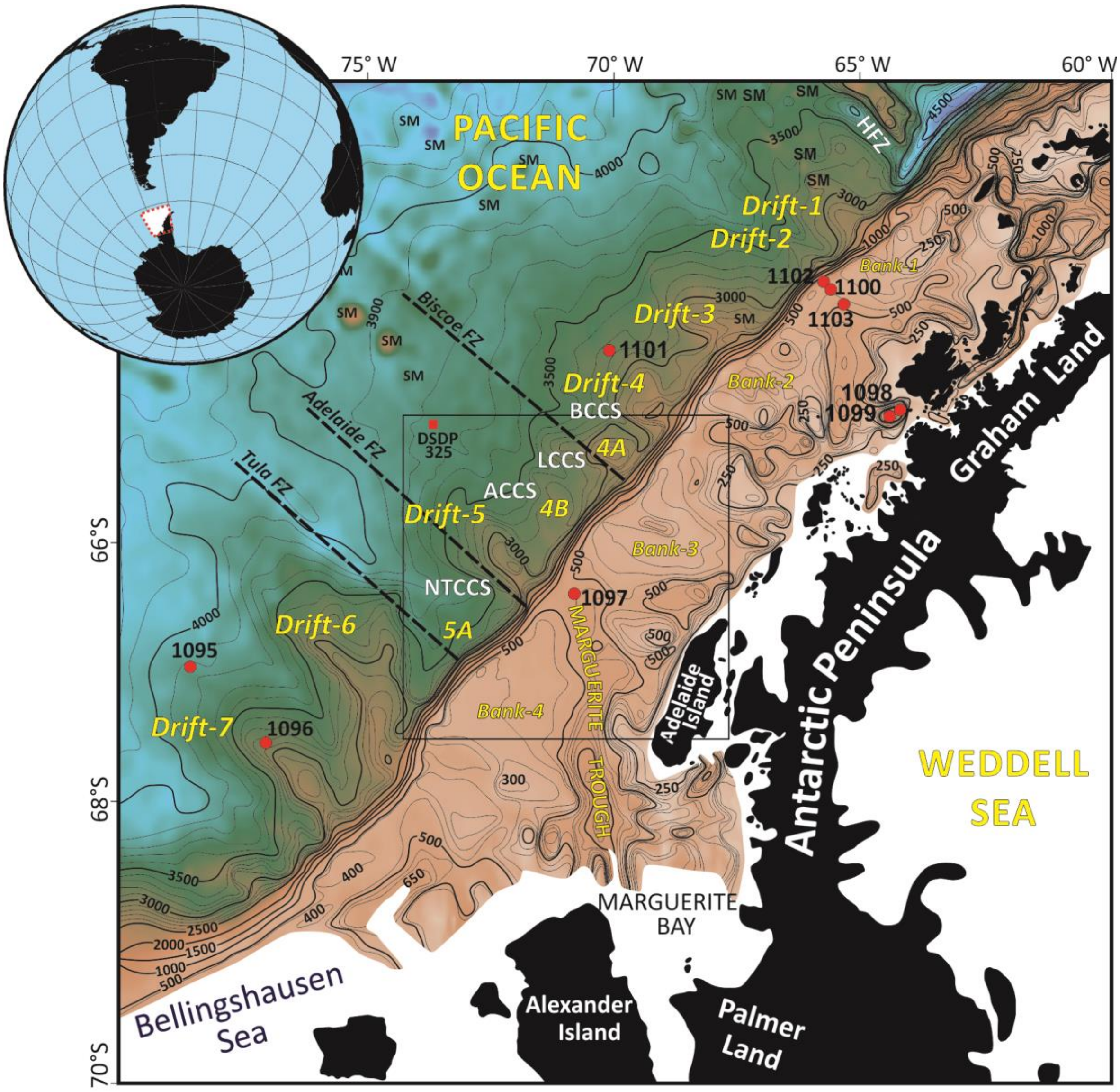

75° W
70° W
65° W
60° W
66°S
68°S
70°S
PACIFIC OCEAN
Drift-1
Drift-2
Drift-3
Drift-4
Drift-5
Drift-6
Drift-7
Bank-1
Bank-2
Bank-3
Bank-4
HFZ
Biscoe FZ
Adelaide FZ
Tula FZ
1095
1096
1097
1098
1099
1100
1101
1102
1103
DSDP 325
BCCS
LCCS
ACCS
NTCCS
4A
4B
5A
MARGUERITE TROUGH
MARGUERITE BAY
Adelaide Island
Alexander Island
Palmer Land
Graham Land
Antarctic Peninsula
WEDDELL SEA
Bellingshausen Sea

Figure - 1

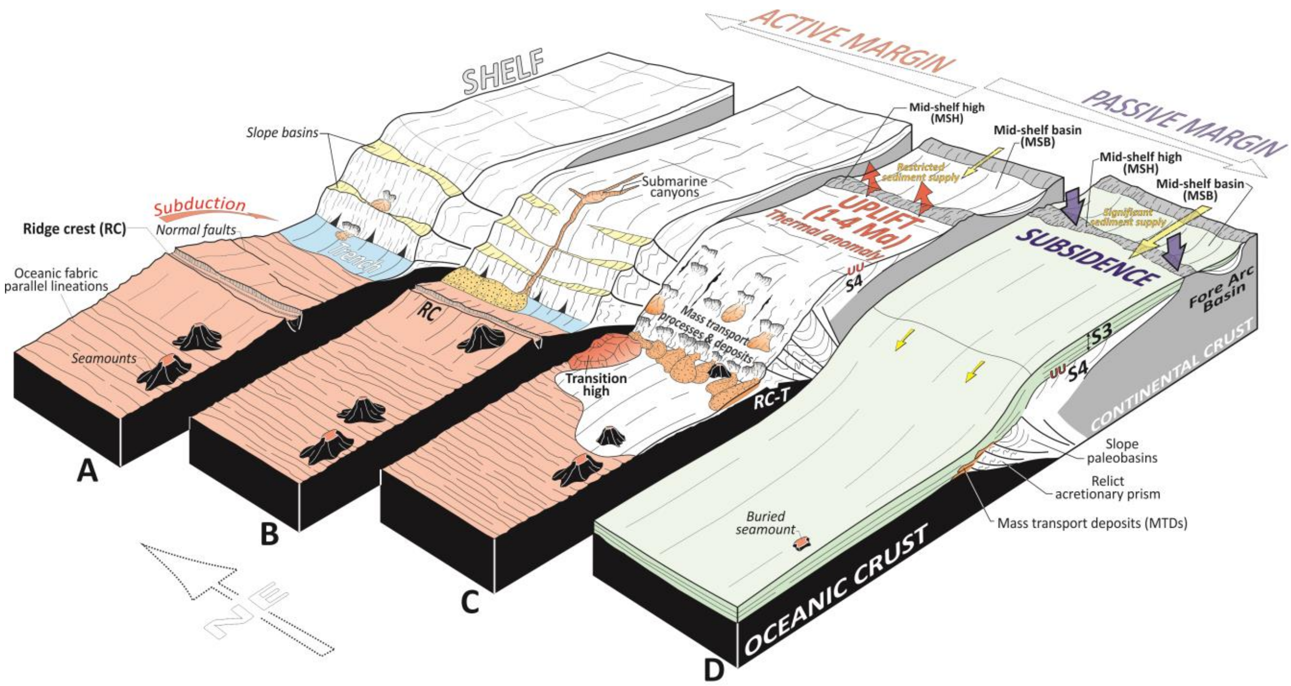

ACTIVE MARGIN
PASSIVE MARGIN
SHELF
Slope basins
Submarine canyons
Mid-shelf high (MSH)
Mid-shelf basin (MSB)
Restricted sediment supply
Significant sediment supply
UPLIFT (1-4 Ma)
Thermal anomaly
SUBSIDENCE
Fore Arc Basin
CONTINENTAL CRUST
Subduction
Ridge crest (RC)
Normal faults
Trench
Oceanic fabric parallel lineations
Seamounts
RC
Mass transport processes & deposits
Transition high
RC-T
S4
S3
Slope paleobasins
Relict acretionary prism
Mass transport deposits (MTDs)
Buried seamount
OCEANIC CRUST
A
B
C
D
N
E

Figure - 2

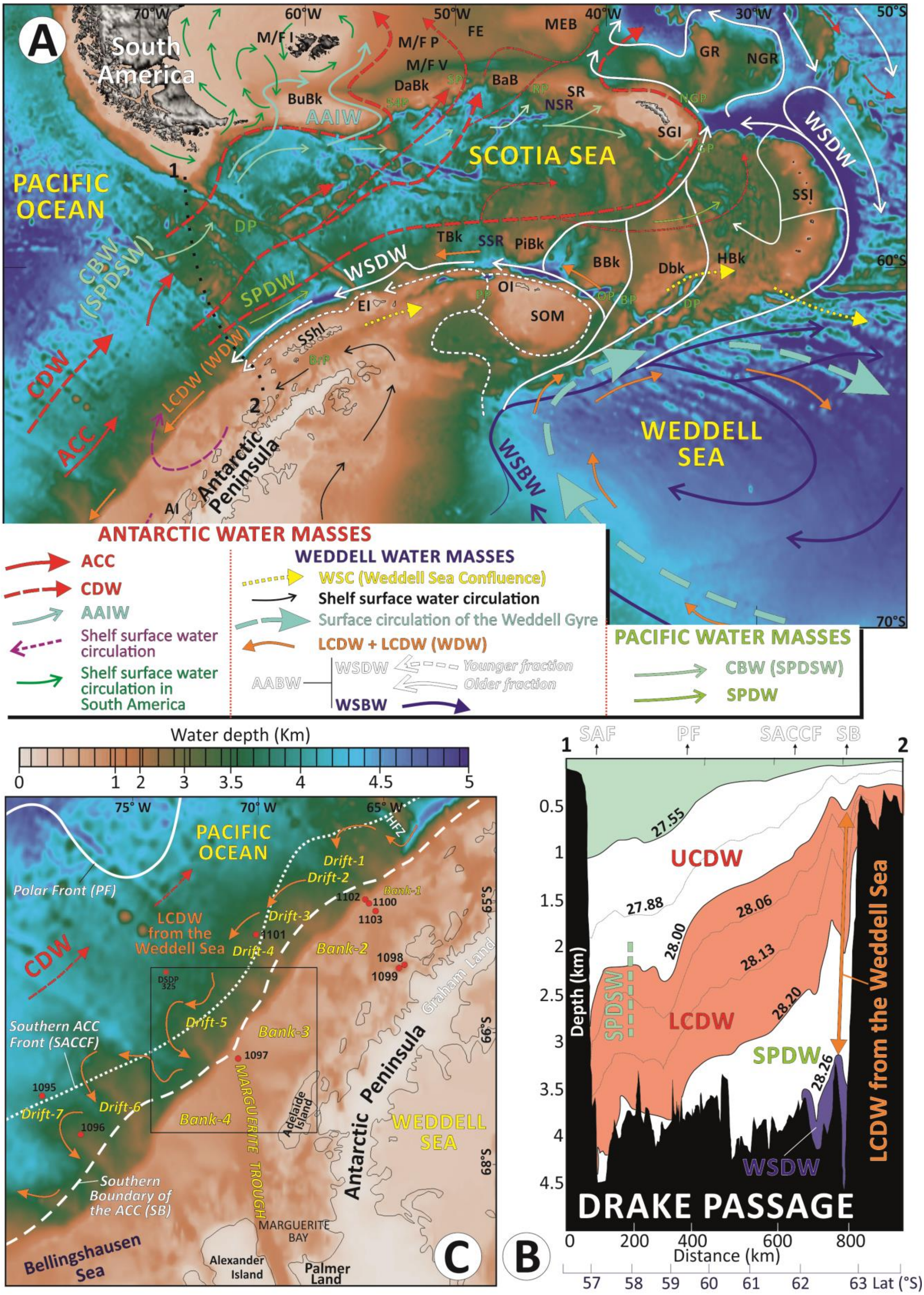

A
South America
PACIFIC OCEAN
SCOTIA SEA
WEDDELL SEA
Antarctic Peninsula
AAIW
WSDW
CBW (SPDSW)
SPDW
LCDW (WDW)
CDW
ACC
WSBW
ANTARCTIC WATER MASSES
ACC
CDW
AAIW
Shelf surface water circulation
Shelf surface water circulation in South America
WEDDELL WATER MASSES
WSC (Weddell Sea Confluence)
Shelf surface water circulation
Surface circulation of the Weddell Gyre
LCDW + LCDW (WDW)
AABW
WSDW
Younger fraction
Older fraction
WSBW
PACIFIC WATER MASSES
CBW (SPDSW)
SPDW
Water depth (Km)
C
PACIFIC OCEAN
Polar Front (PF)
LCDW from the Weddell Sea
CDW
Southern ACC Front (SACCF)
Southern Boundary of the ACC (SB)
Bellingshausen Sea
Alexander Island
Palmer Land
MARGUERITE BAY
MARGUERITE TROUGH
Adelaide Island
Graham Land
WEDDELL SEA
B
DRAKE PASSAGE
UCDW
LCDW
SPDW
SPDSW
WSDW
LCDW from the Weddell Sea
Depth (km)
Distance (km)
Lat (°S)

Figure - 3

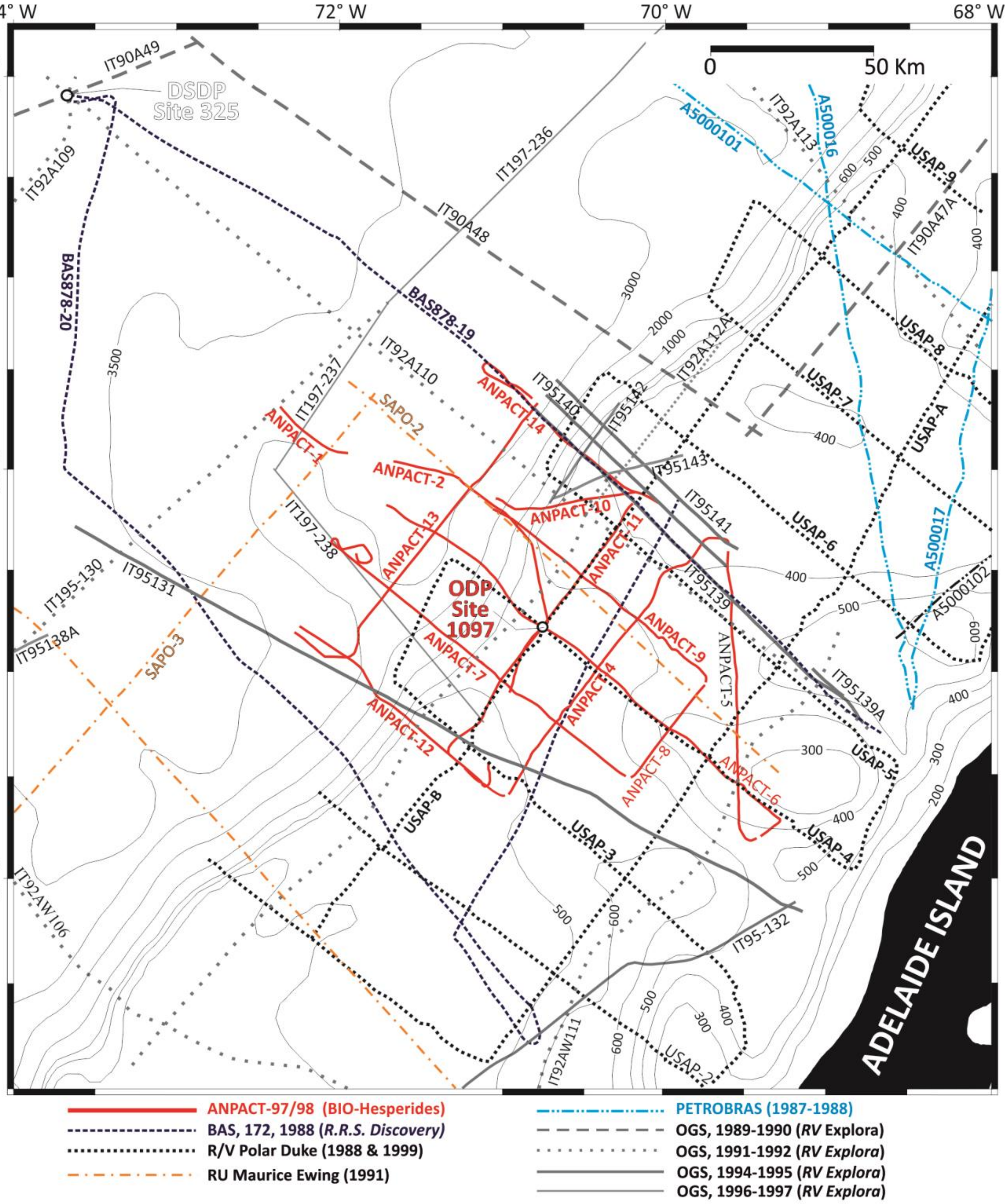
74° W
72° W
70° W
68° W
65° S
66° S
67° S
0
50 Km
DSDP Site 325
ODP Site 1097
ADELAIDE ISLAND
ANPACT-97/98 (BIO-Hesperides)
BAS, 172, 1988 (R.R.S. Discovery)
R/V Polar Duke (1988 & 1999)
RU Maurice Ewing (1991)
PETROBRAS (1987-1988)
OGS, 1989-1990 (RV Explora)
OGS, 1991-1992 (RV Explora)
OGS, 1994-1995 (RV Explora)
OGS, 1996-1997 (RV Explora)

Figure -4

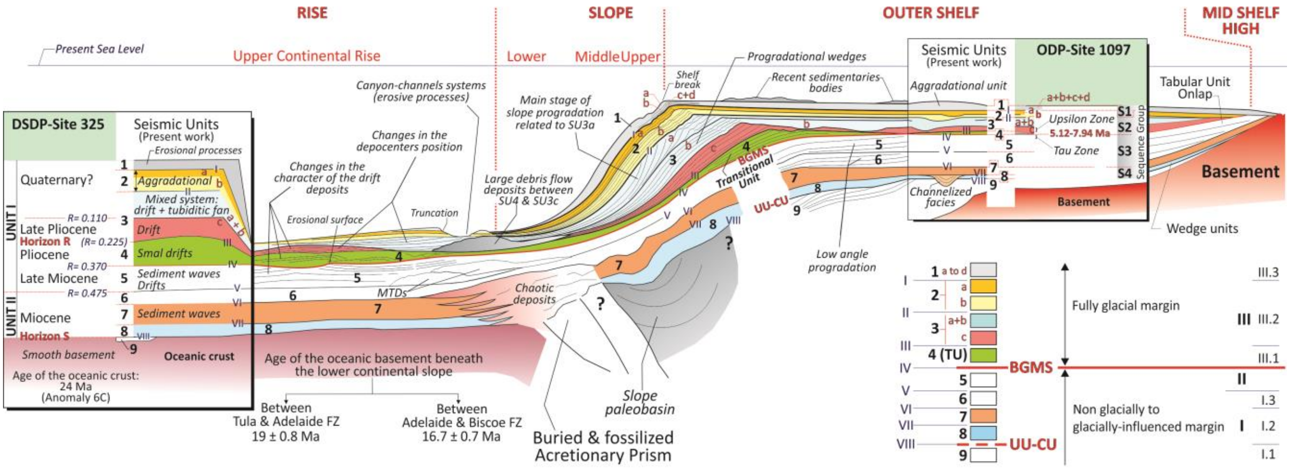

Figure-5

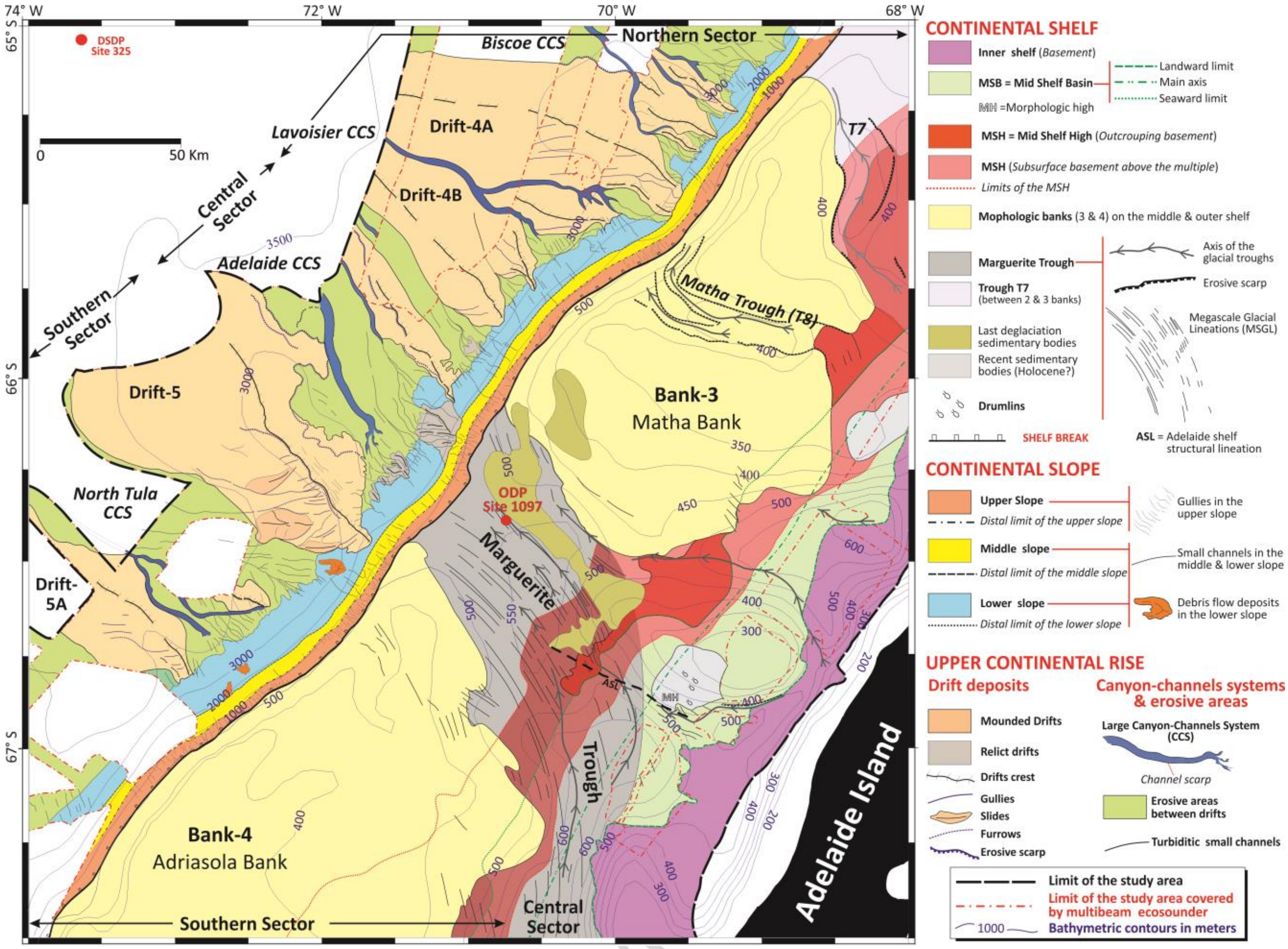

74° W
72° W
70° W
68° W
65° S
66° S
67° S
DSDP Site 325
Biscoe CCS
Northern Sector
Lavoisier CCS
Central Sector
Southern Sector
Adelaide CCS
Drift-4A
Drift-4B
Drift-5
North Tula CCS
Drift-5A
ODP Site 1097
Marguerite Trough
Matha Trough (T8)
T7
Bank-3
Matha Bank
Bank-4
Adriasola Bank
Central Sector
Adelaide Island
ASL
MH
0
50 Km
CONTINENTAL SHELF
Inner shelf (Basement)
MSB = Mid Shelf Basin
Landward limit
Main axis
Seaward limit
MH =Morphologic high
MSH = Mid Shelf High (Outcrouping basement)
MSH (Subsurface basement above the multiple)
Limits of the MSH
Mophologic banks (3 & 4) on the middle & outer shelf
Marguerite Trough
Trough T7 (between 2 & 3 banks)
Last deglaciation sedimentary bodies
Recent sedimentary bodies (Holocene?)
Drumlins
Axis of the glacial troughs
Erosive scarp
Megascale Glacial Lineations (MSGL)
SHELF BREAK
ASL = Adelaide shelf structural lineation
CONTINENTAL SLOPE
Upper Slope
Distal limit of the upper slope
Middle slope
Distal limit of the middle slope
Lower slope
Distal limit of the lower slope
Gullies in the upper slope
Small channels in the middle & lower slope
Debris flow deposits in the lower slope
UPPER CONTINENTAL RISE
Drift deposits
Mounded Drifts
Relict drifts
Drifts crest
Gullies
Slides
Furrows
Erosive scarp
Canyon-channels systems & erosive areas
Large Canyon-Channels System (CCS)
Channel scarp
Erosive areas between drifts
Turbiditic small channels
Limit of the study area
Limit of the study area covered by multibeam ecosounder
1000
Bathymetric contours in meters

Figure 6

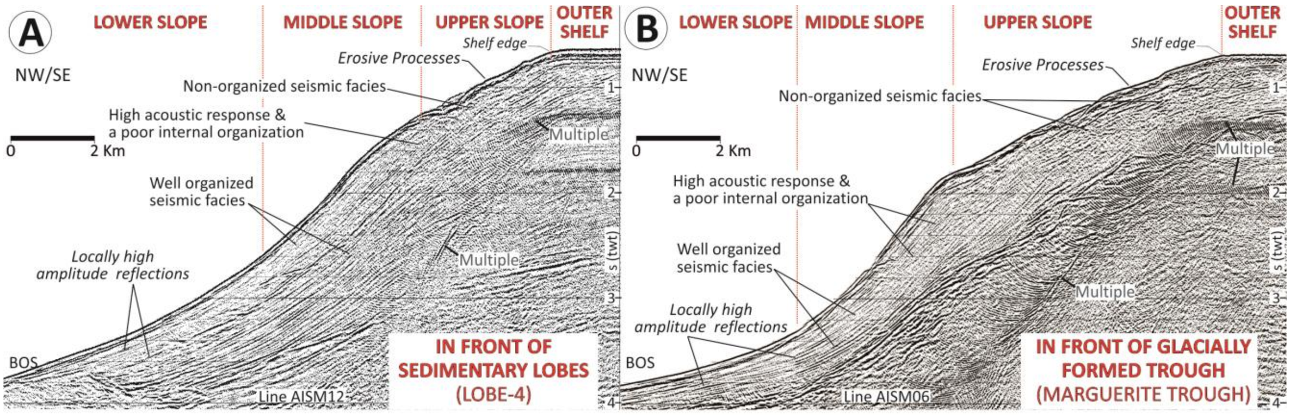

A
LOWER SLOPE
MIDDLE SLOPE
UPPER SLOPE
OUTER SHELF
NW/SE
Shelf edge
Erosive Processes
Non-organized seismic facies
High acoustic response & a poor internal organization
0
2 Km
Multiple
Well organized seismic facies
Locally high amplitude reflections
Multiple
s (twt)
BOS
Line AISM12
IN FRONT OF SEDIMENTARY LOBES (LOBE-4)
B
LOWER SLOPE
MIDDLE SLOPE
UPPER SLOPE
OUTER SHELF
NW/SE
Shelf edge
Erosive Processes
Non-organized seismic facies
0
2 Km
Multiple
High acoustic response & a poor internal organization
Well organized seismic facies
Multiple
Locally high amplitude reflections
BOS
Line AISM06
IN FRONT OF GLACIALLY FORMED TROUGH (MARGUERITE TROUGH)
s (twt)

Figure 7

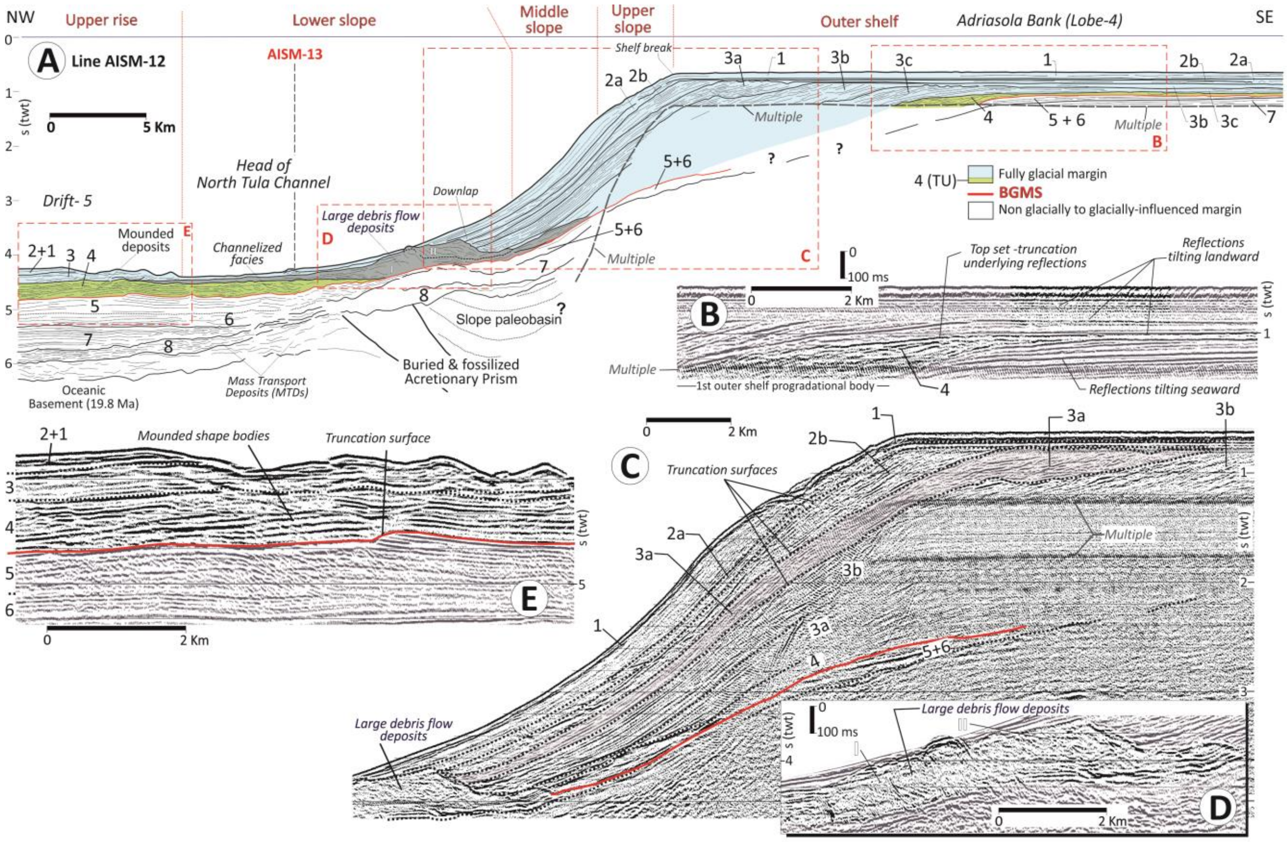
NW
SE
Upper rise
Lower slope
Middle slope
Upper slope
Outer shelf
Adriasola Bank (Lobe-4)
Line AISM-12
AISM-13
Shelf break
Head of North Tula Channel
Drift- 5
Large debris flow deposits
Downlap
Mounded deposits
Channelized facies
Multiple
Slope paleobasin
Buried & fossilized Acretionary Prism
Oceanic Basement (19.8 Ma)
Mass Transport Deposits (MTDs)
Fully glacial margin
BGMS
Non glacially to glacially-influenced margin
Top set -truncation underlying reflections
Reflections tilting landward
Reflections tilting seaward
1st outer shelf progradational body
Mounded shape bodies
Truncation surface
Truncation surfaces
s (twt)
0
5 Km
2 Km
100 ms

Figure-8

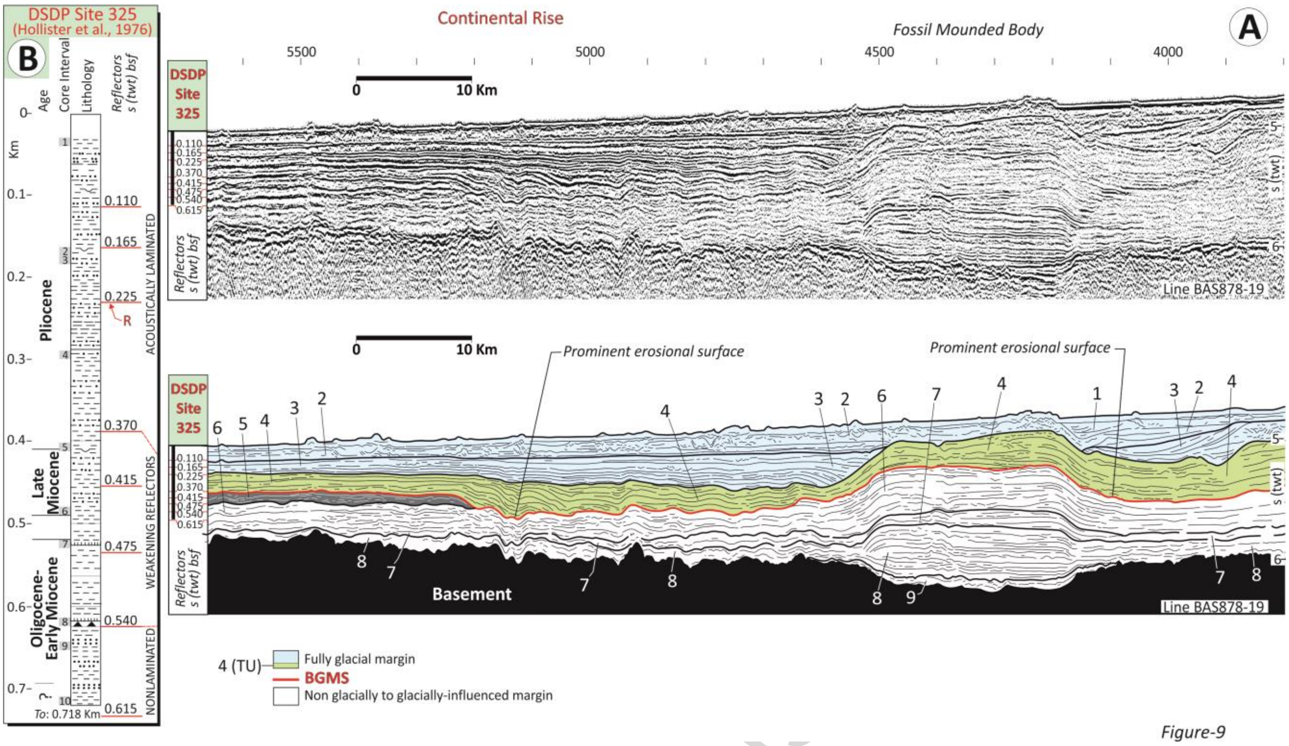
DSDP Site 325
(Hollister et al., 1976)
B
Age
Core Interval
Lithology
Reflectors s (twt) bsf
Km
Pliocene
Late Miocene
Oligocene-Early Miocene
ACOUSTICALLY LAMINATED
WEAKENING REFLECTORS
NONLAMINATED
0.110
0.165
0.225
R
0.370
0.415
0.475
0.540
0.615
To: 0.718 Km
Continental Rise
Fossil Mounded Body
A
5500
5000
4500
4000
0
10 Km
DSDP Site 325
Line BAS878-19
Prominent erosional surface
Basement
4 (TU)
Fully glacial margin
BGMS
Non glacially to glacially-influenced margin

Figure-9

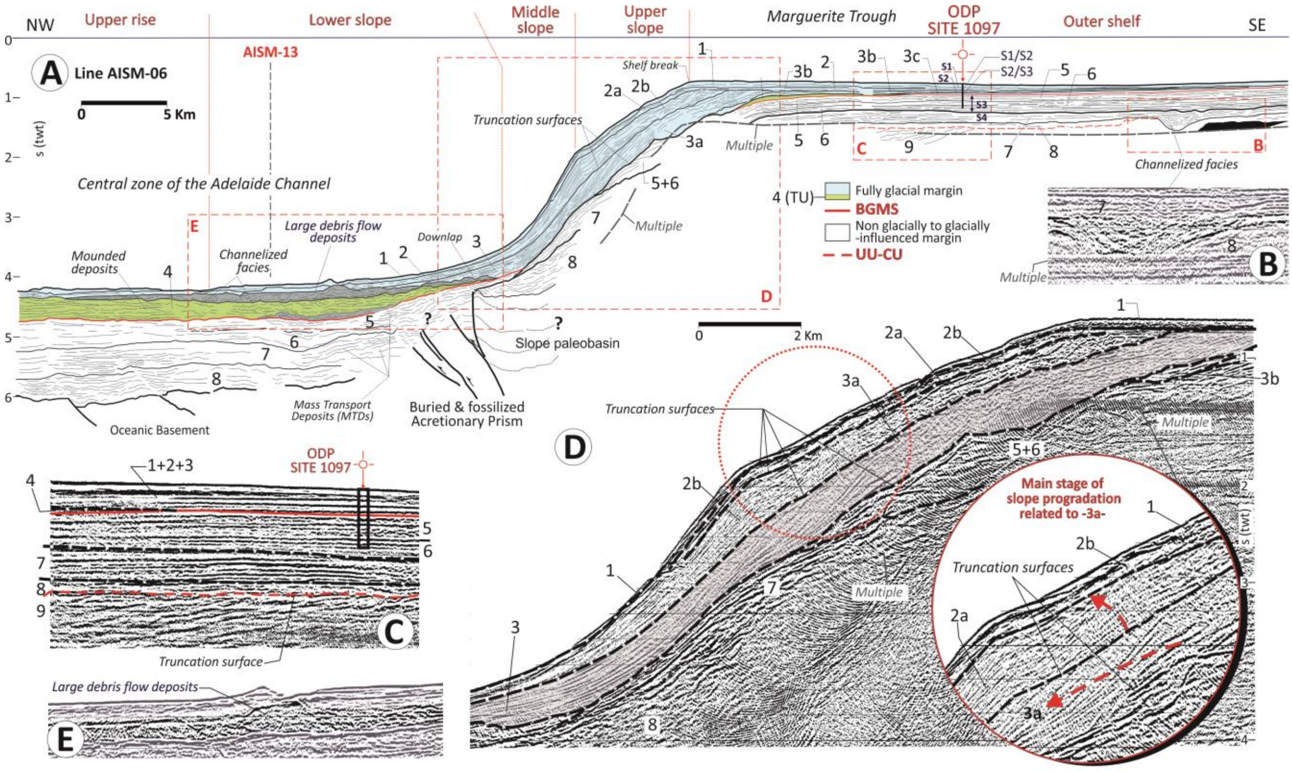

NW
Upper rise
Lower slope
Middle slope
Upper slope
Marguerite Trough
ODP SITE 1097
Outer shelf
SE
A
Line AISM-06
AISM-13
0
5 Km
s (twt)
Shelf break
Truncation surfaces
Central zone of the Adelaide Channel
Multiple
Fully glacial margin
BGMS
Non glacially to glacially -influenced margin
UU-CU
4 (TU)
Large debris flow deposits
Mounded deposits
Channelized facies
Downlap
Slope paleobasin
Mass Transport Deposits (MTDs)
Buried & fossilized Acretionary Prism
Oceanic Basement
Channelized facies
B
C
D
E
0
2 Km
S1/S2
S2/S3
ODP SITE 1097
1+2+3
Truncation surface
Large debris flow deposits
Truncation surfaces
Main stage of slope progradation related to -3a-

Figure-10

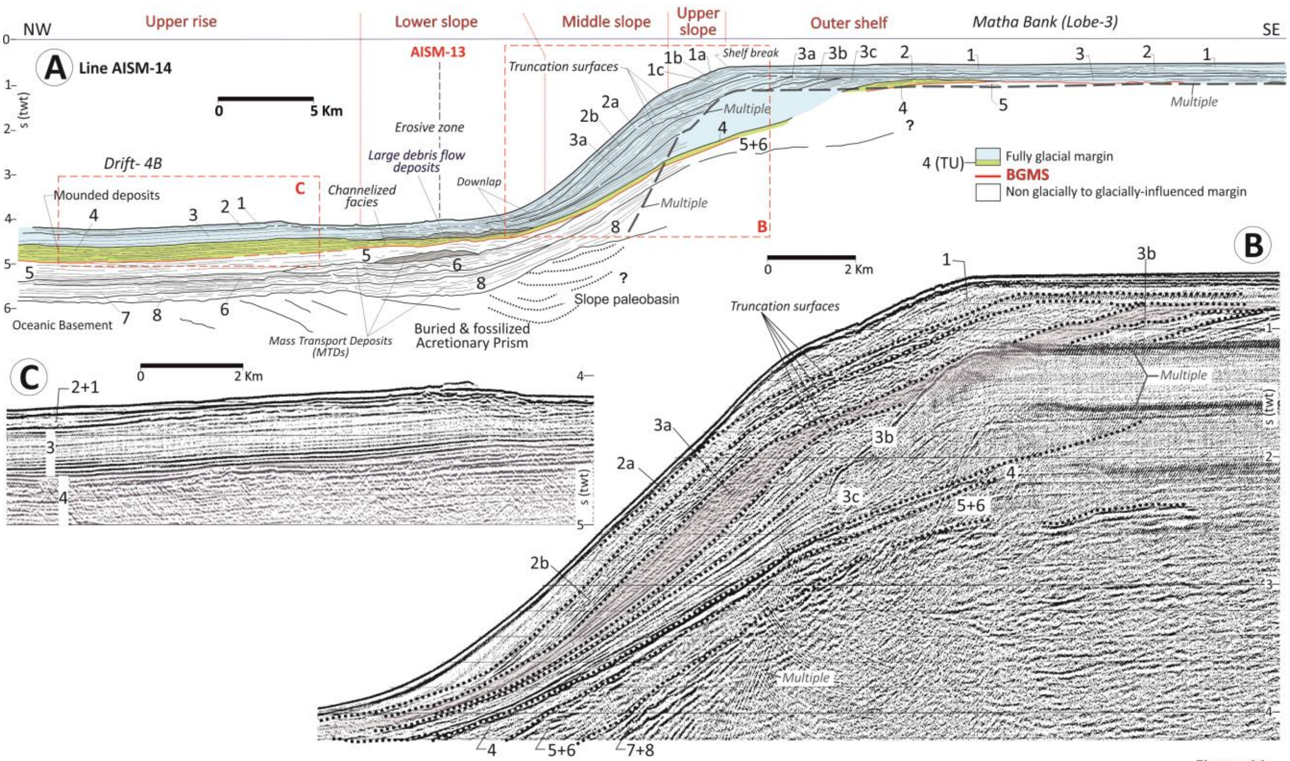

NW
Upper rise
Lower slope
Middle slope
Upper slope
Outer shelf
Matha Bank (Lobe-3)
SE
A
Line AISM-14
AISM-13
Truncation surfaces
Shelf break
Erosive zone
Large debris flow deposits
Channelized facies
Downlap
Drift- 4B
Mounded deposits
Multiple
Fully glacial margin
BGMS
Non glacially to glacially-influenced margin
4 (TU)
Oceanic Basement
Mass Transport Deposits (MTDs)
Buried & fossilized Acretionary Prism
Slope paleobasin
s (twt)
5 Km
2 Km
B
C

Figure-11

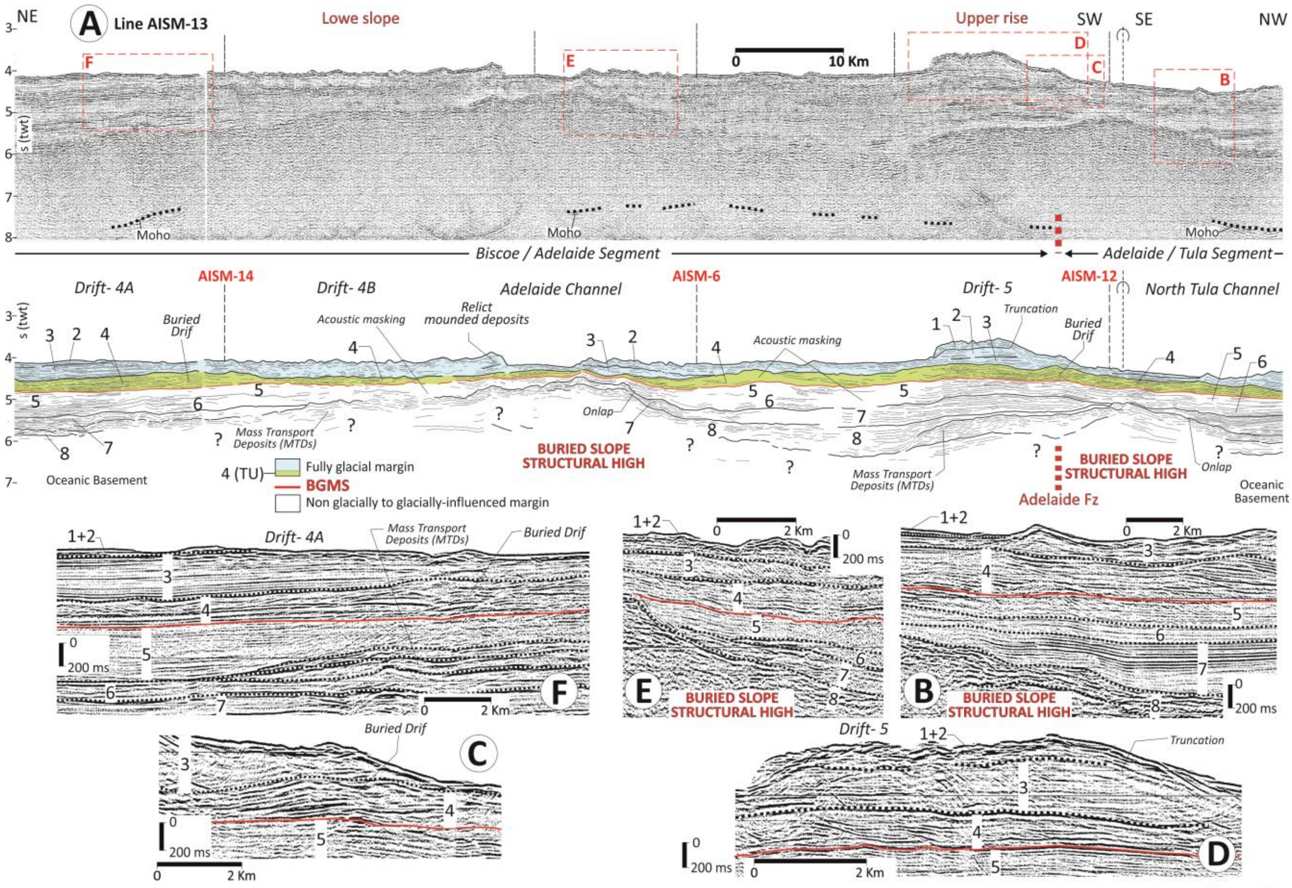

A Line AISM-13
NE
Lowe slope
Upper rise
SW
SE
NW
0 10 Km
s (twt)
Moho
Biscoe / Adelaide Segment
Adelaide / Tula Segment
Drift- 4A
AISM-14
Drift- 4B
Adelaide Channel
AISM-6
Drift- 5
AISM-12
North Tula Channel
Buried Drif
Acoustic masking
Relict mounded deposits
Truncation
Onlap
Mass Transport Deposits (MTDs)
BURIED SLOPE STRUCTURAL HIGH
Oceanic Basement
4 (TU)
Fully glacial margin
BGMS
Non glacially to glacially-influenced margin
Adelaide Fz
1+2
200 ms
2 Km

Figure-12

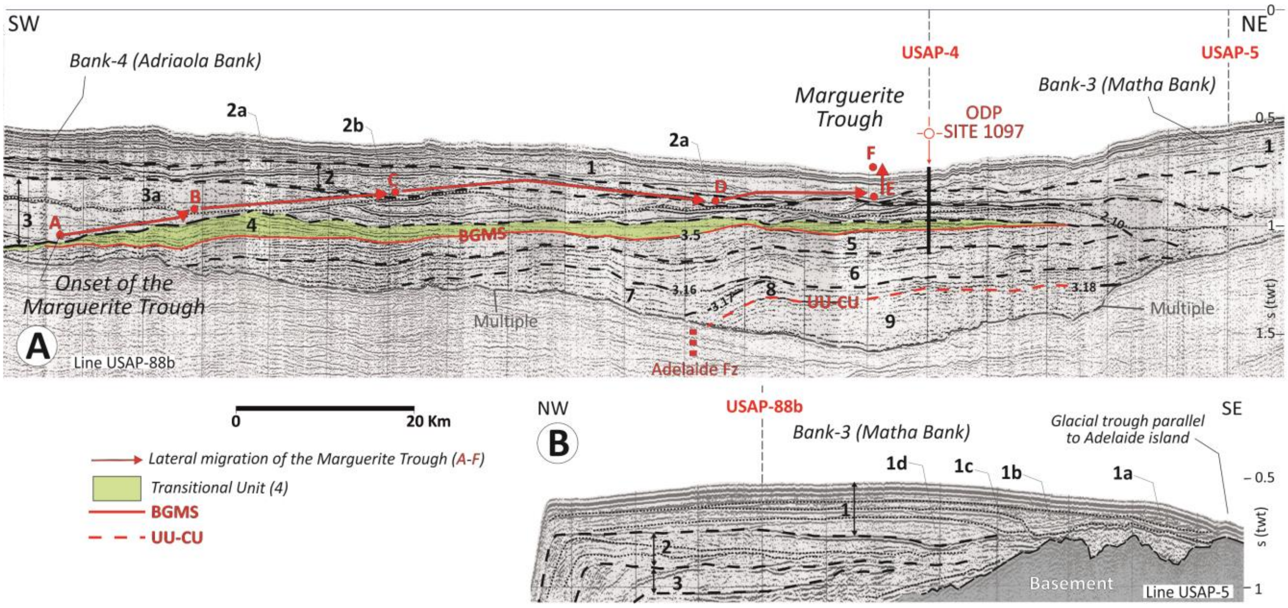

SW
NE
Bank-4 (Adriaola Bank)
USAP-4
USAP-5
Marguerite Trough
ODP SITE 1097
Bank-3 (Matha Bank)
Onset of the Marguerite Trough
BGMS
UU-CU
Multiple
Adelaide Fz
A
Line USAP-88b
s (twt)
0
20 Km
Lateral migration of the Marguerite Trough (A-F)
Transitional Unit (4)
BGMS
UU-CU
NW
USAP-88b
SE
Bank-3 (Matha Bank)
Glacial trough parallel to Adelaide island
B
Basement
Line USAP-5

Figure - 13

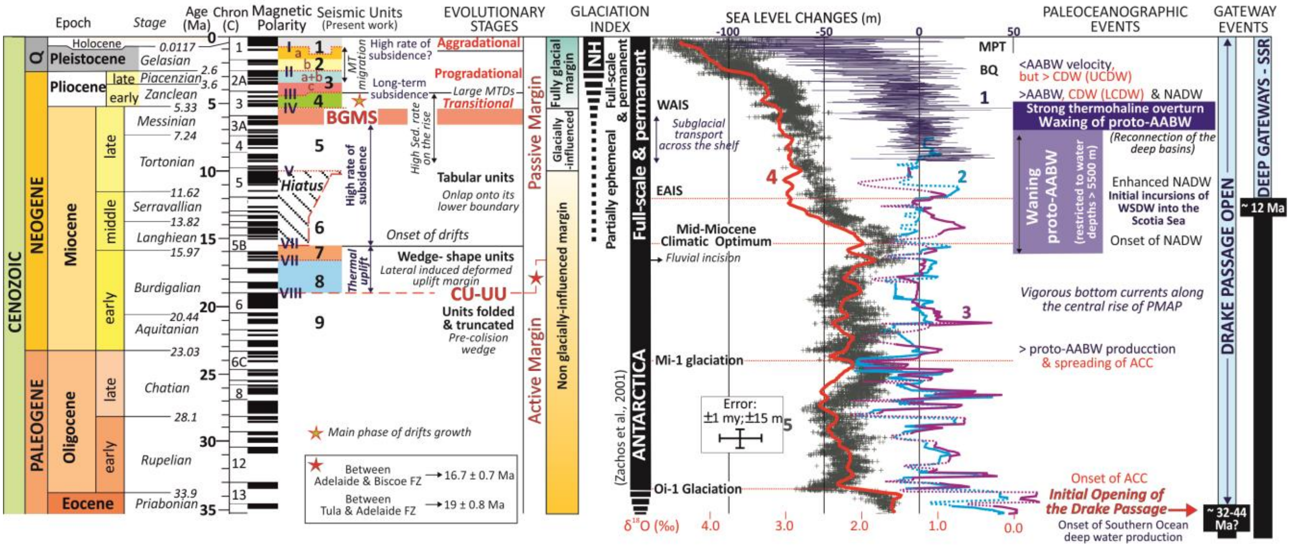

Epoch
Stage
Age (Ma)
Chron (C)
Magnetic Polarity
Seismic Units (Present work)
EVOLUTIONARY STAGES
GLACIATION INDEX
SEA LEVEL CHANGES (m)
PALEOCEANOGRAPHIC EVENTS
GATEWAY EVENTS
CENOZOIC
NEOGENE
PALEOGENE
Q
Pleistocene
Pliocene
Miocene
Oligocene
Eocene
Holocene
Gelasian
Piacenzian
Zanclean
Messinian
Tortonian
Serravallian
Langhian
Burdigalian
Aquitanian
Chatian
Rupelian
Priabonian
late
early
middle
0.0117
2.6
3.6
5.33
7.24
11.62
13.82
15.97
20.44
23.03
28.1
33.9
High rate of subsidence?
MT migration
Aggradational
Progradational
Long-term subsidence
Large MTDs
Transitional
BGMS
High Sed. rate on the rise
High rate of subsidence
Hiatus
Tabular units
Onlap onto its lower boundary
Onset of drifts
Thermal uplift
Wedge- shape units
Lateral induced deformed uplift margin
CU-UU
Units folded & truncated
Pre-colision wedge
Main phase of drifts growth
Between Adelaide & Biscoe FZ → 16.7 ± 0.7 Ma
Between Tula & Adelaide FZ → 19 ± 0.8 Ma
Passive Margin
Active Margin
Fully glacial margin
Glacially -influenced
Non glacially-influenced margin
NH
Full-scale & permanent
Partially ephemeral
Full-scale & permanent
ANTARCTICA
(Zachos et al., 2001)
WAIS
Subglacial transport across the shelf
EAIS
Mid-Miocene Climatic Optimum
Fluvial incision
Mi-1 glaciation
Error: ±1 my; ±15 m
Oi-1 Glaciation
δ18O (‰)
4.0
3.0
2.0
1.0
0.0
-100
-50
0
50
MPT
BQ
<AABW velocity, but > CDW (UCDW)
>AABW, CDW (LCDW) & NADW
Strong thermohaline overturn
Waxing of proto-AABW
(Reconnection of the deep basins)
Waning proto-AABW
(restricted to water depths > 5500 m)
Enhanced NADW
Initial incursions of WSDW into the Scotia Sea
Onset of NADW
Vigorous bottom currents along the central rise of PMAP
> proto-AABW producction & spreading of ACC
Onset of ACC
Initial Opening of the Drake Passage
Onset of Southern Ocean deep water production
DRAKE PASSAGE OPEN
DEEP GATEWAYS - SSR
~ 12 Ma
~ 32-44 Ma?

Figure-14

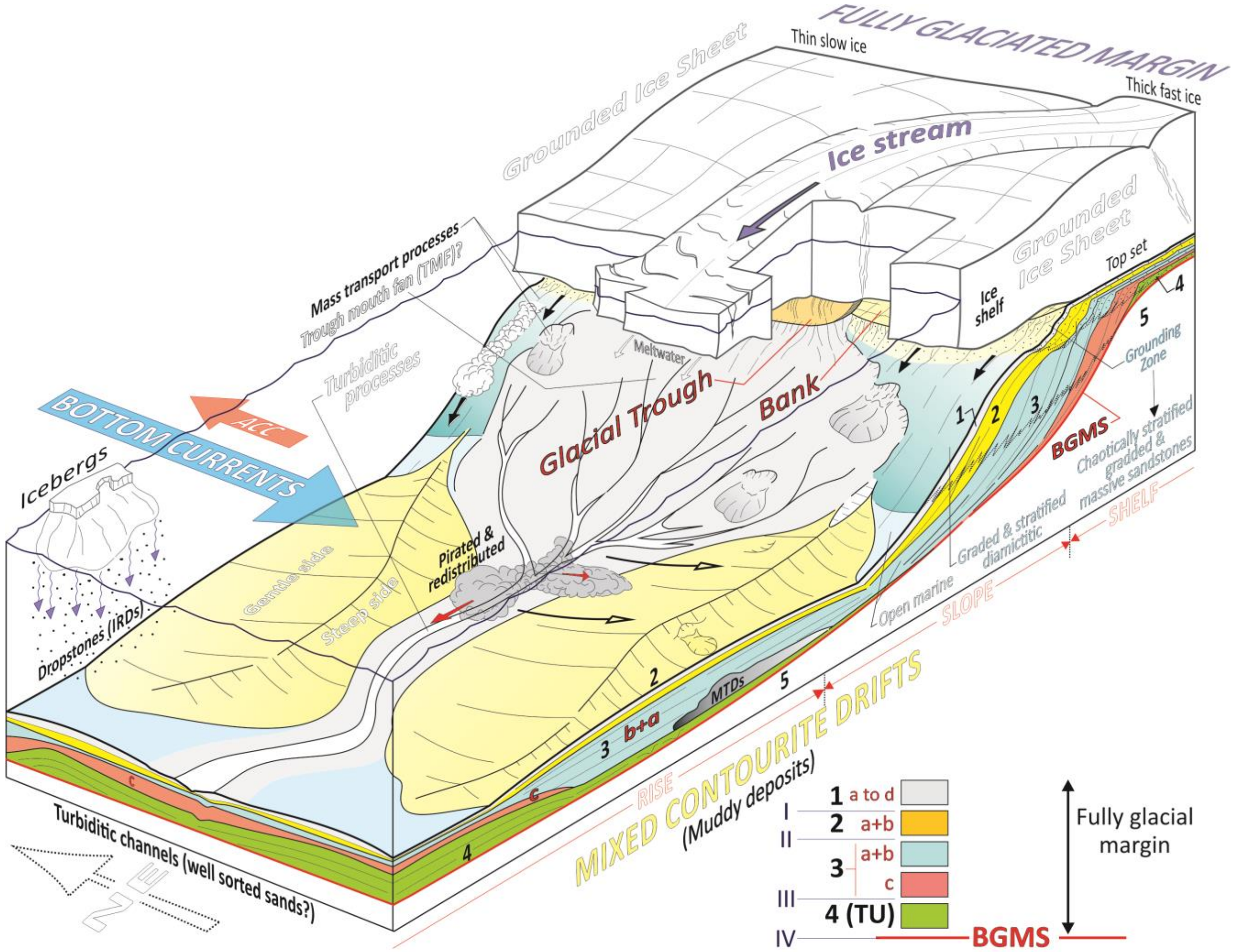
FULLY GLACIATED MARGIN
Thin slow ice
Thick fast ice
Grounded Ice Sheet
Ice stream
Grounded Ice Sheet
Top set
Ice shelf
Mass transport processes
Trough mouth fan (TMF)?
Turbiditic processes
Meltwater
Glacial Trough
Bank
Grounding Zone
BGMS
Chaotically stratified gradded & massive sandstones
Graded & stratified diamictitic
Open marine
SHELF
SLOPE
RISE
BOTTOM CURRENTS
ACC
Icebergs
Dropstones (IRDs)
Pirated & redistributed
Gentle side
Steep side
MTDs
b+a
MIXED CONTOURITE DRIFTS
(Muddy deposits)
Turbiditic channels (well sorted sands?)
1 a to d
2 a+b
3 a+b
c
4 (TU)
I
II
III
IV
BGMS
Fully glacial margin

Figure - 15

Table 1

<table>
<tr><th rowspan="2">Intervals</th><th rowspan="2">Stages</th><th rowspan="2">Seismic Units</th><th colspan="7">Seismic Facies</th></tr>
<tr><th colspan="3">Shelf</th><th>Slope</th><th colspan="2">Rise</th></tr>
<tr><td rowspan="4">III</td><td>III.3: Aggradational</td><td>SU1 (a,b,c, & d)</td><td>Aggradational configuration</td><td colspan="2" rowspan="4">Wedge shape (shelf+ slope)</td><td rowspan="3">Upper slope: chaotic facies. Frequent internal erosion surfaces
Middle slope: poorly organized facies. High acoustic response and irregular reflections.
Lower slope: more uniform facies. Transparent-to-weak acoustic response. Occasional higher amplitude reflections with concave patterns.</td><td colspan="2">Aggradational configuration</td></tr>
<tr><td rowspan="2">III.2: Progradational</td><td>SU2 (a & b)</td><td rowspan="2">Progradational configuration Transparent</td><td rowspan="2">Low-angle progradation (SU3). Aggradational configuration (SU2) Weak acoustic response Some reflections with high amplitude and good lateral continuity</td><td rowspan="2">Thin sedimentary wedges</td></tr>
<tr><td>SU3 (a,b & c)</td></tr>
<tr><td>II.1: Transitional</td><td>SU4</td><td>Reflections with very high acoustic response. High angle progradation (shelf break & upper slope). Sigmoid-oblique configuration.</td><td>Lower slope: moderate to high acoustic response. Large, irregular, lens-shaped deposits with chaotic, transparent facies.</td><td colspan="2">Sheeted, lightly mounded deposit, marked by very high amplitude reflections</td></tr>
<tr><td>II</td><td></td><td>SU5</td><td>Weak-to-moderate acoustic response. Some reflections with high amplitudes and good lateral continuity. Onlap.</td><td rowspan="2">Tabular shape</td><td rowspan="4">Aggradational configuration</td><td>Lower slope: mounded and lens shaped deposits with chaotic, massive facies and irregular high amplitude reflections.</td><td colspan="2">Moderate-to-high acoustic response. High amplitude reflections with good lateral continuity. Aggradational configuration. Sheeted deposits.</td></tr>
<tr><td rowspan="3">I</td><td>I.3</td><td>SU6</td><td>Homogeneous, with some reflections of high amplitude and good lateral continuity. Onlap</td><td></td><td colspan="2">Uniform with weak acoustic response</td></tr>
<tr><td rowspan="2">I.2</td><td>SU7</td><td>High acoustic response with irregular but laterally continuous reflections.</td><td rowspan="2">Sheeted deposits</td><td rowspan="2">Irregular to semi-chaotic features represented by an amalgam of high amplitude reflections</td><td>Very high acoustic response (>SU8), which decreases towards the base of the section,</td><td rowspan="2">Wedge deposits</td></tr>
<tr><td>SU8</td><td>Weak to medium acoustic</td><td>Medium-to-high acoustic response, and</td></tr>
</table>

ACCEPTED MANUSCRIPT

			response. Some irregular reflections with high acoustic response but poor lateral continuity.				contains some unusual reflections with variable lateral continuity	
	I.1	**SU9**	High acoustic response. Some high amplitude reflections with poor lateral continuity			---	High amplitude reflections, with good lateral continuity. Aggradational configuration. Onlap	

Acoustic basement

Table 2

Intervals	**Stages**	**Seismic Units**	**Sedimentary thickness (ms, TWT)**								
			Outer Shelf (proximal to distal)			**Slope**			**Rise**		
			Sectors			**Sectors**			**Sectors**		
			South	*Central*	*North*	*South*	*Central*	*North*	*South*	*Central*	*North*
III	III.3 Aggradational	**SU1**	~100	~50-100	~200	~250	~50	~50-100	~50-100	Eroded ?	~50
	III.2 Progradational	**SU2**	~100-350	~50-300	~50-260	~200	~300	~250	~100	~150	~50-60
		SU3	~200-1300	~50 to 450	~100 to 500	~500 700	~300	~500	~150	~100	~250
	II.1Transitional	**SU4**	~300	100	160	--	--	~50-100	~200 -260	~300-350	~325 -250
II		**SU5**	~150	~200	~150	50?	50?	Eroded ?	~50 to 300. Average=100		
I	I.3	**SU6**	100	~150	~250	~100	~200	~150	~200	~200	~120
	I.2	**SU7**	~450	~150	~200	~150 -300	~360	~100?	~450	~400	~400
		SU8	~200	~150	Multiple	~50-250	~400	~250-750	~200	~400	~200
	I.1	**SU9**	Multiple	~350-150	Multiple	--	--	--	Up to 150		

Acoustic basement

Highlights

- Neogene to Quaternary evolution of the Pacific Margin of the Antarctica Peninsula (PMAP)
- It shifted from a non-glacial, to a glacially-influenced, then fully glaciated margin
- Major shifts in sedimentary evolution at late Miocene, latest Pliocene and ~0.9 Ma
- Present morphosedimentary features were established between latest Pliocene and ~0.9 Ma
- Tectonic, climatic, glacial & palaeoceanographic changes influenced margin deposition